Phylogenetic relationships of the genus *Mischonyx* Bertkau, 1880, with taxonomic changes and three new species description (Opiliones: Gonyleptidae). (#52148)

First submission

Guidance from your Editor

Please submit by **9 Oct 2020** for the benefit of the authors (and your $200 publishing discount) .

Structure and Criteria
Please read the 'Structure and Criteria' page for general guidance.

Custom checks
Make sure you include the custom checks shown below, in your review.

Raw data check
Review the raw data.

Image check
Check that figures and images have not been inappropriately manipulated.

Privacy reminder: If uploading an annotated PDF, remove identifiable information to remain anonymous.

Files

Download and review all files from the materials page.

32 Figure file(s)
2 Table file(s)
8 Raw data file(s)

Custom checks

DNA data checks

- Have you checked the authors data deposition statement?
- Can you access the deposited data?
- Has the data been deposited correctly?
- Is the deposition information noted in the manuscript?

Field study

- Have you checked the authors field study permits?
- Are the field study permits appropriate?

New species checks

- Have you checked our new species policies?

- Do you agree that it is a new species?
- Is it correctly described e.g. meets ICZN standard?

Structure and Criteria

Structure your review

The review form is divided into 5 sections. Please consider these when composing your review:

1. **BASIC REPORTING**
2. **EXPERIMENTAL DESIGN**
3. **VALIDITY OF THE FINDINGS**
4. General comments
5. Confidential notes to the editor

You can also annotate this PDF and upload it as part of your review

When ready submit online.

Editorial Criteria

Use these criteria points to structure your review. The full detailed editorial criteria is on your guidance page.

BASIC REPORTING

- Clear, unambiguous, professional English language used throughout.
- Intro & background to show context. Literature well referenced & relevant.
- Structure conforms to PeerJ standards, discipline norm, or improved for clarity.
- Figures are relevant, high quality, well labelled & described.
- Raw data supplied (see PeerJ policy).

EXPERIMENTAL DESIGN

- Original primary research within Scope of the journal.
- Research question well defined, relevant & meaningful. It is stated how the research fills an identified knowledge gap.
- Rigorous investigation performed to a high technical & ethical standard.
- Methods described with sufficient detail & information to replicate.

VALIDITY OF THE FINDINGS

- Impact and novelty not assessed. Negative/inconclusive results accepted. *Meaningful* replication encouraged where rationale & benefit to literature is clearly stated.
- All underlying data have been provided; they are robust, statistically sound, & controlled.
- Speculation is welcome, but should be identified as such.
- Conclusions are well stated, linked to original research question & limited to supporting results.

Standout reviewing tips

The best reviewers use these techniques

Tip	*Example*
Support criticisms with evidence from the text or from other sources	*Smith et al (J of Methodology, 2005, V3, pp 123) have shown that the analysis you use in Lines 241-250 is not the most appropriate for this situation. Please explain why you used this method.*
Give specific suggestions on how to improve the manuscript	*Your introduction needs more detail. I suggest that you improve the description at lines 57- 86 to provide more justification for your study (specifically, you should expand upon the knowledge gap being filled).*
Comment on language and grammar issues	*The English language should be improved to ensure that an international audience can clearly understand your text. Some examples where the language could be improved include lines 23, 77, 121, 128 – the current phrasing makes comprehension difficult.*
Organize by importance of the issues, and number your points	*1. Your most important issue* *2. The next most important item* *3. …* *4. The least important points*
Please provide constructive criticism, and avoid personal opinions	*I thank you for providing the raw data, however your supplemental files need more descriptive metadata identifiers to be useful to future readers. Although your results are compelling, the data analysis should be improved in the following ways: AA, BB, CC*
Comment on strengths (as well as weaknesses) of the manuscript	*I commend the authors for their extensive data set, compiled over many years of detailed fieldwork. In addition, the manuscript is clearly written in professional, unambiguous language. If there is a weakness, it is in the statistical analysis (as I have noted above) which should be improved upon before Acceptance.*

Phylogenetic relationships of the genus *Mischonyx* Bertkau, 1880, with taxonomic changes and three new species description (Opiliones: Gonyleptidae).

Caio Gueratto [Corresp., 1], **Alípio Benedetti** [2], **Ricardo Pinto-da-Rocha** [1]

[1] Departamento de Zoologia/ Instituto de Biociências, Universidade de São Paulo, São Paulo, São Paulo, Brazil

[2] Centro Universitário Metodista Izabela Hendrix, Belo Horizonte, Minas Gerais, Brazil

Corresponding Author: Caio Gueratto
Email address: caio.gueratto@gmail.com

The type species of *Mischonyx* Bertkau 1880, *Mischonyx squalidus*, was described based on a juvenile, which holotype is lost. Based on revision publications, the genus includes 11 Brazilian species. The objectives of this research are: to propose a phylogenetic hypothesis for *Mischonyx* based on Total Evidence (TE); to propose taxonomic changes based on the phylogeny; and analyse the phylogenetic hypothesis biogeographically as well. We studied 54 individuals, 15 ~~of external~~ group and 39 ~~of internal~~ group for seven molecular markers (28S, 12S, 16S, COI, CAD, ITS e H3), totalizing 3742 bp. and we raised 128 morphological characters. We analysed the dataset under two optimality criteria: Maximum likelihood (ML) and ~~Maximum~~ parsimony (MP). We described three new species: *Mischonyx minimus* **sp. nov.** (type locality: Petrópolis, Rio de Janeiro), *Mischonyx intervalensis* **sp. nov.** (type locality: Ribeirão Grande, São Paulo) and *Mischonyx tinguaensis* **sp. nov** (type locality: Nova Iguaçu, Rio de Janeiro). The genus *Urodiabunus* is considered a junior synonym of *Mischonyx*. *Weyhia spinifrons* Mello-Leitão, 1923; *Weyhia clavifemur* Mello-Leitão, 1927 and *Geraeocormobius reitzi* Vasconcelos, 2005b were transferred to *Mischonyx*. *M. cuspidatus* Roewer, 1913 is a junior synonym of *M. squalidus* Bertkau, 1880. By the phylogenetic hypothesis ~~of relationship~~, *Gonyleptes antiquus* Mello-Leitão, 1934 (former *Mischonyx antiquus*) cannot be considered a *Mischonyx* species, therefore we reestablish the original combination. The new composition for *Mischonyx* comprises 17 species, with 7 new combinations. We discuss the transformation of character states throughout the phylogeny, the different phylogenetic hypothesis using different datasets and the congruence of evidence between the clades in the phylogenetic hypothesis with the biogeographical hypothesis on Atlantic Forest areas of endemism.

Phylogenetic relationships of the genus *Mischonyx* Bertkau, 1880, with taxonomic changes and three new species description (Opiliones: Gonyleptidae).

Caio Guerratto[1], Alípio Benedetti[2], Ricardo Pinto-da-Rocha[1]

[1] Departamento de Zoologia, Instituto de Biociências, Universidade de São Paulo, 05508-090, Rua do Matão, travessa 14, número 321, São Paulo, SP, Brazil.
[2] Centro Universitário Metodista Izabela Hendrix, 30160-012, Rua da Bahia, 2020, Belo Horizonte, MG, Brazil.

Corresponding Author:
Caio Gueratto[1]
Departamento de Zoologia, Instituto de Biociências, Universidade de São Paulo, 05508-090, Rua do Matão, travessa 14, número 321, São Paulo, SP, Brazil.
caio.gueratto@gmail.com

Abstract

The type species of *Mischonyx* Bertkau 1880, *Mischonyx squalidus*, was described based on a juvenile, which holotype is lost. Based on revision publications, the genus includes 11 Brazilian species.

The objectives of this research are: to propose a phylogenetic hypothesis for *Mischonyx* based on Total Evidence (TE); to propose taxonomic changes based on the phylogeny; and analyse the phylogenetic hypothesis biogeographically as well. We studied 54 individuals, 15 of external group and 39 of internal group for seven molecular markers (28S, 12S, 16S, COI, CAD, ITS e H3), totalizing 3742 bp. and we raised 128 morphological characters. We analysed the dataset under two optimality criteria: Maximum likelihood (ML) and Maximum parsimony (MP).

We described three new species: *Mischonyx minimus* **sp. nov.** (type locality: Petrópolis, Rio de Janeiro), *Mischonyx intervalensis* **sp. nov.** (type locality: Ribeirão Grande, São Paulo) and *Mischonyx tinguaensis* **sp. nov** (type locality: Nova Iguaçu, Rio de Janeiro). The genus *Urodiabunus* is considered a junior synonym of *Mischonyx*. *Weyhia spinifrons* Mello-Leitão, 1923; *Weyhia clavifemur* Mello-Leitão, 1927 and *Geraeocormobius reitzi* Vasconcelos, 2005b were transferred to *Mischonyx*. *M. cuspidatus* Roewer, 1913 is a junior synonym of *M. squalidus* Bertkau, 1880. By the phylogenetic hypothesis of relationship, *Gonyleptes antiquus* Mello-Leitão, 1934 (former *Mischonyx antiquus*) cannot be considered a *Mischonyx* species, therefore we reestablish the original combination. The new composition for *Mischonyx* comprises 17 species, with 7 new combinations. We discuss the transformation of character states throughout the phylogeny, the different phylogenetic hypothesis using different datasets and the congruence of evidence between the clades in the phylogenetic hypothesis with the biogeographical hypothesis on Atlantic Forest areas of endemism.

Keywords. Atlantic Rainforest; Cladistics; Gonyleptoidea.

Introduction

Laniatores is the most diverse suborder within Opiliones and from its more than 4200 species (Kury, 2020), at least 2,400 are from the Neotropical region (Kury, 2003). Modern taxonomists are trying to organize families and less inclusive groups based on the cladistics paradigm (e.g. Bragagnolo & Pinto-da-Rocha, 2009; Da Silva & Gnaspini, 2010; Pinto-da-Rocha, 2002; Pinto-da-Rocha & Bragagnolo, 2010), including recently molecular data to understand some clade's evolution (e.g. Bragagnolo *et al.*, 2015; Pinto-da-Rocha *et al.*, 2014). However, most families and genera within Laniatores lack evolutionary studies ~~yet~~.

Even though researchers have made progress in phylogenetic systematics and taxonomy recently in Laniatores, there still is a strong influence of Carl F. Roewer's (1881-1963) classification system. Roewer based his nomenclature and groupings on a few arbitrary characters. As a result, he created a lot of monotypic genera and placed close related species in distinct clades (Pinto-da-Rocha *et al*., 2012). Another issue of ~~r~~oewerian's classification system is groups not reflecting phylogenetic relationships.

Gonyleptidae Sundevall, 1833 is one of the families within Laniatores that had many monotypic genera and many artificial groups as well. According to Kury (1990), the literature for the family showed that there were many species cited only once and this fact pointed to the possibility of high degree of synonymies within Gonyleptidae. However, recently researchers studied many subfamilies of Gonyleptidae in the light of phylogenetic systematics and there are cladistic evidences to support several groups (Benedetti & Pinto-da-Rocha, 2019; Bragagnolo & Pinto-da-Rocha, 2012; Da Silva & Gnaspini, 2010; Da Silva & Pinto-da-Rocha, 2010; Pinto-da-Rocha & Bragagnolo, 2010). In addition, with the use of molecular data in phylogenetic inference, Pinto-da-Rocha *et al.* (2014) and Benedetti *et al.* (unpublished data) proposed new relationships among most subfamilies of Gonyleptidae.

However, Gonyleptinae Sundevall, 1833, is one of the gonyleptid subfamilies that needs more phylogenetic research, once its 39 genera (140 species in total) have uncertain phylogenetic relationships (Kury, 2003). Moreover, the diagnosis for this subfamily is based on the number of areas in the dorsal scutum and the absence of features from other subfamilies (Pinto-da-Rocha *et al*., 2014). Thus, probably Gonyleptinae is polyphyletic and, to become monophyletic, some genera must be transferred to other clades.

Mischonyx background

Bertkau (1880) described *Mischonyx squalidus*, type species of the genus by monotypy, from Copacabana, Rio de Janeiro, Brazil. Rower (1923) pointed out that the holotype described in this work was a juvenile, evidenced by the incomplete tarsal segmentation. After Bertkau (1880), the genus remained monotypic until Kury (2003), ~~which~~ synonymized other genera (cited below) within *Mischonyx*.

In the first half of the 20th century, Carl Roewer and Candido Mello-Leitão described genera of interest for this research, namely, *Ilhaia* Roewer, 1913, *Weyhia* Roewer, 1913, *Xundarava* Mello-Leitão, 1927, *Eduardoius* Mello-Leitão, 1931, *Geraecormobiella* Mello-Leitão, 1931 and *Giltaya* Mello-Leitão, 1932. Besides that, Mello-Leitão described and transferred species into these genera and recognized *Weyhia* as a synonym of *Geraeocormobius* (Mello-Leitão, 1940).

In the second half of 20th century, B. Soares and H. Soares synonymized *Ilhaia* with *Eduardoius* (Soares, 1943), *Geraecormobiella* with *Geraeocormobius* Holmberg, 1887 (Soares, 1945) and *Ilhaia* with *Xundarava* (Soares & Soares, 1987). Along with that, the authors synonymized some species of these genus and described more species.

Kury (2003) synonymized *Ilhaia* and *Giltaya* with the almost forgotten genus *Mischonyx*. Besides that, he transferred *G. antiquus* (then in *Paragonyleptes*) to *Mischonyx*. Apparently, *Mischonyx squalidus* holotype is lost and the author based his conclusions on Roewer's drawings and description. In this catalog, Kury considers *Mischonyx* as having 11 species.

Finally, in Vasconcelos (2004, 2005a) the two last *Mischonyx* species were described: *Mischonyx kaisara*, from the coast of São Paulo state, and *Mischonyx poeta*, from the north of Rio de Janeiro state. He also described *Gearaeocormobius reitzi* Vasconcelos, 2005b. Besides these publications, Vasconcelos has an unpublished dissertation regarding *Mischonyx* taxonomy (E Vasconcelos, 2003, unpublished data).

The last published research containing taxonomical remarks regarding the genus,

Pinto-da-Rocha *et al.* (2012) considered 13 valid species within *Mischonyx*: *M. anomalus* (Mello-Leitão, 1936); *M. antiquus* (Mello-Leitão, 1934); *M. cuspidatus* (Roewer, 1913); *M. fidelis* (Mello-Leitão, 1931); *M. insulanus* (Soares, 1972); *M. intermedius* (Mello-Leitão, 1935); *M. kaisara* Vasconcelos, 2004; *M. meridionalis* (Mello-Leitão, 1927); *M. poeta* Vasconcelos, 2005a; *M. processigerus* (Soares & Soares, 1970); *M. scaber* (Kirby, 1819); *M. squalidus* Bertkau, 1880 and *M. sulinus* (Soares & Soares, 1947).

Beyond the taxonomic part, *Mischonyx cuspidatus* is one of the most studied harvestmen species regarding its biology. There are publications regarding its odoriferous glands chemical composition (Rocha *et al.*, 2013), defensive behavior (Dias & Willermart, 2013; Dias *et al.*, 2014; Willemart & Pellegatti-Franco, 2006), odor sensitivity (Dias, 2017) and synanthropic behaviour (Mestre & Pinto-da-Rocha, 2004). As it is possible to see from the historical background, although there was a lot of discussion about *Mischonyx* taxonomy, there is no phylogenetic hypothesis for this genus until the present.

The main goal of this work is to propose a phylogenetic hypothesis for *Mischonyx*, based on a Total Evidence approach, using seven genes and morphological characters, from external morphology and genitalia. In addition, we propose taxonomic~~al~~ changes, new species descriptions and biogeographical remarks for the genus based on the phylogenetic hypothesis.

Material and Methods

Species distribution and areas of endemism

To build an updated map of geographical distribution of *Mischonyx* species, we inserted the geographical coordinates of individuals from different locations of all the species available at Museu de Zoologia da Universidade de São Paulo (MZSP) and from LAL tissue collection into a spreadsheet and used DIVA-GIS to plot the localities on the map. We also included the type localities and records present in Kury (2003) as well. The nomenclature of areas of endemism of the Atlantic Rainforest and their delimitation follows Da Silva, Pinto-da-Rocha & Morrone (2017).

Type and analyzed ingroup specimens

We analyzed (see table 1) at least one type specimen from each valid *Mischonyx* species listed in Kury (2003), except the holotype of *Mischonyx squalidus*, which is lost. Type specimens were compared with harvestmen tissue collection present at Arachnology Lab (Instituto de Biociências - Universidade de São Paulo) to determine them correctly. We analyzed them through a stereomicroscope (Zeiss Stemi DV4). We conducted expeditions to obtain fresh material to extract DNA. Individuals that resembled *Mischonyx* species and did not match ~~with the~~ existing species were included in the analysis. The ingroup for this work is listed at Table 02.

Outgroup selection

We chose as outgroup species from different gonyleptid subfamilies to have a broader representativeness for this family. Species from Caelopyginae Sørensen, 1884,

Gonyleptinae, Hernandariinae Sørensen, 1884, Mitobatinae Simon, 1879, Pachylinae Sørensen, 1884, Progonyleptoidellinae Soares & Soares, 1985, Sodreaninae Soares & Soares, 1985 are included as outgroup. We have chosen at most two species of each subfamily in order to reduce the computational demand of parsimony analysis, ~~once we used~~ dynamic homology search algorithms. All information regarding the specimens is at Table 01.

Molecular data ~~acquirement~~

We keep all the collected specimens in 92 – 98% ethanol and at -20°C. For those species which did not have the DNA extracted, we extracted muscular tissue from the coxa IV of individuals (Pinto-da-Rocha *et al.*, 2014). Alternatively, when the individual was small, we used tissue~~s~~ from chelicerae and pedipalps. We used the kit Agencourt® DNAdvance System (Beckman Coulter, California, EUA) for extractions and modified the protocols according to Pinto-da-Rocha *et al*. (2014).

From the extracted DNA, we amplified seven molecular *loci*: the ribosomal nuclear gene 28S; the ribosomal mitochondrial genes 12S and 16S; the nuclear ~~I~~nternal ~~T~~ranscribed ~~S~~pacer subunit ~~II~~ (ITS2), carbamoylphosphate synthetase 2 (CAD) and the coding histone H3 gene (H3); and the mitochondrial ~~C~~ytochrome ~~O~~xidase subunit ~~coding gene~~ (COI). For polymerase chain reactions (PCRs), we used Thermo-fisher Taq kit, following the concentration present in Pinto-da-Rocha *et al.* (2014).

The primers used to amplify the genes were:

- 28S: overlap of two primer sets: 28SRDIAF – 28SRD4B (Arango & Wheeler, 2007 and Edgecombe & Giribet, 2006, respectively) and 28SD3AP – 28SB (Reyda & Olson, 2003 and De Ley *et al.*, 1999, respectively);
- 16S: 16SpotFN – 16SBR (Pinto-da-Rocha *et al.*, 2014 and Palumbi, 1996, respectively);
- 12S: 12SAIN – 12SOP2RN (Pinto-da-Rocha *et al.*, 2014);
- COI: dgLCO1490 – dgHCO2198 (Meyer 2003). Alternatively, LCO1490 – HCO2198 (Folmer *et al.*, 1994) and LCO1490 – HCOout (Folmer *et al.*, 1994 and Prendini, Weygoldt & Wheeler, 2005, respectively);
- H3: H3AF – H3AR (Colgan *et al.*, 1998). Alternatively, H3AF_edit (5'-GCVMGVAAGTCYACVGGMGG-3') – H3AR_edit (5'-ATGGTSACTCTCTTGGCGTGR-3'), made at the Molecular Systematics Laboratory of IBUSP;
- ITS: 5.8SF – CAS28Sb1d (Ji, Zhang & He, 2003);
- CAD: op_cad_F1 – op_cad_R1 (Peres *et al.*, 2018).

We conducted PCR reactions in an Eppendorf Mastercycler® gradient thermal cycler and the cycles and temperature used in this work are the same present in Pinto-da-Rocha *et al.* (2014). Afterwards, we inspected the PCR products using agarose gel electrophoresis (2% agarose), purified the products using Agencourt Ampure XP (Beckman Coulter) and quantified the products using a Thermo Scientific NanoDrop spectrophotometer. In order to prepare the products for sequencing, we used the BigDye® Terminator v3.1 Cycle Sequencing Kit (Applied Biosystems). The precipitation was with

sodium acetate and the sequencing process was in an ABI PRISM® 3100 Genetic Analyser/HITACHI (Applied Biosystems).

We assembled the contiguous sequences using Consed/PhredPhrap package (Ewing & Green, 1998; Ewing *et al.*, 1998; Gordon, Abajian & Green, 1998; Gordon, Desmarais & Green, 2001). We queried the contigs against the online NCBI BLAST database to check for contamination from other external sources. we aligned the sequences using MAFFT (Katoh *et al.*, 2002), visualized, and edited the results in Aliview (Larsson, 2014). We searched for stop codons in the coding genes (COI, CAD and H3) in Aliview. We trimmed the coding genes sequences to match the first base of the sequences with the first codon position. All sequences are at GenBank and their respective access codes are at Tables 01 and 02.

Morphological data acquisition, terminology and new species drawings

We obtained the external morphological characters analyzing both the type material and other individuals from the species under a Zeiss Stemi DV4 stereomicroscope. We used Scanning Electron Microscopy (SEM) to obtain male genitalia characters. We followed Pinto-da-Rocha (1997) to dissect and prepare the genitalia for Scanning Electron Microscope (Zeiss DSM940, from Instituto de Biociências, Universidade de São Paulo). We used Mesquite 3.51 (Maddison & Maddison, 2017) to build the character matrix and we coded the characters treating them preferentially as binary, in order to avoid ~~the~~ redundancy and to assure the principle of characters independence (Strong & Lipscomb, 1999). Nonetheless, to avoid building non-comparable characters, in some cases, we used multistate characters and we treated them as unordered. The character descriptions follow Sereno (2007). The complete character matrix is available online, at MorphoBank (http://morphobank.org/permalink/?P3599 – for reviewers, the password is Squalidus).

The terminology follows, in general, DaSilva & Gnaspini (2010). Granules refer to minute elevations, concentrated in a particular region or article. Tubercles are elevations which are clearly distinguishable from granules by their height and width and can have blunt or acuminated apex. Spines are acuminated elevations present on the ocularium. Apophyses are those armatures present on coxa IV, free tergites, anterior and posterior margins and can show several shapes. The terminology for dorsal scutum shapes follows Kury & Medrano (2016). The terminology for penis macrosetae follows Kury & Villareal (2015).

We used a stereomicroscope with *camara lucida* to make drawings. We digitalized them and used Adobe Photoshop Lightroom 6.0® to remove background inconsistencies.

Nomenclatural acts and collecting license

The electronic version of this article in Portable Document Format (PDF) will represent a published work according to the International Commission on Zoological Nomenclature (ICZN), and hence the new names contained in the electronic version are effectively published under that Code from the electronic edition alone. This published work and the nomenclatural acts it contains have been registered in ZooBank, the online registration system for the ICZN. The ZooBank LSIDs (Life Science Identifiers) can be resolved and the associated information viewed through any standard web browser by

appending the LSID to the prefix http://zoobank.org/. The LSIDs for this publication are: urn:lsid:zoobank.org:act:A6F34641-1AF1-4BE2-A16A-4A4497ECA1FC; urn:lsid:zoobank.org:act:3DDE0A87-E9F6-4504-9C54-6DC37D202A0E; urn:lsid:zoobank.org:act:5FA4CC13-EC27-4E3A-AB19-81A97FE74177. The online version of this work is archived and available from the following digital repositories: PeerJ, PubMed Central and CLOCKSS.

Field expeditions and collections were approved by Ministério do Meio Ambiente (MMA), Instituto Chico Mendes de Conservação da Biodiversidade (ICMBio), Sistema de Autorização e Informação em Biodiversidade (SISBIO) (License number: 57281-2).

Molecular dating

Firstly, we used only COI to estimate *Mishconyx* divergence time, given that, from all the genes used, it has more sequences from different Gonyleptidae species present at GenBank. We used only one terminal from each species, totalizing 122 terminals. We used the program BEAUti to set the priors for BEAST 2.5 analysis (Bouckaert *et al.*, 2019). As priors, we used Beast Model Test to set the site model, a lognormal relaxed clock with substitution rate of 0.005 (according to Bragagnolo *et al.*, 2015 and Peres *et al.*, 2019) with Yule tree and constrained the root using a normal distribution. We dated three clades in this initial analysis: Gonyleptidae root, with T_{MRCA} 140 ± 40 Mya, based on Sharma & Giribet (2011); Sodreaninae Kury, 2003 clade (*sensu* Peres *et al.*, 2019), with T_{MRCA} 31.5 ± 10 Mya, based on Peres *et al.* (2019); *Promitobates* Rower, 1913, with T_{MRCA} 58.5 ± 3.9 Mya, based on Bragagnolo *et al.* (2015). We ran two independent analyses, with 10 million generations each, sampling trees every 10,000 generations. We verified both runs in TRACER 1.7 (Rambaut *et al.*, 2018) and checked for EES > 200 and combined the results in LOGCOMBINER 2.5.

Then, we applied the T_{MRCA} estimated for *Mischonyx* to calibrate the multilocus species tree using *BEAST, with the seven genes cited above and the terminals from Table 02, using BEAST 2.5 as well. We pruned the dataset to one sequence per haplotype per species. We used all the priors from the first step and performed two independent analyses with 100 million generations, sampling trees each 5,000 generations. We checked the output from the analyses, using Tracer 1.7 and combined trees using LOGCOMBINER 2.5. The maximum clade credibility was annotated and the first 10% was discarded, using TREEANNOTATOR 2.5. Finally, we analysed the final tree using FigTree 1.4.4 (Rambaut, 2010).

Phylogenetic inferences

We ran three analyses: using morphological data only, molecular data only and combined evidence (Total Evidence Analysis). For each of them, we used two optimality criteria: Maximum parsimony (MP) and maximum likelihood (ML).

Maximum likelihood. For morphological analysis (ML1), we inserted the dataset as input in IQ-TREE version 1.6.10 (Nguyen *et. al.*, 2015), using the best model found by the program, which uses BIC (*Bayesian information criterion*) (Schwarz, 1978) to analyse which model is the best for that specific dataset. The analysis displayed by the program is

the same described for the molecular data below. To analyse character changes, we inserted the phylogeny output from IQ-TREE on Winclada 1.61 (Nixon, 2002).

For molecular (ML2) and TE (ML3) analysis, we aligned the sequences on MAFFT and analyzed them on Aliview. We built a FASTA file with all the sequences concatenated using SequenceMatrix 1.8 (Vaidya, Lohman & Meier, 2011). We ran the analysis on IQ-TREE version 1.6.10 (Nguyen *et. al.*, 2015). All the partitions coming from the seven different genes present in the concatenated FASTA file (and the morphological dataset for TE) were first analyzed on IQ-TREE through the partition model (Chernomor, von Haeseler & Minh, 2016), using the "-spp" command. The program selected the best substitution model for each gene partition under the BIC (Schwarz, 1978), using the program ModelFinder (Kalyaanamoorthy *et al.*, 2017), through the command "-m TESTNEWMERGE". We ran the likelihood analysis with 10,000 search iterations, through the command "-s -n 10000". Afterwards, we ran a bootstrap analysis. Through the command "-bb 1000", the program ran 1,000 iterations of ultrafast bootstrap (Minh *et al.*, 2013). Finally, we analyzed the output using FigTree 1.4.4 (Rambaut, 2010), considering *Promitobates ornatus* Mello-Leitão, 1922 as the root, once, in Pinto-da-Rocha *et al.* (2014), this species is the furthest from *Mischonyx cuspidatus* in their topology when comparing to the other species chosen as outgroup in the present research. We used a parsimony method to analyse character change because, as pointed by Cheng & Kuntner (2014), the aim is to "understand the evolutionary changes of characters rather than the probability of particular ancestral states on the phylogeny".

Maximum parsimony. We carried out the analysis using morphological characters only (MP1) on TNT (Goloboff, Farris & Nixon, 2008), through the heuristic search, with the TBR algorithm, making 10,000 replicates and retaining 100 trees per replicate. We used the command "collapse branches after search" to eliminate non-supported nodes, and searches using Ratchet (Nixon, 1999) and Tree Fusing (Goloboff, 1999). The characters were treated as unordered and unweighted. To analyse character change throughout the phylogeny, we used Winclada 1.61. We considered *Promitobates ornatus* as the root as well (reason explained above).

The molecular only (MP2) and TE (MP3) analysis were implemented using the program POY 5.1.1 (Varón, Vinh & Wheeler, 2010), which did the searches using direct optimization (hereafter DO) of unaligned sequences (Wheeler, 1996), strategy referred as Dynamic Homology (Wheeler 2001 a,b). This strategy differs from traditional static homology search because the former integrates both alignment and tree searches, while the last treats them as two separated searches. DO is able to insert in a static matrix the tests of possible homology hypothesis for unaligned nucleotides dynamically, optimizing these sequences directly on the available trees and, concomitantly, converts of the transformation series of pre-aligned sequences (Kluge & Grant, 2006; Grant & Kluge, 2009; Sánchez-Pacheco *et al.*, 2017).

At first, we ran DO analysis for five searches, specifying search time (from two hour to ten hours, ~~totalizing~~ 30 hours search). This was an exploratory search and allowed us to check which one of these five search times presented the lowest tree scores as outputs and, consequently, the optimal search time for DO ("max_time" parameter). The best tree scores for our dataset was with a maximum search time of 2 h. Then, we submitted the

dataset to the analysis, treating H3, COI and CAD sequences as pre-aligned, because they are coding genes, and 28S, 12S, 16S and ITS to be aligned using dynamic homology methods ("transform" command in POY). We treated morphological characters as unordered and transformations as equally weighted. The program performed five rounds of searches using the "max_time" (with "search" command). In POY each "search" round implements Tree Bisection and Reconnection (TBR), Wagner tree building, Subtree Pruning and Regrafting (SPR), Branch Swapping (RAS+swapping, as in Goloboff, 1999), Tree fusing (Goloboff, 1999) and Parsimony Ratchet (Nixon, 1999). We used the final trees from this previous analysis in an exact iterative pass (IP) analysis (Wheeler, 2003). Costs for all the previous optimal trees were calculated and POY generated the implied alignment of this final analysis (Wheeler, 2003). We used TNT 1.5 (Goloboff & Catalano, 2016) to calculate Bootstrap values and Bremer support, with "hold" command of 10000000 trees, "mult" command of 1000 replicates, holding 10 trees per replicate. Finally, we analyse the character changes through the phylogeny using parsimony on Winclada 1.61.

Results

Molecular data

In total, we sequenced 54 individuals of almost all *Mischonyx* species. We could not obtain fresh tissue for two species, namely, *Urodiabunus arlei* and *Mischonyx scaber*. The fragments sequenced have the following lengths: 28S has 972 bp, 16S has 386 bp, 12S has 408 bp, CAD has 639 bp, COI has 570 bp, H3 has 309 bp and ITS has 456 bp, ~~totalizing~~ 3742 bp for all the sequences. From all the 54 individuals, we could sequence 88% of all the fragments. We included in the analysis terminals that had at least five of the seven fragments sequenced (see Table 2).

Morphological data

For morphological data, we coded 128 characters. The ones taken from literature are properly acknowledged. We included 45 characters from dorsal scutum, 44 characters from appendages, 6 characters from free tergites, 27 characters from male genitalia and two characters from general aspect.

List of Morphological Characters and States

1. Dorsal scutum, shape (males) (Kury & Medrano, 2016): 0, Gamma P; 1, Gamma R; 2, Gamma; 3, Gamma T; 4, Non-Gamma;
2. Dorsal scutum, shape (females) (Kury & Medrano, 2016): 0, Alfa; 1, Gamma; 2, Gamma T; 3, Gamma P; 4, Non-Gamma;
3. Pedipalp, length: 0, Short (shorter than the dorsal scutum); 1, Long (longer than the dorsal scutum);
4. Pedipalp, tibia and tarsus, thickness: 0, Same thickness of femur; 1, Clearly more expanded than femur;
5. Dorsal scutum, anterior margin, lateral tubercles (Mendes, 2011): 0, Absence; 1, Presence;

6. Dorsal scutum, anterior margin, lateral tubercles, number: 0, Three on each lateral; 1, Two on each lateral; 2, Four or more in each lateral;
7. Dorsal scutum, anterior margin, lateral tubercles, size: 0, All tubercles with the same size; 1, One of the tubercles clearly more developed than the others;
8. Dorsal scutum, frontal hump, elevation: 0, Low (smaller than the ocularium height, without considering the median armature); 1, Elevated (bigger than the ocularium height, without considering the median armature) (Figs. 19 – 27);
9. Dorsal scutum, frontal hump, tubercles: 0, Absent; 1, Present;
10. Dorsal scutum, frontal hump, tubercles, number: 0, One (single armature); 1, Two (one pair) (Fig. 22C); 2, Four (2 pairs);
11. Dorsal scutum, number of areas: 0, Three; 1, Four;
12. Dorsal scutum, ocularium, median armature: 0, Absence; 1, Presence;
13. Dorsal scutum, ocularium, median armature, number: 0, One; 1, Two (one pair) (Figs. 19 – 27); 2, Three pairs;
14. Dorsal scutum, ocularium, median armature, size: 0, Tubercle (smaller than the ocularium height) (Fig. 19D); 1, Spine (longer than the ocularium height) (Fig. 22C);
15. Dorsal scutum, ocularium, median armature, merge: 0, Not merged (Figs. 19 – 27); 1, Apex merged;
16. Dorsal scutum, ocularium, anterior granule: 0, Absent (Fig. 25D); 1, Present (Fig. 19C);
17. Dorsal scutum, ocularium, posterior granulation: 0, Absent (Fig. 20D); 1, Present (Fig. 21C);
18. Dorsal scutum, prosoma, lateral granulation: 0, Absent 1, Present (Fig. 16A);
19. Dorsal scutum, prosoma, posterior armature: 0, Absence; 1, Presence;
20. Dorsal scutum, prosoma, posterior armature, number: 0, Pair of tubercles (Figs. 19 – 27); 1, Several tubercles;
21. Dorsal scutum, mid-bulge, lateral margin, armature: 0, Absence; 1, Presence;
22. Dorsal scutum, mid-bulge, lateral margin, armature distribution: 0, Present in the whole extension (Fig. 20B); 1, Present on the posterior half only (Fig. 21B);
23. Dorsal scutum, mid-bulge, lateral margin, armature, size: 0, Large tubercles (Fig. 27A); 1, Small tubercles (Fig. 20C);
24. Dorsal scutum, mid-bulge, lateral margin, armature, shape: 0, Rounded (Figs. 19 – 27); 1, Pointed;
25. Dorsal scutum, mid-bulge, lateral margin, armature, color (in ethanol): 0, Clearer than the rest of the body (Fig. 27A); 1, Darker than the rest of the body (Fig. 25A); 2, Same color of the rest of the body (Fig. 19B);
26. Dorsal scutum, mid-bulge, lateral margin, posterior armature, merge: 0, Merged, forming large tubercles (Fig. 27A); 1, Not merged (Fig. 20B);
27. Dorsal scutum, area I, longitudinal groove: 0, Absent; 1, Present;
28. Dorsal scutum, area I, paired median armature: 0, Absent; 1, Present;
29. Dorsal scutum, area I, paired median armature, size: 0, Small tubercles (Fig. 20B); 1, Conspicuous tubercles (Fig. 19B);
30. Dorsal scutum, area I, paired median armature, color (in ethanol): 0, Clearer than the rest of the body (Fig. 19B); 1, Darker than the rest of the body (Fig. 19A); 2, Same color of the rest of the body;
31. Dorsal scutum, area I, paired median armature, length in comparison to median armatures of area III: 0, Larger than the median armatures from area III (Fig. 19B); 1,

Smaller than the median armatures from area III (Fig. 19A); 2, Same size of the median armatures from area III;

32. Dorsal scutum, area II, paired median armature: 0, Absent; 1, Present;
33. Dorsal scutum, area II, lateral tubercle: 0, Absent (Fig. 24B); 1, Present (Fig. 21A);
34. Dorsal scutum, area II, paired median armature, color (in ethanol): 0, Lighter than the rest of the body (Fig. 23A); 1, Darker than the rest of the body (Fig. 22A); 2, Same color of the rest of the body;
35. Dorsal scutum, area II, paired median armature, size in comparison to median armatures of area III: 0, Larger than the median armatures from area III (Fig. 23A); 1, Smaller than the median armatures from area III (Fig. 22A); 2, Same size of the median armatures from area III;
36. Dorsal scutum, area III, armature: 0, Absent; 1, Present;
37. Dorsal scutum, area III, median armature, number: 0, One pair; 1, Single;
38. Dorsal scutum, area III, paired median armature, color (in ethanol): 0, Lighter than the rest of the body (Fig. 24A); 1, Darker than the rest of the body (Fig. 23B); 2, Same color of the rest of the body;
39. Dorsal scutum, area III, paired median armature, form: 0, Rounded; 1, Elliptic (Fig. 23B); 2, Sharp (Fig. 19D);
40. Dorsal scutum, area III, elliptic paired median armature: 0, Slightly compressed laterally (Fig. 23B); 1, Strongly compressed laterally (Fig. 27A);
41. Dorsal scutum, area III, lateral tubercles: 0, Absent; 1, Present (Fig. 27A);
42. Dorsal scutum, area III, lateral armature, size: 0, Small tubercles (Fig. 21A); 1, Well-developed tubercles (Fig. 27A);
43. Dorsal scutum, area III, lateral armature, color (in ethanol): 0, Clearer than the rest of the body (Fig. 24B); 1, Darker than the rest of the body (Fig. 27A); 2, Same color of the rest of the body (Fig. 19B);
44. Dorsal scutum, area III, lateral armature, form: 0, Rounded (Fig. 21A); 1, Elliptic (Fig. 23B);
45. Dorsal scutum, posterior margin, armature: 0, Absent; 1, Present;
46. Dorsal scutum, posterior margin, armature, size: 0, Small tubercles (Fig. 19A); 1, Presence of central tubercle more developed or apophysis (Fig. 27B); 2, All tubercles well-developed;
47. Dorsal scutum, granulation, density (DaSilva & Pinto-da-Rocha, 2010): 0, Low (scattered granules, some regions of dorsal scute smooth); 1, Median (granules scattered throughout dorsal scute); 2, High;
48. Free tergite I, armature: 0, Absente; 1, Present;
49. Free tergite I, armature, size: 0, Small tubercles (Fig. 19A); 1, Presence of central tubercle more developed or apophysis (Fig. 27B); 2, All tubercles well-developed;
50. Free tergite II, armature: 0, Absent; 1, Present;
51. Free tergite II, armature, size: 0, Small tubercles (Fig. 19A); 1, Presence of central tubercle more developed or apophysis (Fig. 24B); 2, All tubercles well-developed;
52. Free tergite III, armature: 0, Absent; 1, Present;
53. Free tergite III, armature, size: 0, Small tubercles (Fig. 19A); 1, Presence of central tubercle more developed or apophysis (Fig. 24B); 2, All tubercles well-developed;
54. Leg II, basitarsus, segmentation, number: 0, Six; 1, Seven; 2, Eight; 3, Nine; 4, more than nine;

55. Leg III, trochanter, armature: 0, Absence; 1, Presence;
56. Leg III, trochanter, armature, type: 0, Trochanter with many tubercles; 1, Trochanter with a prolateral basal apophysis;
57. Leg IV, coxa, apical width of males in ventral view (compared to coxa III) (modified from Benedetti & Pinto-da-Rocha, 2019): 0, Coxa III and IV with the same width; 1, Coxa IV 2 times larger than coxa III; 2, Coxa IV 4 times larger than coxa III;
58. Leg IV, coxa, apical prolateral apophysis on males: 0, Absent; 1, Present;
59. Leg IV, coxa, apical prolateral apophysis, length (compared to trochanter IV) (modified from Benedetti & Pinto-da-Rocha, 2019): 0, Shorter than trochanter IV (Fig. 21B); 1, Similar size of trochanter IV (Fig. 21A); 2, Longer than trochanter IV; 3, Much smaller than trochanter IV (as a tubercle);
60. Leg IV, coxa, apical prolateral apophysis, basal tubercle: 0, Absent; 1, Present (Fig. 20B);
61. Leg IV, coxa, apical prolateral apophysis, secondary subdistal lobe (Benedetti & Pinto-da-Rocha, 2019): 0, Absent; 1, Present (Fig. 22A);
62. Leg IV, coxa, apical prolateral apophysis, direction in dorsal view (Benedetti & Pinto-da-Rocha, 2019): 0, Slightly inclined relative to the axis of the base of coxa IV (Fig. 22A); 1, Transversal; 2, Oblique (Fig. 21B);
63. Leg IV, coxa, apical prolateral apophysis, apex width (modified from Benedetti & Pinto-da-Rocha, 2019): 0, Base more than 4 times larger than the apex (Fig. 20B); 1, Base 2 times larger than the apex (Fig. 27B); 2, Base as large as the apex;
64. Leg IV, coxa, apical prolateral apophysis, thickness: 0, Robust (Fig. 23B); 1, Sharp (Fig. 23A);
65. Leg IV, coxa, apical prolateral apophysis in females (Benedetti & Pinto-da-Rocha, 2019): 0, Absent; 1, Smaller than the male;
66. Leg IV, coxa, apical retrolateral apophysis in males (Benedetti & Pinto-da-Rocha, 2019): 0, Absent; 1, Present (Fig. 26B);
67. Leg IV, coxa, apical retrolateral apophysis, size (Benedetti & Pinto-da-Rocha, 2019): 0, Tubercle; 1, Apophysis;
68. Leg IV, coxa, apical retrolateral apophysis, number of branches: 0, One; 1, Two;
69. Leg IV, trochanter, prolateral armature in males: 0, Absent; 1, Present;
70. Leg IV, trochanter, retrolateral apical armature: 0, Absent; 1, Present;
71. Leg IV, trochanter, retrolateral apical armature, size: 0, Tubercle; 1, Apophysis (Fig. 19B);
72. Leg IV, trochanter, retrolateral armature, number: 0, One (Fig. 22B); 1, Two (Fig. 25B); 2, Three (forming a line);
73. Leg IV, femur, thickness: 0, Short and robust (Fig. 23B); 1, Long and thin (Fig. 21B);
74. Leg IV, femur, prolateral curvature: 0, Straight (not curved) (Fig. 21B); 1, Curved (Fig. 24B);
75. Leg IV, femur, retrolateral basal apophysis: 0, Absent; 1, Present (Fig. 20D);
76. Leg IV, femur, dorso-basal apophysis (DBA) (Benedetti & Pinto-da-Rocha, 2019): 0, Absent; 1, Present (Fig. 20D);
77. Leg IV, femur, dorso-basal apophysis, size: 0, Small (Fig. 26D); 1, large (longer than larger) (Fig. 20D); 2, Very small (Tubercle) (Fig. 19D);
78. Leg IV, femur, dorso-basal apophysis, apex direction: 0, Apex anteriorly directed (Fig. 27B); 1, Apex dorsally directed (Fig. 23D); 2, Apex retrolaterally directed (Fig. 24B);

3, Apex prolaterally directed;

79. Leg IV, femur, dorso-basal apophysis, apex width: 0, Base more than 4 times wider than apex (Fig. 20D); 1, Base 2 times wider than apex (Fig. 27B); 2, Base as wide as apex (Fig. 26D);
80. Leg IV, femur, dorso-basal apophysis, shape: 0, Digitiform (Fig. 24C); 1, Falciform (Fig. 25D); 2, Blunt; 3, Branched (Fig. 27B); 4, Conic (Fig. 20D);
81. Leg IV, femur, branched dorso-basal apophysis, bigger branch: 0, Retrolateral (Fig. 24B); 1, Dorsal (Fig. 22C);
82. Leg IV, femur, prolateral row of tubercles in males: 0, Absent; 1, Present;
83. Leg IV, femur, prolateral row of tubercles, development: 0, Equally developed (Fig. 27A); 1, Median larger (Fig. 24B); 2, Apical larger (Fig. 24A);
84. Leg IV, femur, prolateral row of tubercles, single apical apophysis: 0, Absent; 1, Present (Fig. 21B);
85. Leg IV, femur, dorsal row of tubercles: 0, Absent (dorsally smooth) (Fig. 21D); 1, Present (Fig. 20C);
86. Leg IV, femur, dorsal row of tubercles, apophysis after DBA: 0, Absent (Fig. 20D); 1, Present (Fig. 20C);
87. Leg IV, femur, dorsal row of tubercles, apophysis after DBA, number: 0, One (Fig. 23D); 1, Two (Fig. 22C); 2, Three – Six (Fig. 20C); 3, More than six;
88. Leg IV, femur, row of tubercles between the dorsal and retrolateral lines: 0, Absent; 1, Present;
89. Leg IV, femur, retrolateral row of tubercles: 0, Absent; 1, Present;
90. Leg IV, femur, retrolateral row of tubercles, position of the larger apophysis: 0, Basal third; 1, Medial third (Fig. 27A); 2, Apical Third (Fig. 23B);
91. Leg IV, femur, retrolateral row of tubercles, number of apophysis on the basal half: 0, Absence of apophysis on the basal half) (Fig. 21B); 1, One (Fig. 21A); 2, Two (Fig. 22A); 3, Three – Six (Fig. 24A); 4, More than 6;
92. Leg IV, femur, retrolateral row of tubercles, median apophysis: 0, Absent (Fig. 24B); 1, Present (Fig. 22A) ;
93. Leg IV, femur, retrolateral row of tubercles, number of apophysis on the apical half: 0, Absence of apophysis on the apical half; 1, One (Fig. 25D); 2, Two (Fig. 19A); 3, Three – Six (Fig 21B); 4, More than 6;
94. Leg IV, femur, retrolateral row of tubercles, more developed apical tubercle: 0, Absent; 1, Present (Fig. 19B);
95. General body color (in ethanol): 0, Brownish; 1, Black; 2, Yellowish; 3, Reddish;
96. Body totally or partially covered with debris (DaSilva & Pinto-da-Rocha, 2010): 0, Absent; 1, Present;
97. Penis, ventral plate, form in lateral view: 0, Globose (Fig. 29E); 1, Thin (Fig. 30E);
98. Penis, ventral plate, form in dorsal view: 0, Longer than larger (thin) (Fig. 30D); 1, Larger than longer (developed lateral expansions) (Fig. 30A);
99. Penis, ventral plate, ventral side, T1 microsetae: 0, Absence; 1, Presence;
100. Penis, ventral plate, ventral side, T1 microsetae, distribution: 0, Sparse or present in some regions (Fig. 29F); 1, Presence in the whole extension (Fig. 31C);
101. Penis, ventral plate, ventral side, medio-apical excavation: 0, Absence; 1, Presence;
102. Penis, ventral plate, ventral side, degree of the medio-apical excavation: 0, Slightly excavated (Fig. 29C and 29I); 1, Very excavated (Fig. 31F);

103. Penis, ventral plate, apical cleft (Kury, 1992): 0, Absent; 1, Present;
104. Penis, ventral plate, apical cleft, depth: 0, Shallow (in dorsal view, reaches at most the line of the first MS C) (Fig. 30D); 1, Deep (in dorsal view it is more basal than the MS C) (Fig. 28G);
105. Penis, ventral plate, apical cleft, format: 0, Edges slightly sloped (Fig. 28A); 1, Edges very sloped (Fig. 28G);
106. Penis, ventral plate, Macrosetae C (MS C), number: 0, Two; 1, Three (Fig. 30D); 2, Four;
107. Penis, ventral plate, Macrosetae C (MS C), shape: 0, Straight; 1, Helicoidal (Fig. 29G); 2, Curved (Fig. 30D);
108. Penis, ventral plate, Macrosetae C (MS C), position: 0, Distal (Fig. 28A); 1, Sub-distal (Fig. 30D);
109. Penis, ventral plate, Macrosetae A (MS A), number: 0, Two (Fig. 31D); 1, Three (Fig. 18G); 2, Four (Fig. 28A);
110. Penis, ventral plate, Macrosetae A (MS A), position on the ventral plate: 0, Linear in dorso-ventral direction (Fig. 29A); 1, Triangle shaped (Fig. 31D); 2, Parable shaped (Fig. 29H); 3, Linear in baso-apical direction;
111. Penis, ventral plate, Macrosetae B (MS B), size: 0, Small (clearly smaller than the MS A) (Fig. 18B); 1, Large (same size of the MS A) (Fig 18G);
112. Penis, ventral plate, Macrosetae D (MS D): 0, Absent (Fig. 31E); 1, Present (Fig. 28H);
113. Penis, ventral plate, Macrosetae D (MS D), number: 0, One (Fig. 28H); 1, Two; 2, Three;
114. Penis, ventral plate, Macrosetae D (MS D), size: 0, Small (Fig. 28H); 1, Large (Fig. 18B);
115. Penis, ventral plate, Macrosetae D (MS D), position in lateral view: 0, Ventral to the MS C (Fig. 29A); 1, Dorsal to the MS C;
116. Penis, ventral plate, Macrosetae E (MS E): 0, Absent; 1, Present;
117. Penis, ventral plate, Macrosetae E (MS E), number: 0, One; 1, Two;
118. Penis, ventral plate, Macrosetae E (MS E), position of the most basal MS E: 0, Ventral and aligned to the MS C (Fig. 30B); 1, Ventral and medial to the MS C (Fig. 28H);
119. Penis, ventral plate, well-developed lateral lobes (modified from Kury, 1992): 0, Absent (Fig. 30D); 1, Present (Fig. 30A);
120. Penis, ventral plate, lateral lobes, position: 0, Medial (Fig. 30A); 1, Basal (Fig. 30D);
121. Penis, ventral process: 0, Absent; 1, Present;
122. Penis, ventral process, flabellum: 0, Absent; 1, Present;
123. Penis, ventral process, flabellum, shape: 0, As long as large (Fig. 31A); 1, Longer than wide (thin) (Fig. 31D);
124. Penis, ventral process, flabellum, lateral parts: 0, Serrated (Fig. 29A); 1, Smooth (Fig. 28G);
125. Penis, ventral process, flabellum, apex: 0, Without a longer central terminal; 1, With a longer central terminal (Fig. 29H);
126. Penis, stylus, apex, microsetae: 0, Absence (Fig. 28D); 1, Presence (Fig. 31B);
127. Penis, stylus, apex, format: 0, Inclined relative to the penis axis; 1, Straight;
128. Penis, stylus, apex, keel: 0, Absence; 1, Presence.

Geographical Distribution and Areas of Endemism

The geographical distribution of all *Mischonyx* species is depicted on Figures 01 – 03. All species occur from Santa Catarina to Espirito Santo States, throughout the Atlantic Forest and in some Cerrado areas in Brazil (e.g. Minas Gerais and Mato Grosso do Sul). The species that occur in Cerrado areas are *M. intermedius* and *M. squalidus*. In general, all species are restricted to a narrow range, with exception of *M. anomalus*, which occurs in the whole state of Paraná, and *M. squalidus* which is a widespread species. This species is widespread throughout the genus distribution and even in some regions in which other species of the genus do not occur, such as Espírito Santo state. Moreover, this species shows a synanthropic behavior (Mestre & Pinto-da-Rocha, 2004) and can be found in degraded areas, such as regions with *Pinus* plantation, pasture areas and even in cities.

Regarding the Areas of Endemism (AoE) proposed by Da Silva, Pinto-da-Rocha & Morrone (2017), ~~the~~ most of the ~~genus~~ species are endemic/restricted to one AoE. The only exception is *M. squalidus*. *M. reitzi* **comb.nov.** and *M. clavifemur* **comb.nov.** are restricted to SC AoE; *M. anomalus* is restricted to PR AoE; *M. intervalensis* **sp. nov.** is restricted to SSP; *M. insulanus* and *M. kaisara* are restricted to SMSP; *M. processigerus* is restricted to Boc; *M. fidelis, M. scaber* and *M. parvus* **comb. nov.** are restricted to LSRJ; *M. arlei* **comb. nov.**, *M. spinifrons* **comb.nov.**, *M. minimus* **sp. nov.**, *M. tinguaensis* **sp. nov.** and *M. poeta* are restricted to Org. Clearly, the AoE with more endemic species is Org. Each species locality plotted at the map of Figures 01 – 03 are in different colors, each of them representing one different AoE, as the legend explains.

Phylogenetic analyses

Morphological analyses

In both analyses using strictly morphological data, under maximum likelihood (hereon ML1, fig. 04) and under maximum parsimony (heron MP1, fig. 05) criteria, the first lineage which branches off inside *Mischonyx* clade is composed by *M. arlei* **comb.nov**., *M. minimus* **sp. nov.** and *M. intermedius*, followed by the divergence of *G. antiquus* (former *Mischonyx antiquus*, before this work). Moreover, both analyses recover the clade formed by *M. anomalus, M. clavifemur* **comb.nov.** and *M. reitzi* **comb.nov.**, which agrees with molecular and TE results (Figs. 06 – 14). In ML1, both *Multumbo* species are within *Mischonyx* clade, while in MP1 they are not. This last result agrees with our TE results (see below). Both analyses presented low bootstrap values. *Mischonyx* clade present 25 of bootstrap value in ML1 and 7 in MP1. All internal branches inside the genus have values below 50 in both analyses (Figs. 04 and 05).

Molecular analyses

In both analysis using strictly molecular data, under maximum likelihood (hereon ML2, fig. 06) and under maximum parsimony (heron MP2, fig. 07) criteria, *Mischonyx* is monophyletic if *G. antiquus* (former *Mischonyx antiquus*) is removed from the genus. However, in MP2, there is a clade formed by *Deltaspidium* and *Multumbo* species, which is inside the clade that holds all the other *Mischonyx* species. These other genera are inside the clade with species from SMSP, SSP, PR and SC AoE. This group is sister to another clade

with the rest of *Mischonyx* species, which are from Boc, Esp, LSRJ and Org AoE.

ML2 differs from MP2 by not presenting the *Deltaspidium* and *Multumbo* species inside the clade with all *Mischonyx* species. Besides this difference, the main relationships inside the clade are the same found in MP2: a clade with species from SMSP, SSP, PR and SC AoE sister to the lineage with species from Boc, Esp, LSRJ and Org AoE.

Bootstrap values for both criteria are high. *Mischonyx* clade have 92 bootstrap value in ML2 and 100 in MP2. In MP2, the node which presents the lower bootstrap value is the one holding *Deltaspidium*, *Multumbo* and some *Mischonyx* species (cited above). In ML2, the lowest value inside *Mischonyx* clade is 67 (Figs. 06 and 07).

Bayesian analysis and Molecular dating

The Bayesian analysis (hereon B1, fig. 08) corroborates the topologies from the other molecular analyses, with the difference in the position of *M. poeta*. While in B1, this species is sister to *M. spinifrons* **comb.nov.**, in ML2 it is sister to a bigger clade, which includes *M. spinifrons* **comb.nov.**, *M. fidelis*, *M. parvus* **comb.nov.** and *M. squalidus*. The more inclusive clades have the same composition and same relationships in B1 and ML2: one clade including the species from LSRJ, Boc, Org and SEsp AoE and another with species from SMSP, SSP, PR and SC AoE. The main divergence time of *Mischonyx* clade occurred at 50.53 Mya (95% HPD = 44.07 – 57.12), when occurred the split of the two speciose clades. The first split time inside these two clades are very similar: 48.94 Mya (95% HPD = 39.65 – 54.60), for the one holding species from SMSP, SSP, PR and SC AoE and 44.80 (95% HPD = 35.57 – 52.32) for the other clade. Within the former clade, the formation of the lineage containing from SSP, PR and SC areas of endemism happened at approximately 28 Mya. The main divergence time after *M. intermedius* divergence from the remaining species of the clade occurred at 34.24 Mya (95% HPD = 27.07 – 41.38).

Total Evidence analyses

Both TE analyses, under maximum likelihood (hereon ML3, figs. 09 – 11) and maximum parsimony (heron MP3, fig. 12 – 14), have very similar results. *G. antiquus* (former *Mischonyx antiquus*) is placed outside *Mischonyx* genus. Inside the genus, there are two major clades. One of them with the lineage containing species of SMSP AoE as sister to the clade containing species from SSP, PR and SC AoE. The other, with a clade holding *M. intermedius* as sister to *M. arlei* **comb.nov.** and *M. minimus* **sp. nov.** and this lineage as sister to the clade which contains species from Boc, LSRJ and Org AoE. Inside this last clade, there are some differences between the analyses. While in MP3 the species from LSRJ + *M. squalidus* form a clade sister to species from Org (excepting *M. arlei* **comb.nov.** and *M. minimus* **sp. nov.** which have already diverged), in ML3, two species from Org (*M. poeta* and *M. scaber*) branches off in a clade, followed by *M. spinifrons* **comb.nov.**, which is sister to the lineage containing the species from LSRJ + *M. squalidus*. Both analyses have bootstrap values over 50 for inner branches inside *Mischonyx*. Bootstrap values for *Mischonyx* node are 89 in ML3 and 81 in MP3. Bremer support in MP3 for *Mischonyx* clade is 4 (Fig. 12).

From now on, we are going to consider ML3 as the phylogeny to present the further results regarding character state changes and to discuss relationships and character

evolution.

Character change through ML3

In ML3, *Mischonyx* clade is supported by the following character changes: Lateral tubercles on anterior margin of dorsal scutum with the same size (#7-0), elliptic tubercles on area III (#39-1), absence of prolateral apophysis on females (#65-0), femur prolaterally curved (#74-1), three to six apophysis on the apical half of retrolateral row on femur IV (#93-3) and brown as the general body color (#95-0). The clade with species from SMSP, SSP, PR and SC AoE is supported by presence of median apophysis on retrolateral row of femur IV (#92-1). Inside this clade, the lineage with species from SMSP is supported by nine segments on basitarsus II (#54-3) and falciform DBA (#80-1). The clade holding specie from SSP, PR and SC is supported by median armature on ocularium longer than the its height (#14-1), small tubercles on free tergite II (#51-0), thin ventral plate (#98-0) and MSA forming a parable (#110-2). The group with species from PR and SC is supported by #25-1, #47-2, retrolateral apophysis on trochanter IV (#71-1), two apophysis on the apical half on retrolateral row of femur IV (#93-2) and ventral plate thin in lateral view (#97-1).

The other lineage inside the clade, with species from Boc, Esp, LSRJ, and Org, is supported by flabellum as long as large (#123-0). Inside this clade, the lineage formed by *M. arlei* **comb.nov.**, *M. intermedius* and *M. minimus* **sp. nov.** is supported by median armature on area I larger than the median armatures from area III (#31-0), median armature on area II larger than the median armatures from area III (#35-0), low density of granulation on dorsal scutum (#47-0), prolateral apophysis on coxa IV shorter than trochanter IV (#59-0), prolateral apophysis on coxa IV oblique on dorsal view (#62-2) and thin ventral plate (#98-0) and the clade with *M. arlei* **comb.nov.** and *M. minimus* **sp. nov.** is supported by large tubercles on lateral margin of dorsal scutum (#23-0), median armature on area III with the same color of the rest of the body (#38-2), femur straight (#74-0), absence of retrolateral basal apophysis on femur IV (#75-0). The less inclusive clade holding species from Boc, LSRJ and remaining species from Org AoE is supported by rounded lateral armatures on area III (#44-1), branched DBA (#80-3) and absence of apophysis after DBA (#86-0). Inside this last group, the lineage with species from LSRJ and remaining Org species is supported by small tubercles on free tergite II (#51-0) and sparse T1 microsetae on ventral side of ventral plate (#100-0). The clade with *M. scaber*, *M. poeta*, *M. spinifrons* **comb.nov.** and species from LSRJ is supported by basal tubercle on prolateral apophysis on coxa IV (#60-1), absence of a more developed apical tubercle on retrolateral row on femur IV (#94-0) and ventral plate thin on dorsal view (#98-0). The lineage holding *M. scaber* and *M. poeta* is supported by absence of secondary distal lobe on prolateral apophysis of coxa IV (#61-0), absence of retrolateral basal apophysis on femur IV (#75-0), small DBA (#77-0) and one apophysis on apical half of retrolateral row of d=femur IV (#93-1). The group with *M. spinifrons* **comb.nov.** and species from LSRJ is supported by ventral plate thin on lateral view (#97-1), absence of well-developed lateral lobes on ventral plate (#119-0) and flabellum longer than wide (#123-1). The clade with species from LSRJ is supported by DBA with its base four times wider than the apex (#79-0) and lateral parts on flabellum smooth (#124-1). Finally, the clade holding *M. squalidus* and *M. parvus* **comb.nov.** is supported by presence of lateral tubercles on area II (#33-1), free tergite II with more developed central tubercle/ apophysis (#51-1), free tergite III with more developed central tubercle/apophysis (#53-1) and absence of retrolateral basal

apophysis on femur IV (#75-0).

Taxonomic changes

Mischonyx new combinations and diagnosis

Before this publication, *Mischonyx* included the following 12 species, listed in Kury (2003) and Pinto-da-Rocha *et al.* (2012): *M. anomalus* (Mello-Leitão, 1936); *M. antiquus* (Mello-Leitão, 1934); *M. cuspidatus* (Roewer, 1913); *M. fidelis* (Mello-Leitão, 1931); *M. insulanus* (Soares, 1972); *M. intermedius* (Mello-Leitão, 1935); *M. kaisara* Vasconcelos, 2004; *M. poeta* Vasconcelos, 2005a; *M. processigerus* (Soares & Soares, 1970); *M. scaber* (Kirby, 1819); *M. squalidus* Bertkau, 1880 and *M. sulinus* (Soares & Soares, 1947).

Based on ML3 hypothesis, we propose new combinations, composition and diagnosis for this genus:

***Mischonyx* Bertkau, 1880**

Mischonyx Bertkau, 1880: 106 (type species: *Mischonyx squalidus* Bertkau, 1880, by monotypy); Mello-Leitão, 1935: 22; Soares & Soares, 1949: 221; Kury, 2003: 132; Vasconcelos, 2004: 129; 2005: 229; Pinto-da-Rocha *et al*. 2012: 51 .
Ilhaia Roewer, 1913: 221; (type species *Ilhaia cuspidata* Roewer, 1913, by monotypy). Junior subjective synonym of *Mischonyx*, Bertkau, 1880: by Kury, 2003. In the present paper considered as a junior objective synonym of *Mischonyx*, Bertkau, 1880.
Jlhaia (misspelling): Roewer, 1930: 362.
Eugonyleptes Roewer, 1913: 219 (type species *Gonyleptes scaber* Kirby, 1819, by monotypy). Junior subjective synonym of *Mischonyx* Bertkau, 1880: by Pinto-da-Rocha *et al*, 2012.
Xundarava Mello-Leitão, 1927: 19 (type species *Xundarava holacantha* Mello-Leitão, 1927, by original designation). Junior subjective synonym of *Mischonyx* Bertkau, 1880: by Kury, 2003.
Gonazula Roewer, 1930: 417 (type species *Gonazula gibbosa* Roewer, 1930, by monotypy). Junior subjective synonym of *Mischonx* Bertkau, 1880: by Pinto-da-Rocha *et al.*, 2012.
Eduardoius Mello-Leitão, 1931: 94 (type species *Eduardoius fidelis* Mello-Leitão, 1931, by original designation). Junior subjective synonym of *Mischonyx*, Bertkau, 1880: by Kury, 2003.
Cryptomeloleptes Mello-Leitão, 1931: 137 (type species *Criptomeloleptes spinosus* Mello-Leitão, 1931, by original designation).Junior subjective synonym of *Mischonyx*, Bertkau, 1880: by Kury, 2003.
Geraecormobiella Mello-Leitão, 1931: 127; B. Soares, 1945: in a footnote [= *Geraeocormobius* Holmberg, 1887] (type species *Geraecormobiella convexa* Mello-Leitão, 1931, by original designation). **Syn.nov.**
Ariaeus Sørensen, 1932; Vasconcelos, 2005b: 2 [= *Geraeocormobius* Holmberg, 1887] (type species *Ariaeus tuberculatus* Sørensen, 1932, by monotypy). **Syn.nov.**
Giltaya Mello-Leitão, 1932: 466 (type species *Giltaya solitaria* Mello-Leitão, 1932, by original designation). Junior subjective synonym of *Mischonyx*, Bertkau, 1880: by Kury,

2003.
Brunoleptes Mello-Leitão, 1935: 398. (type species *Brunoleptes armatus* Mello-Leitão, 1935, by original designation). Junior subjective synonym of *Mischonyx*, Bertkau, 1880: by Kury, 2003.
Arleius Mello-Leitão, 1935: 22 (type species *Arleius incisus* Mello-Leitão, 1935, by original designation). Junior subjective synonym of *Mischonyx*, Bertkau, 1880: by Kury, 2003.
Urodiabunus Mello-Leitão, 1935: 396; 1935: 104; Soares & Soares, 1949: 219. (type species *Urodiabunus arlei* Mello-Leitão, 1935, by original designation). **Syn.nov.**
Penygorna Mello-Leitão, 1936: 30 (type species *Penygorna infuscata* Mello-Leitão, 1936, by original designation). Junior subjective synonym of *Mischonyx*, Bertkau, 1880: by Kury, 2003.

Composition: *Mischonyx. anomalus* (Mello-Leitão, 1936); *Mischonyx arlei* (Mello-Leitão, 1935b) **comb.nov.**,, *Mischonyx clavifemur* (Mello-Leitão, 1927a) **comb.nov.**; *Mischonyx fidelis* (Mello-Leitão, 1931b); *Mischonyx insulanus* (H. Soares, 1972); *Mischonyx intermedius* (Mello-Leitão, 1935b); *Mischonyx intervalensis* **sp. nov.**; *Mischonyx kaisara* Vasconcelos, 2004; *Mischonyx minimus* **sp. nov.**; *Mischonyx parvus* (Roewer, 1917) **comb. nov.**; *Mischonyx poeta* Vasconcelos, 2005a; *Mischonyx processigerus* (Soares & Soares, 1970); *Mischonyx reitzi* (Vasconcelos, 2005b) **comb.nov.**; *Mischonyx scaber* (Kirby, 1819); *Mischonyx spinifrons* (Mello-Leitão, 1923) **comb.nov.**; *Mischonyx squalidus* Bertkau, 1880; *Mischonyx tinguaensis* **sp. nov.**.

Taxonomic remarks: we transferred *Geraeocormobius reitzi* Vasconcelos, 2005b, *Urodiabunus arlei* Mello-Leitão, 1935, *Weyhia clavifemur* Mello-Leitão, 1927, *Weyhia spinifrons* Mello-Leitão, 1923 and *Weyhia parva* Roewer, 1917 to *Mischonyx* based on the molecular and morphological evidence. Other new combinations we have proposed based on the morphological analysis of the types as well. The only exception is *M. squalidus*, which we had to analyze original figures and description from Bertkau to propose this new synonym. Vasconcelos (2003, unpublished data), in his master's dissertation, and Benedetti (2017, unpublished data), in his PhD thesis, have already proposed most of these combinations. However, they have not published their works and, according to ICZN (1999), nomenclatural acts in thesis or dissertations are not valid if they are not officially published.

Besides that, by this new phylogenetic analysis, we restablish here the original combination of *Gonleptes antiquus* Mello-Leitão, 1934, removing the species from *Mischonyx* genus. This species was considered a member of *Mischonyx* by Kury (2003) and Pinto-da-Rocha *et al.* (2012). Now it returns to the genus in which it was originally described. Consequently, we remove the genus *Anoploleptes* Piza, 1940 from *Mischonyx*'s junior subjective synonym list, as established by Kury (2003), since *Anoploleptes dubium* (type species of *Anoploleptes*) is a junior synonym of *Gonyleptes antiquus* (see B. Soares, 1943). Therefore, *Anoploleptes* is a junior synonym of *Gonyleptes* as established by B. Soares (1943).

As pointed out by Acosta, Kury & Juárez (2007) "the correct (original) spelling of generic name is *Geraeocormobius*". Accordingly, we use the correct spelling in the synonymic lists below.

Diagnosis. Small size Gonyleptinae (3 –6 mm of dorsal scutum length). Dorsal scutum outline γP in males, with coda involved by the mid-bulge, which is very distinct. Females have dorsal scutum outline α, with coda long and clearly separated from mid-bulge. Anterior margin with lateral armature, normally two or three tubercles on each side. Frontal hump is high and narrow, with a pair of median tubercles (except in *M. processigerus*, which has two pairs). Lateral margin of prosoma with several granules, posterior to the ozopore. *Ocularium* is narrow and not very high, armed with median spines or tubercles. Some species have small tubercles anterior or posterior to the eye (or both). Posterior margin of prosoma with a pair of tubercles. Dorsal scutum with three areas. Mesotergal area I is divided by a longitudinal groove. Areas I and II armed with median tubercles (which are big and whitish in *M. arlei* **comb.nov.** and *M. minimus* **sp. nov.**). Area III with a pair of median elliptic tubercles (except in *M. arlei* **comb.nov.** and *M. minimus* **sp. nov.**), which can vary in size and lateral compression. Some species have other elliptic tubercles besides the median ones (e.g. *M. spinifrons* **comb.nov.**). Lateral margin of dorsal scutum (mid-bulge) with rounded tubercles, which can be fused in some species (e.g. *M. spinifrons* **comb.nov.**). Distitarsi of all legs with three segments. Basitarsus of leg I with three or four segments. Basitarsus II variable from 4 – 8 segments. Basitarsi III and IV with four or five segments. Ventral face of coxae I generally with more developed tubercles than the ones on the other coxa. Coxa IV with apical prolateral apophysis, generally robust and can present ventral process and a basal tubercle. Trochanter IV short and robust, with a blunt prolateral apophysis and with at least one retrolateral armature. Femur IV with DBA, which can be small (as in *M. arlei* **comb.nov.** and *M. minimus* **sp. nov.**), or large in most species. DBA can be branched or not and varies in shape and size in every species. Retrolateral row of tubercles generally with some large apophysis. Penis with ventral plate trapezoidal with an apical parabolic groove; three pairs of MS A and one pair of MS B on the lateral projections; three pairs of helicoidal MS C, two pairs of reduced MS E, one pair of MS D, venter of ventral plate with microsetae type T1 covering its whole extension or the basal half. Glans with ventral process, which present *flabellum,* which can be serrated or smooth. Stylus with microsetae, inclined in relation to the penis axis and presenting a ventral groove.

Species new combinations

Besides the combinations and synonyms present in Kury (2003) and Pinto-da-Rocha *et al.* (2012), the following new combinations are here proposed:

***Mischonyx. anomalus* (Mello-Leitão, 1936) (Figs. 19A, 19C, 28A –C)**

Xundarava anomala Mello-Leitão, 1936: 13, fig 10; B. Soares, 1945d: 192; 1945h: 366; H. Soares, 1945a: 210; Soares & Soares, 1949b: 220 (Male and female syntypes, Brazil, Paraná, Antonina; MNRJ 42282).

Ilhaia anomala: Soares & Soares, 1987: 7.

Mischonyx anomalus: Kury, 2003: 133; Pinto-da-Rocha *et al*, 2012: 52.

Ilhaia sulina Soares & Soares, 1947: 215 (Male lectotype and female paralectotype; Brazil Paraná, Florestal; MHNCI 3618 and MHNCI 3619, respectively). **Syn. nov.**

Mischonyx sulinus: Kury, 2003: 134; Pinto-da-Rocha *et al.*, 2012: 52.

Diagnosis. *Mischonyx anomalus* resembles *M. clavifemur* **comb. nov.** by: prolateral apophysis of coxa IV with its apex directed posteriorly; prolateral apophysis of trochanter IV small when compared to other species; retrolateral row of femur IV with median apophysis larger than the other armatures of this row; ventral plate of the penis with MS A forming a baso-apical, reduced MS B, MS E slightly medial when compared to the MS C, ventral side entirely covered with microsetae, lateral lobes basal. It differs from *M. clavifemur* **comb.nov.** by: its reduced size (4 – 4.5 mm of dorsal scutum length) (5 – 6 mm in *M. clavifemur* **comb.nov.**); Dorsal scutum is narrower than in *M. clavifemur* **comb.nov.**; Mesotergal Area III with a pair of large median tubercles (reduced in *M. clavifemur* **comb.nov.**); retrolateral side of trochanter IV with a row of small tubercles (two tubercles in *M. clavifemur* **comb.nov.**, with the apical more developed than the other); ventral plate longer than wider (as wide as long in *M. clavifemur* **comb.nov.**) dorsal row of femur IV with small tubercles only after DBA (three big tubercles after DBA in *M. clavifemur* **comb.nov.**) apical groove reaching the line of the second MS C (reaching deeper than the MS C in *M. clavifemur* **comb.nov.**).

***Mischonyx arlei* (Mello-Leitão, 1935b) comb.nov. (Fig. 19B, 19D, 28D –F)**

Urodiabunus arlei Mello-Leitão, 1935: 397, fig 22 (1 Male 1 female syntypes; Brazil, Rio de Janeiro, Petrópolis; MNRJ 42476).

Diagnosis. *Mischonyx arlei* **comb. nov.** resembles *M. minimus* **sp. nov.** by the combinations of following characters: mesotergal area I with a pair of well-developed median tubercles, which are clearer (whitish) than the rest of the body's color (dark brown); median armatures on mesotergal area III are spines; lateral margin of dorsal scutum with several small tubercles; Free Tergite II with a well-developed median apophysis; prolateral apophysis on coxa IV small and pointing posteriorly; retrolateral side of trochanter IV with two armatures; femur IV with several small apophysis on dorsal and retrolateral row of tubercles; femur IV with a well-developed terminal tubercle on pro and retrolateral rows of tubercles; ventral plate with three subdistal MS C on each side; MS B smaller than MS A; *flabellum* with serrated ends. It differs from *M. minimus* **sp. nov.** by: its size (7 – 8 mm) (3 – 3.5 mm in *M. minimus* **sp. nov.**); mesotergal area II with median tubercles small and darker than the rest of the body (median tubercles whitish and as big as the median tubercles on mesotergal area I in *M. minimus* **sp. nov**); basitarsus II with seven segments (four in *M. minimus* **sp. nov**); leg IV curved in dorsal view (straight in *M. minimus* **sp. nov**); MS D reduced (well-developed in *M. minimus* **sp. nov**).

***Mischonyx clavifemur* (Mello-Leitão, 1927a) comb.nov. (Figs. 20A, 20C, 28G –I)**

Weyhia clavifemur Mello-Leitão, 1927: 416; Roewer, 1930: 356; Mello-Leitão, 1932: 286, fig 177 (Male holotype; Brazil, Santa Catarina, Blumenau; MNRJ 1496).

Geraeocormobius clavifemur: Mello-Leitão, 1940b: 22; B. Soares, 1945h: 354; Soares & Soares, 1949b: 169; Vasconcelos, 2005b: 3, figs. 1 –9; Pinto-da-Rocha et al, 2014: 12, 16.

Ilhaia meridionalis Mello-Leitão, 1927a: 417 (female holotype; Brazil, Santa Catarina, Blumenau; MNRJ 1474); Vasconcelos, 2005b:3. Synonymy established by Vasconcelos, 2005b.

Jlhaia meridionalis (misspelling): Roewer, 1930: 363.

Mischonyx meridionalis: Kury, 2003: 133 –134.

Ariaeus tuberculatus Sørensen, 1932: 282 (female holotype; Brazil, Santa Catarina, Blumenau; BMNH); Vasconcelos, 2005b: 3. Synonymy established by Vasconcelos, 2005b.

Diagnosis. *Mischonyx clavifemur* **comb. nov.** resembles *M. anomalus***.** by the combinations of following characters: prolateral apophysis of coxa IV with its apex directed posteriorly; prolateral apophysis of trochanter IV small when compared to other species; retrolateral row of femur IV with median apophysis larger than the other armatures of this row; ventral plate of the penis with MS A forming a baso-apical, reduced MS B, MS E slightly medial when compared to the MS C, ventral side entirely covered with microsetae, lateral lobes basal. It differs from *M. anomalus* by: its size (5 – 6 mm of dorsal scutum) (4 – 4.5 mm in *M. anomalus*); mesotergal area III with small median tubercles (more developed in *M. anomalus*); retrolateral side of trochanter IV with two tubercles, with the apical more developed than the other (a row of small tubercles in *M. anomalus*); ventral plate of the penis as wide as long (longer than wider in *M. anomalus*) dorsal row of femur IV with three large tubercles after DBA (small tubercles only after DBA in *M. anomalus*), apical groove reaching deeper than the line of the last MS C (reaching the line of the second MS C in *M. anomalus*).

***Mischonyx fidelis* (Mello-Leitão, 1931b) (Figs. 20B, 20D, 29A –C)**

Eduardoius fidelis Mello-Leitão, 1931a: 95; 1932: 344 (2 syntypes; Brazil, Rio de Janeiro, Piraí; MNRJ 1408).

Ilhaia fidelis: B. Soares, 1943f: 56 [by implication]; 1945h: 358; Soares & Soares, 1946a: 76; 1949b: 186.

Mischonyx fidelis: Kury, 2003: 133; Pinto-da-Rocha *et al*, 2012: 52.

Diagnosis. *M. fidelis* resembles *M. parvus* **comb. nov.** by the combinations of following characters: pair of tubercles on the frontal hump and lateral margins of the dorsal scutum whitish (in ethanol); median tubercles on mesotergal area III big and elliptic; prolateral apophysis of trochanter IV big, when compared to other species (e.g. *M. spinifrons* **comb.nov.**); DBA conic and the tallest of the genus (almost as tall as the whole body), with a tubercle on the anterior side of the apophysis; prolateral row of femur IV with median tubercles more developed than the others on this row; retrolateral row of femur IV with the largest tubercle on the distal third; penis truncus apex not globose in lateral view; ventral plate with microsetae only on the basal half; apical groove shallow, reaching the line of the most apical MS C; lateral projections basal; MS A forming a dorso-ventral line; MS E basal when compared to the MS C; flabellum with the median large projection. It differs from *M. parvus* **comb. nov.** by: prolateral apophysis on coxa IV with small ventral lobe (ventral lobe as developed as the main projection in *M. parvus* **comb.nov.**); retrolateral side of trochanter IV with three small tubercles (two big tubercles in *M. parvus* **comb.nov.**); dorsal row of femur IV with an elevation basal to the DBA (absence of an elevation basal to the DBA in *M. parvus* **comb.nov.**); dorsal row of femur IV with small tubercles only after DBA (one big tubercle after DBA in *M. parvus* **comb.nov.**); retrolateral row of femur IV with three big tubercles on the basal half (without big tubercles tubercles on the basal half in *M. parvus* **comb.nov.**); ventral plate of the penis as large as wide (larger than wider in

M. parvus **comb.nov.**); lateral lobes projected (not projected in *M. parvus* **comb.nov.**); MS B ventral to MS A (MS B apical to the MS A in *M. parvus* **comb.nov.**); MS C more distal than in *M. parvus* **comb.nov.**.

***Mischonyx insulanus* (H. Soares, 1972) (Figs. 21A, 21C, 29D –F)**

Ilhaia insulana H. Soares, 1972: 65, figs 1 –4 (Male holotype, 1female paratype; Brazil, São Paulo, São Sebastião; HSPC 361).

Mischonyx insulanus: Kury, 2003: 133; Pinto-da-Rocha *et al*, 2012: 52.

Diagnosis. *M. insulanus* resembles *M. processigerus* by the combinations of following characters: median tubercles on ocularium smaller than the ocularium height; ocularium with small tubercles on the anterior and posterior sides; mesotergal area III with small median tubercles when compared to other species (e.g. *M. fidelis*); Free Tergites II and III with median apophysis; prolateral row of femur IV with median tubercles bigger than the others in this row; dorsal row of femur IV with small tubercles after DBA; retrolateral row of femur IV with the biggest apophysis on the distal third; ventral side of the ventral plate of the penis with microsetae only on the laterals; lateral lobes well-developed; apical groove of the ventral plate reaching the line of the second MS C; MS A forming a dorso-ventral line; reduced MS B. It differs from *M. processigerus* by: prolateral apophysis of coxa IV with ventral lobe as big as the main projection and close to each other (ventral lobe smaller and more separated from the main projection of the apophysis in *M. processigerus*); retrolateral apophysis of coxa IV not visible on dorsal view; (visible in *M. processigerus*); DBA not branched (branched in *M. processigerus*); retrolateral row of femur IV with two big apophysis (one in *M. processigerus*); retrolateral row of femur IV with small tubercles besides the two apophysis (several big tubercles in *M. processigerus*); *flabellum* with smooth apex (serrated in *M. processigeus*); stylus without microsetae (stylus with microsetae in *M. processigerus*); MS B closer to MS E when compared to *M. processigerus*.

***Mischonyx intermedius* (Mello-Leitão, 1935) (Figs. 21B, 21D, 29G –I)**

Ilhaia intermedia Mello-Leitão, 1935e: 401, fig 25; 1935b: 107 (Maleholotype; Brazil, Minas Gerais, Viçosa; IBSP 46).

Penygorna infuscata Mello-Leitão, 1936b: 31, fig 26 (1Male 2female syntypes; Brazil, Minas Gerais; Viçosa; MNRJ 42695). Synonymy established by B. Soares, 1944i.

Mischonyx intermedius: Kury, 2003: 133; Pinto-da-Rocha *et al*, 2012: 52.

Diagnosis. *M. intermedius* resembles *M. arlei* **comb. nov.** by the combinations of following characters: lateral margin of dorsal scutum with several small tubercles; mesotergal area III with median tubercles that are not elliptic; prolateral apophysis of coxa IV smaller than trochanter IV, blunt and oblique to the body axis; femur IV thin and long; retrolateral row of femur IV with an apical sharp tubercle; MS B reduced; MS E in the same dorso-basal line of the MS C; *flabellum* with serrated ends. It differs from *M. arlei* **comb. nov.** by: median tubercles on mesotergal area I smaller than the median tubercle of the other mesotergal areas and darker than the rest of the body color (in ethanol) (bigger and whitish in *M. arlei* **comb. nov.**); Free Tergite II with small tubercles only (big median apophysis in *M. arlei* **comb. nov.**); retrolateral apophysis of coxa IV not visible in dorsal

view (visible in *M. arlei* **comb. nov.**) prolateral apophysis of trochanter IV big (reduced in *M. arlei* **comb. nov.**); retrolateral side of trochanter IV with a line of three tubercles (two n *M. arlei* **comb. nov.**); DBA big in relation to the other armature on the dorsal row and with its apex directed anteriorly (DBA almost with the same size of other tubercles on the row and with its apex directed dorsally in *M. arlei* **comb. nov.**); prolateral ros of femur IV with a large number of tubercles when compared to other species (e.g. *M. spinifrons* **comb. nov.** and *M. arlei* **comb. nov.**); retrolateral row of femur IV with tubercles increasing in size apically (retrolateral row with minute armature in *M. arlei* **comb. nov.**); ventral side of the ventral plate of the penis with microsetae on the basal half (ventral side entirely covered with microsetae in *M. arlei* **comb. nov.**); apical groove of the ventral plate of the penis reaches the line of the most basal MS C (apical groove reaches the line of the median MS C in *M. arlei* **comb. nov.**); MS A forming a parable (MS A forming a diagonal baso-apical line in *M. arlei* **comb. nov.**); MS D more apical, when compared to *M. arlei* **comb. nov.**, that has the MS D medial on the ventral plate;

***Mischonyx kaisara* Vasconcelos, 2004 (Figs. 22B, 22D, 30A –C)**

Mischonyx kaisara Vasconcelos, 2004: 130, fig. 1 –9. (Male holotype; 5 Male paratypes; Brazil, São Paulo, Ilha Bela; MNRJ 17437 and MZSP 23147, respectively)

As *M. kaisara* was recently described and there is no new combination for the species, Vasconcelos (2004) diagnosis for the species remains unaltered and with no necessity to add information.

***Mischonyx parvus* (Roewer, 1917) comb. nov. (Figs. 23B, 23D, 30D –F)**

Weyhia parva Roewer, 1917: 133 (Male holotype, Brazil, São Paulo. Santos; SMF 1331).

Geraeocormobius parva: Mello-Leitão, 1940b: 22.

Geraeocormobius parvus: B. Soares, 1945: 355; Soares & Soares, 1949b: 171.

Ilhaia parva: Soares & Soares, 1987a: 6.

Cryptomeloleptes spinosus Mello-Leitão, 1931d: 138 (holotype; Brazil, Rio de Janeiro, Rio de Janeiro; MNRJ 11392). Synonymy established by Soares & Soares, 1987a.

Arleius incisus Mello-Leitão, 1935a: 22 (holotype; Brazil,Rio de Janeiro, Rio de Janeiro; MNRJ 41759). Synonymy established by Soares & Soares, 1987.

Ilhaia incisa: Soares & Soares, 1946a: 76; H.Soares, 1974: 354, fig 2. [= *Bunoleptes armatus* Mello-Leitão, 1935e; = *Geraecormobius cervicornis* Mello-Leitão, 1940b].

Bunoleptes armatus Mello-Leitão, 1935e: 398 (Male holotype, 2 Male paratypes; Brazil, Rio de Janeiro, Rio de Janeiro; MNRJ 42477 and MZSP 2328) Synonymy established by Soares & Soares, 1987a.

Geraecormobius cervicornis Mello-Leitão, 1940b: 17 (Male holotype lost; Brazil, Rio de Janeiro, Mangaritiba; MNRJ 53924). Synonymy established by Soares & Soares, 1987a.

Diagnosis. *M. parvus* **comb. nov.** resembles *M. fidelis* by the combinations of following characters: pair of tubercles on the frontal hump and lateral margins of the dorsal scutum whitish (in ethanol); median tubercles on mesotergal area III big and elliptic; prolateral apophysis of trochanter IV big, when compared to other species (e.g. *M. spinifrons* **comb.**

nov.); DBA conic and the tallest of the genus (almost as tall as the whole body), with a tubercle on the anterior side of the apophysis; prolateral row of femur IV with median tubercles more developed than the others on this row; retrolateral row of femur IV with the biggest tubercle on the distal third; penis not globose in lateral view; ventral plate with microsetae only on the basal half; apical groove shallow, reaching the line of the most apical MS C; lateral projections basal; MS A forming a dorso-ventral line; MS E basal when compared to the MS C; flabellum with the median projection big. It differs from *M. fidelis* by: prolateral apophysis on coxa IV with ventral lobe as developed as the main projection (ventral lobe reduced in *M. fidelis*); retrolateral side of trochanter IV with two big tubercles (small in *M. fidelis*); dorsal row of femur IV without an elevation basal to the DBA (presence of an elevation basal to the DBA in *M. fidelis*); dorsal row of femur IV with a big tubercle after DBA (small tubercles only after DBA in *M. fidelis*); retrolateral row of femur IV without big tubercles on the basal half (three big tubercles on the basal half in *M. fidelis*); ventral plate of the penis larger than wider (as large as wide in *M. fidelis*); lateral lobes not very projected, with the MS A and MS B close to the penis base (projected in *M. fidelis*); MS B apical to MS A (MS B ventral to the MS A in *M. fidelis*); MS C more median than in *M. fidelis.*

Taxonomic remarks: Kury (2003) synonymized this species with *M. squalidus*. However, the distribution of *M. parvus* does not match with the original location of the described individual in Bertkau (1880). In this last work, the location of the specimen is "Copacabana, Rio de Janeiro". By the distribution map in the figures 01 –03, the registers from this species are from Mangaratiba and Angra dos Reis, which are to the south of Rio de Janeiro state. For this reason, we removed this species from the synonymy created by Kury (2003).

***Mischonyx poeta* Vasconcelos, 2005 (Figs. 24A, 24C, 30G –I)**

Mischonyx poeta Vasconcelos, 2005a: 229, fig. 1 –9.(Male holotype; Brazil, Rio de Janeiro, Casimiro de Abreu; MNRJ 17460)

As *M. poeta* was recently described and there is no new combination for the species, Vasconcelos (2005a) diagnosis for the species remains unaltered and with no necessity to add information.

***Mischonyx processigerus* (Soares & Soares, 1970) (Figs. 24B, 24D, 31A –C)**

Ilhaia processigera Soares & Soares, 1970: 340, figs 1 –3 (Male holotype, 1 female paratype; Brazil, Rio de Janeiro, Itatiaia; MZUSP 4501).

Mischonyx processigerus: Kury, 2003: 134; Pinto-da-Rocha *et al*, 2012: 52.

Diagnosis. *M. processigerus* resembles *M. insulanus* by the combinations of following characters: median tubercles on ocularium smaller than the ocularium height; ocularium with small tubercles on the anterior and posterior sides; mesotergal area III with small median tubercles when compared to other species (e.g. *M. fidelis*); Free Tergites II and III with median apophysis; prolateral row of femur IV with median tubercles bigger than the others in this row; dorsal row of femur IV with small tubercles after DBA; retrolateral row of femur IV with the biggest apophysis on the distal third; ventral side of the ventral plate of the penis with microsetae only on the laterals; lateral lobes well-developed; apical

groove of the ventral plate reaching the line of the second MS C; MS A forming a dorso-ventral line; reduced MS B. It differs from *M. insulanus* by: prolateral apophysis of coxa IV with ventral lobe small and separated from the main projection (ventral lobe as big as the main projection and close to each other in *M. insulanus*); retrolateral apophysis of coxa IV visible on dorsal view; (not visible in *M. insulanus*); DBA branched (not branched in *M. insulanus*); retrolateral row of femur IV with one big apophysis (two in *M. insulanus*); retrolateral row of femur IV with big tubercles besides the apophysis (small tubercles in *M. insulanus*); *flabellum* with serrated apex (smooth in *M. insulanus*); stylus with microsetae (stylus without microsetae in *M. insulanus*); MS B distant from MS E when compared to *M. insulanus*.

***Mischonyx reitzi* (Vasconcelos, 2005) comb.nov. (Figs. 25A, 25C, 32A –C)**

Geraeocormobius reitzi Vasconcelos, 2005b: 6, figs. 10 –19. (Malee holotype; Brazil, Santa Catarina, Ilhota; MNRJ 6949)

Diagnosis. *M. reitzi* **comb. nov.** resembles *M. tinguaensis* **sp. nov.** by the combinations of following characters: Median armature on mesotergal area III small when compared to other species (e.g. *M. spinifrons* **comb.nov.**) and elliptic; no median armature on Free Tergites I – III; prolateral apophysis on coxa IV with its apex directed laterally, as big as the trochanter IV and with ventral lobe; a small tubercles basal to DBA on the dorsal row; DBA branched; dorsal row of femur IV with small tubercles only; prolateral row with tubercles of the same size; apical groove on ventral plate of the penis reaching the line of the most basal MS C; MS A forming a baso-apical line; stylus with microsetae. It differs from *M. tinguaensis* **sp. nov.** by: lateral margin of dorsal scutum with small tubercles which have the same color of the rest of the body (whitish than the rest of the body in *M. tinguaensis* **sp. nov.**); median armature on ocularium smaller than the ocularium height (bigger in *M. tinguaensis* **sp. nov.**); trochanter IV with two retrolateral tubercles (three in *M. tinguaensis* **sp. nov.**); median apophysis on retrolateral row of femur IV is the biggest on this row (biggest apophysis is on the apical third in *M. tinguaensis* **sp. nov.**); MS B reduced (as big as MS A in *M. tinguaensis* **sp. nov.**)

***Mischonyx scaber* (Kirby, 1817) (Figs. 25B, 25D)**

Gonyleptes scaber Kirby, 1819: 453 (3 males & 1 female syntypes; Brazil; NHM 1863.41)

Eugonyleptes scaber: Roewer, 1913: 219; Kury, 2003: 123.

Xundarava holacantha Mello-Leitão, 1927b: 20 (female holotype; Brazil, Rio de Janeiro, Niteroi; MNRJ 1469). Synonymy established by Pinto-da-Rocha *et al.*, 2012.

Weyhia vellardi Mello-Leitão *in litteris*: Soares & Soares, 1987a: 7.

Ilhaia holacantha: Soares & Soares, 1987a: 7, figs 27 –28.

Weyhia absconsa Mello-Leitão, 1932: 284, fig 175; Soares & Soares, 1987: 7 [= *Xundarava holacantha* Mello-Leitão, 1927].(Male holotype; Brazil, Rio de Janeiro, Niteroi; MNRJ 1501). Synonymy established by implication in Pinto-da-Rocha *et al.*, 2012.

Geraeocormobius absconsa: Mello-Leitão, 1940b: 22.

Geraeocormobius absconsus: B. Soares, 1945h: 354; Soares & Soares, 1949b: 167.

Geraeocormobius carioca Mello-Leitão, 1940b: 18, fig 22; Soares & Soares, 1949b: 168; Soares & Soares, 1987: 7 [= *Xundarava holacantha* Mello-Leitão, 1927].

(Male and female syntypes; Brazil, Rio de Janeiro, Rio de Janeiro; MNRJ 53927, lost). Synonymy established by implication in Pinto-da-Rocha *et al.*, 2012.

Mischonyx holacanthus: Kury, 2003: 133.

Diagnosis. *M. scaber* resembles *M. fidelis* by the combinations of following characters: median tubercles on frontal hump whitish when compared to the rest of the body (in ethanol); lateral margin of dorsal scutum with whitish tubercles when compared to the rest of the body (in ethanol); dorsal row of tubercles with an elevation before DBA; DBA with its apex directed anteriorly; no apophysis after DBA on the dorsal row of femur IV; prolateral row with median tubercles bigger than the others in this row; retrolateral row with the biggest apophysis on the apical third. It differs from *M. fidelis* by: lateral margin of dorsal scutum with smaller tubercles when compared to *M. fidelis*; prolateral apophysis on coxa IV with its apex directed dorsally (Fig. 25D) (prolateral apophysis with apex directed posteriorly in *M. fidelis*); retrolateral apophysis on coxa IV visible in dorsal view (not visible in *M. fidelis*); prolateral apophysis on trochanter IV small when compared to *M. fidelis*; retrolateral side of trochanter IV with three big tubercles (small tubercles in *M. fidelis*); DBA small, much smaller than the body height (almost as big as the body height in *M. fidelis*); retrolateral row with tubercles increasing in size from the base to the middle of the row (small tubercles only in *M. fidelis*); after the apophysis on the retrolateral row, there is no big tubercles (two big tubercles in *M. fidelis*).

***Mischonyx spinifrons* (Mello-Leitão, 1923) comb.nov. (Figs. 26A, 26C, 31D –F)**

Weyhia spinifrons Mello-Leitão, 1923: 137; Roewer, 1930: 355; Mello-Leitão, 1932: 283, fig. 173 (Female holotype, Brazil, Rio de Janeiro, Petrópolis; MNRJ, lost)

Geraeocormobius spinifrons: Mello-Leitão, 1940: 21; Soares & Soares, 1949: 172; Soares & Soares, 1987: 7, figs. 23-26.

Weyhia bresslaui Roewer, 1927: 344; 1930: 356, pl. 6, fig. 1; Mello-Leitão, 1931d: 127; 1932: 285, fig. 178; 1933b: 143 (Male and female syntypes; Brazil, Rio de Janeiro, Teresópolis; SMF 1420). Synonymy established by Soares & Soares, 1987.

Geraeocormobius bresslaui: Mello-Leitão, 1940: 21; Soares & Soares, 1949: 168.

Geraecormobiella convexa Mello-Leitão, 1931d: 128, fig 16 (Male lectotype, 5 paralectotypes; Brazil, Rio de Janeiro; Rio de Janeiro; MNRJ 18203). **Syn. nov.**

Geraeocormobius convexus: Soares & Soares, 1949b: 169

Weyhia montis Mello-Leitão, 1935: 389, fig. 15; 1935: 106 (Male holotype, Brazil, Rio de Janeiro, Petrópolis, Independência; MNRJ 42461). Synonymy established by Soares & Soares, 1987.

Geraeocormobius montis: Mello-Leitão, 1940: 21; B. Soares, 1945: 355; Soares & Soares, 1949: 170.

Geraeocormobius cheloides Mello-Leitão, 1940b: 19, fig 23; Soares & Soares, 1987: 4 [= *Geraecormobiella convexa* Mello-Leitão, 1931] (holotype; Brazil, Rio de Janeiro, Rio de Janeiro; MNRJ 58236). **Syn. nov.**

Diagnosis. *Mischonyx spinifrons* **comb. nov.** resembles *Mischonyx tinguaensis* **sp. nov.** by the combinations of following characters: anterior margin of dorsal scutum with two tubercles on each side; tubercles on mesotergal area III, besides the median ones, elliptic; lateral margin of dorsal scutum with the most posterior lateral tubercles fused (forming

bigger tubercles); all free tergites with small tubercles; retrolateral apophysis on coxa IV apparent on dorsal view; dorsal row on leg IV with a tubercle anterior to the DBA; retrolateral row on leg IV with a large median apophysis; ventral plate with three pairs of apical MS C. It differs from *Mischonyx tinguaensis* **sp. nov.** by: median tubercles on mesotergal area III strongly compressed (elliptic but not strongly compressed laterally in *Mischonyx tinguaensis* **sp. nov**); lateral margin of dorsal scutum with small tubercles (big in *Mischonyx tinguaensis* **sp. nov**); prolateral apophysis on coxa IV smaller than trochanter IV (approximately with the same length in *Mischonyx tinguaensis* **sp. nov**); DBA not branched (branched in *Mischonyx tinguaensis* **sp. nov**); dorsal row of tubercles of leg IV with three big tubercles after DBA (without big tubercles after DBA in *Mischonyx tinguaensis* **sp. nov**); retrolateral row of leg IV with big tubercles (small in *Mischonyx tinguaensis* **sp. nov**); MS B reduced much smaller than MS A (as big as the the MS A in *Mischonyx tinguaensis* **sp. nov**); MS A forming a triangle and hidden behind the ventral process (forming a dorso-ventral line and apparent in *Mischonyx tinguaensis* **sp. nov.**); *flabelum* with smooth ends (serrated in *Mischonyx tinguaensis* **sp. nov**).

***Mischonyx squalidus* Bertkau, 1880 (Figs. 26B, 26D, 31G –I)**

Mischonyx squalidus Bertkau, 1880: 107, pl.2, fig. 38; Roewer, 1913: 468; 1923: 584; Soares & Soares, 1949: 221; Pinto-da-Rocha *et al.*, 2012: 52 (Female holotype; Brazil, Rio de Janeiro, Copacabana; ISNB)

Ilhaia cuspidata Roewer, 1913: 221 (Male holotype; Brazil, Rio de Janeiro, Ilha Grande, SMF 900). **Syn.nov.**

Jlhaia cuspidata: Roewer, 1930: 363 misspelling*)*.

Mischonyx cuspidatus: Kury 2003: 133; Pinto-da-Rocha *et al.* 2012: 53; Pinto-da-Rocha *et al.*, 2014: 4, 16 –18.

Ilhaia fluminensis Mello-Leitão, 1922: 334; B. Soares, 1943: 56 [= *Ilhaia cuspidata* Roewer, 1913] (13 syntypes; Brazil, Rio de Janeiro, Piraí; MZSP 503) **Syn.nov.**

Jlhaia fluminensis: Roewer, 1930: 363, fig 4*(lapsus calami)*.

Gonazula gibbosa Roewer, 1930: 418, fig. 32; Pinto-da-Rocha *et al.*, 2012: 53 [= *Ilhaia cuspidata* Roewer, 1913] (Male holotype, Brazil, Santa Catarina, Serra Azul. SMF 1328). **Syn.nov.**

Eduardoius granulosus Mello-Leitão, 1931a: 95; B. Soares, 1944: 171 [= *Ilhaia cuspidata* Roewer, 1913] (holotype; Brazil, Rio de Janeiro, Piraí; MNRJ 1479). **Syn.nov.**

Ilhaia granulosa: B. Soares, 1943f: 56.

Giltaya solitaria Mello-Leitão, 1932: 467; Kury, 2003: 133 [= *Ilhaia cuspidata* Roewer, 1913] (Male holotype; Brazil, Rio de Janeiro, Rio de Janeiro. MNRJ 1473). **Syn.nov.**

Eduardoius lutescens Roewer, 1943: 44; Soares & Soares, 1970: 340 [= *Ilhaia cuspidata* Roewer, 1913] (Male and female syntypes; Brazil, Rio de Janeiro, Mendes. SMF 5392/58). **Syn.nov.**

Ilhaia lutescens: B. Soares, 1943f: 56.

Taxonomic remarks: Vasconcelos (2003, unpublished data) proposed this new combination in his dissertation. In this research, we have analyzed Bertkau's original drawing (Bertkau, 1880, fig. 38) and the original description for *M. squalidus*. We could not analyze the holotype because it is lost. The collection in which it was deposited is at the

Institut Royal des Sciences Naturelles de Belgique. Part of the description translated from German is presented below:

"... The first abdominal dorsal segment is almost fused with the thorax, and in general the articulation skin between each segment is not very flexible. **The first three [abdominal] segments have in their superior part a line of "dots", of which the median ones stand out in height, like little spines**." (Bertkau, 1880, pp. 107)

By this excerpt, it is possible to conclude that possibly the only species which has one median armature on each free tergite in females and juveniles in the region Bertkau collected the specimen (Copacabana, Rio de Janeiro) is the traditionally called *M. cuspidatus*. Therefore, we propose that *Ilhaia cuspidata* is a junior synonym of *M. squalidus.* We know the holotype is a juvenile by the image in Bertkau (1880), by Roewer (1923), where the author states that the specimen is a juvenile, and by Kury (2003).

Diagnosis. *M. squalidus* resembles *M. spinifrons* **comb. nov.** by the combinations of following characters: lateral margin of dorsal scutum with whitish tubercles (in ethanol); posterior tubercles on lateral margin of dorsal scutum fused; retrolateral apophysis of coxa IV visible on dorsal view; DBA with apex directed anteriorly; dorsal row on femur IV with three tubercles after DBA, on the distal half; retrolateral row on femur IV with median apophysis more developed than the others in this row; ventral side of ventral plate without microsetae on the distal half; lateral projections of ventral plate projected dorsally and behind the ventral projection of the glans; MS A forming a triangle; MS B reduced; apical groove of ventral plate reaching the line of the most basal MS C. It differs from *M. spinifrons* **comb. nov.** by: median tubercles on mesotergal area III strongly compressed and big (small and elliptic but not strongly compressed laterally in *M. spinifrons* **comb. nov.**); prolateral apophysis on coxa IV approximately with the same length of trochanter IV (smaller in *M. spinifrons* **comb. nov.**); Free Tergites I – III with median apophysis (without median apophysis in *M. spinifrons* **comb. nov.v**); prolateral row with median tubercles bigger than the others in this row (all tubercles with the same size in *M. spinifrons* **comb. nov.**); retrolateral row on femur IV with several (7 – 8) big tubercles basal to the median apophysis (three tubercles basal, followed by a gap and one tubercle after this gap in *M. spinifrons* **comb. nov.**).

New Species Description

***Mischonyx minimus* sp. nov.**
(Figures: 15, 18A –C, 23A and 23C)

Type material. BRAZIL. Rio de Janeiro: Teresópolis (Parque Nacional da Serra dos Órgãos, Barragem Beija-flor, 22°26'16.4"S 43°36'35.4"W), C. Gueratto & M. Abrão leg., 29.VII.2017, male holotype (MZSP); same data, males and females paratypes, (IBSP); same data, A. Benedetti *et al.* leg., 30.IV.2014.
Etymology. From the Latin adjective *minimus*, *a, um* meaning small, little. This is due to its reduced size when compared to other *Mischonyx* species, specially *Mischonyx arlei* **comb.nov.**, sister species of *M. minimus* **sp. nov.**.

Diagnosis. *Mischonyx minimus* **sp. nov.** resembles *M. arlei* **comb. nov.** by the combinations of following characters: mesotergal area I with a pair of well-developed median tubercles, which are clearer (whitish) than the rest of the body (dark brown); median armatures on mesotergal area III are spines; lateral margin of dorsal scutum with several small tubercles; free tergite II with a well-developed median apophysis; prolateral apophysis on coxa IV small and pointing posteriorly; retrolateral side of trochanter IV with two tubercles; femur IV with several small apophyses on dorsal and retrolateral row of tubercles; femur IV with a well-developed apical tubercle on prolateral and retrolateral rows of tubercles; ventral plate of penis with three subdistal MS C on each side; MS B smaller than MS A; *flabellum* with serrated ends. It differs from *M. arlei* **comb. nov.** by: its reduced size (3 – 3.5 mm) (7 – 8 mm in *M. arlei* **comb. nov.**); mesotergal area II with median tubercles whitish and as large as the median tubercles on mesotergal area I (dark brown and smaller than the ones on mesotergal area I in *M. arlei* **comb. nov.**); basitarsus II with four segments (seven in *M. arlei* **comb. nov.**); leg IV not curved (straight) in dorsal view (curved in *M. arlei* **comb. nov.**); MS D well-developed (reduced in *M. arlei* **comb. nov.**).

Description. Male holotype: *Dorsum* (Figs. 15, 23A, 23C): Measurements: Dorsal scutum: L: 3.2; W:2.9; Prosoma: L:1.3; W: 1.6. Femur IV: 4.4. Scutum outline γP, widest at mesotergal area II. Anterior margin of carapace with three tubercles on each side, with approximately the same size. Frontal hump high, with two spines of the same color from the rest of the body (in ethanol), curved one to the other. Anterior region of the ocularium smooth, ocularium with one pair of median tubercles (as tall as the ocularium height). Posterior region of the ocularium with one pair of small tubercles, right behind the median tubercles. Lateral margin of prosoma with numerous small tubercles. Posterior part of prosoma with a pair of tubercles. Besides these tubercles, prosoma has a low density of granules. Dorsal scutum divided into three mesotergal areas, with low density of granules (DaSilva & Pinto-da-Rocha, 2010). Areas; Area I divided by a median longitudinal groove, with a pair of whitish big median tubercles and no granules; area II with a pair of large whitish median tubercles, with the same size of the tubercles on Area I without granules; Area III with a pair of dark median sharp spines, smaller than the other armatures on other mesotergal areas, a pair of tubercles posterior to the median spines. Lateral margins of dorsal scutum with a row of small tubercles, with the same approximate size, extending from the middle of area I until the posterior margin of Area III; no fusion of tubercles. Posterior margin of dorsal scutum with a line of small tubercles. Free tergite I with a line of small tubercles of the same approximate size. Free tergite II with a big sharp median apophysis and two large tubercles, lateral to the median apophysis; free tergite III with a line of small tubercles. Dorsal anal operculum with small sparse tubercles. *Venter*. Coxa I with several sparse tubercles, larger than the ones in other coxa. Coxa II with sparse numerous granules. Coxa III with an anterior and a posterior basal-apical row of tubercles; coxa IV with sparse numerous granules. Ventral anal operculum with granules. *Chelicerae*. Segment II with several setae, mainly in the apical part. Fix and movable fingers with seven teeth each. *Pedipalps*. Venter of trochanter with few sparse tubercles; tibia setation: prolateral IIi, retrolateral IiIi. Tarsal setation: prolateral IiI, retrolateral III, ventral side with two baso-apical lines of setae. *Legs*. Leg I: trochanter with several ventral tubercles, femur, patella and tibia with granules. Leg II: Trochanter II with several ventral tubercles; femur, patella and tibia with granules. Leg III: trochanter with several ventral tubercles; femur,

patella and tibia with granules; Leg IV: Coxa IV: robust apical oblique prolateral apophysis, smaller than the trochanter size; large retrolateral apophysis, visible in dorsal view. Trochanter IV: prolateral small blunt apophysis; retrolateral side with a line of three big tubercles, two slightly more ventral. Femur IV: long, thin and straight; all tubercles on prolateral row with approximately the same size; DBA small, unbranched, conic, sharp, pointing upwards; dorsal row with several small tubercles after DBA; retrolateral row of with several small tubercles and two more developed tubercles on the apical half; all tubercles on the ventral row small. Tarsal formula: 6(3)-6(3)-4-5. *Male genitalia* (Figs. 18A –C). Ventral plate: Ventral face with microsetae on its whole extension; pronounced apical groove (reaching the line of the first basal MS C); lateral lobes basal when compared to other species (e.g. *Mischonyx intervalensis* **sp. nov.**); three sub-apical helicoidal MS C on each side; two MS E, ventral and in the same baso-apical orientation of MS C; long MS D when compared to other species (e.g. *Mischonyx intervalensis* **sp. nov.**), basal relative to MS C and in the same dorso-ventral orientation of MS C; three spatular MS A, forming a diagonal baso-apical line; one reduce MS B, much smaller than MS A. Glans: Small dorsal process; flabelum triangular, with serrated apex; stylus with subapical microsetae, with the apex inclined relative to the penis axis and keeled. *Color*. Dark brown; pedipalps and trochanters I –III yellow.

Female. Unknown.

***Mischonyx intervalensis* sp. nov.**
(Figs. 16, 18D –F, 22A and 22C)

Type material. BRAZIL. São Paulo: Ribeirão Grande (Parque Estadual Intervales, 24°15'27.1"S 48°16'23.0"W), C. Gueratto *et al.* leg., 25.III.2017, male hololtype (MZSP); same data, males and females paratypes (IBSP); ditto males and females paratypes (MNRJ); same data, Ribeirão Grande (Parque Estadual Intervales, 24°15'27.1"S 48°16'23.0"W), F. Carbayo *et al*. Leg., 12 – 14.XII.2008, males and females paratyes (SMF).
Etymology. Species name derives from “Intervales", due to its first collecting locality, Parque Estadual Intervales, type and only locality registered for this species + the suffix -*ēnsis*, -*ēnse*, in order to form an adjective.

Diagnosis. It resembles *Mischonyx anomalus* by the combinations of following characters: Anterior margin of dorsal scutum with two tubercles on each side; Areas we and II with small median tubercles; area III with well-developed and elliptic median tubercles; other tubercles on area III are rounded; all free tergites with small tubercles; retrolateral row of leg IV with a big median apophysis; retrolateral row of leg IV with several well-developed tubercles. It differs from *M. anomalus* by: prolateral apophysis of coxa IV with ventral process and basal tubercle (not present in *M. anomalus*); retrolateral side of trochanter IV with three tubercles (one in *M. anomalus*); DBA of leg IV branched and the dorsal branch is the biggest (not branched in *M. anomalus*); one apophysis on the dorsal row of tubercles of leg IV after DBA (three in *M. anomalus*); tubercles on prolateral row of tubercles on leg IV small and with the same size (median tubercles bigger in *M. anomalus*); ventral plate with the same approximate height and width (square-shaped) (higher than wider in *M. anomalus*); lateral processes of the ventral plate medial (basal in *M. anomalus*).

Description. Male holotype: *Dorsum* (Figs. 16, 22A and 22C): Measurements: Dorsal scutum: L: 4.5; W:4.6; Prosoma: L:1.8; W: 2.4. Femur IV: 3.9. Scutum outline γP, widest at area II. Anterior margin of carapace with two tubercles on each side, with approximately the same size. Frontal hump high, with two tubercles of the same color from the rest of the body (in ethanol). Anterior face of the ocularium with one pair of tubercles, one pair of median tubercles/spines (taller than the ocularium height). Anterior face of the ocularium with one pair of small tubercles, right before the eyes. Lateral margin of prosoma with numerous small tubercles. Posterior part of prosoma with a pair of tubercles. Besides these tubercles, prosoma has a low density of granules. Dorsal scutum; Area I divided by a median longitudinal groove, with a pair of dark median tubercles and few sparse granules; Area II with a pair of dark median tubercles slightly larger than the tubercles on Area I and few sparse granules; Area III with a pair of dark median elliptic tubercles, larger than the ones on the other mesotergal areas, a pair of rounded tubercles posterior to the median elliptic ones and few sparse granules. Lateral margins of dorsal scutum with a row of small tubercles, increasing in size posteriorly and from sulcus I to the posterior margin of area III; no fusion of tubercles. Posterior margin of dorsal scutum with a line of small tubercles, with the median ones slightly larger than the rest. Dorsal scutum with medium density of granules. Free tergites I–II with a line of small tubercles of the same approximate size. Free tergite III with a row of tubercles larger than the ones on the other free tergites and the central tubercle slightly bigger than the others. Dorsal anal operculum with small sparse tubercles. *Venter*. Coxa I with several sparse tubercles, bigger than the ones in other coxae. Coxae II–IV with sparse numerous granules. Ventral anal operculum with granules. *Chelicerae*. segment II with several setae, mainly in the apical part. Fixed finger with eight and movable finger with 12 teeth. *Pedipalps*. Ventral side of trochanter with few sparse tubercles; tibia setation: prolateral IiIi, retrolateral IiI. Tarsal setation: prolateral IiI, retrolateral II, ventral side with two baso-apical lines of setae. *Legs*. Leg I: trochanter, femur, patellae and tibia with granules. Leg II: Trochanter II with two retrolateral tubercles; femur, patella and tibia with granules. Leg III: trochanter, femur, patella and tibia with granules. Leg IV: coxa IV: robust apical prolateral apophysis, slightly inclined relative to the axis of the base of coxa IV, with ventral process and basal tubercle, with the approximate trochanter size; retrolateral apophysis small, not visible in dorsal view. Trochanter IV: prolateral small blunt apophysis; retrolateral side with a line of three big tubercles, two slightly more ventral. Femur IV: short and robust; all tubercles on prolateral row with approximately the same size; dorsal row of tubercles with a large tubercle before the DBA, DBA branched with the largest branch pointing upwards, one large tubercle after DBA; retrolateral row of with a big median apophysis, eight large tubercles before, three large (yet smaller than the ones anterior to the median apophysis) and three small tubercles posterior to the median apophysis, intercalated; all tubercles on the ventral row small. Tarsal formula: 3(3)-7(3)-4-5. *Male genitalia* (Fig. 18D –F). Ventral plate: Ventral face with microsetae on the whole extension; pronounced apical groove (reaching the line of the most basal MS C); lateral process median when compared to other species (e.g. *Mischonyx tinguaensis* **sp. nov.**); three apical helicoidal MS C on each side; two MS E, ventral and in the same baso-apical orientation of MS C; one small MS D, basal relative to MS C and in the same dorso-ventral orientation of MS C; three spatular MS A, forming a parable line; one spatular MS B, smaller than MS A. Glans: Small dorsal process; flabellum triangular, with serrated margin; stylus with subapical microsetae, with the apex inclined relative to

the penis axis and keeled. *Color*. Brown; dorsal scutum with yellowish tones; pedipalps and trochanters I– III yellow.

Female. (paratype; MZSP): Measurements: Dorsal scutum: L: 4.2; W: 4.0. Prosoma: L: 1.3; W: 2.0; Femur IV: L: 3.9. Dorsal scutum outline α, with a constriction at the area III and evident *coda*; small median tubercles on each area; median tubercles on area III rounded; lateral tubercles of the dorsal scutum small and the most posterior are not fused; absence of prolateral and retrolateral apophysis on coxa IV; trochanter and femur IV unarmed.

***Mischonyx tinguaensis* sp. nov.**
(Figs. 17, 18G – I, 27A, 27B)

Type material. BRAZIL. Rio de Janeiro: Nova Iguaçu, (Reserva Biológica Tinguá/ RPPN CEC/Tinguá, 22°35'23.9"S 43°26'25.7"W), C. Sampaio, F. Uemori & C. T. Olivares leg., 04 –06.IV.2012, male holotype (MZSP).
Etymology. Species name derives from "Tinguá", due to its first collecting locality, Reserva Biológica Tinguá, type and only locality registered for this species + the suffix -*ēnsis*, -*ēnse*, in order to form an adjective.
Diagnosis. It resembles *Mischonyx spinifrons* **comb.nov.** by the combinations of following characters: anterior margin of dorsal scutum with two tubercles on each side; several tubercles on area III elliptical; lateral margin of dorsal scutum with the most posterior lateral tubercles fused (forming bigger tubercles); all free tergites with small tubercles; retrolateral apophysis on coxa IV apparent on dorsal view; dorsal row on leg IV with a tubercle anterior to the DBA; retrolateral row on leg IV with a big median apophysis; ventral plate with three pairs of apical MS C. It differs from *M. spinifrons* **comb.nov.** by: median tubercles on area III elliptic but not strongly compressed laterally (strongly compressed in *M. spinifrons* **comb.nov.**); large tubercles on lateral margin of dorsal scutum (small in *M. spinifrons* **comb.nov.**); prolateral apophysis on coxa IV approximately with the same length of trochanter IV (smaller in *M. spinifrons* **comb.nov.**); DBA branched (not branched in *M. spinifrons* **comb.nov.**); dorsal row of tubercles of leg IV without large tubercles after DBA (three large tubercles after DBA in *M. spinifrons* **comb.nov.**); tubercles on the basal half of the retrolateral row of leg IV small (some are big in *M. spinifrons* **comb.nov.**); MS B as large as the MS A (reduced in *M. spinifrons* **comb.nov.**); MS A forming a dorso-ventral line and apparent (forming a triangle and hidden behind the ventral process); *flabellum* with serrated on margin (smooth in *M. spinifrons* **comb.nov.**).
Description. Male holotype: *Dorsum* (Figs. 17, 27A, 27B): Measurements: Dorsal scutum: L: 4.1; W:4.2; Prosoma: L:1.6; W: 2.1. Femur IV: 4.0. Scutum outline γP, widest at mesotergal area II. Anterior margin of carapace with two tubercles on each side, with approximately the same size. Frontal hump high, with two whitish tubercles (in ethanol). Anterior face of the ocularium with one pair of tubercles, one pair of median tubercles (as tall as the ocularium height). Lateral margin of prosoma with numerous small tubercles. Posterior part of prosoma with a pair of tubercles. Besides these tubercles, prosoma has a low density of granules (DaSilva & Pinto-da-Rocha, 2010). Dorsal scutum: area I divided by a median longitudinal groove, with a pair of dark median tubercles; area II with a pair of dark median tubercles slightly larger than the tubercles on area I; area III with a pair of dark median elliptic tubercles, larger than the ones on the other areas, and some sparse elliptic

tubercles. Lateral margins of dorsal scutum with a row of whitish (in ethanol) big tubercles, reaching the posterior margin of area III; most posterior tubercles fused, forming large tubercles. Posterior margin of dorsal scutum with a line of white (in ethanol) small tubercles of similar size. Dorsal scutum with low density of granules. All free tergites with a line of small tubercles of the same approximate size. Dorsal anal operculum with small sparse tubercles. *Venter*. Coxa I with several sparse tubercles, larger than the one in other coxa. Coxa II with sparse tubercles; the apical are larger. Coxae III and IV with granules. Ventral anal operculum with granules. *Chelicerae*. Middle segment with several setae, mainly in the apical part. Fixed and movable fingers with nine teeth each. *Pedipalps*. Tibia setation: prolateral IiIi, retrolateral IiI. Tarsal setation: prolateral II, retrolateral II, ventral side with two baso-apical lines of setae. *Legs*. Leg I: trochanter, femur, patella and tibia with granules. Leg II: Trochanter II with two retrolateral tubercles; femur, patella and tibia with granules. Leg III: trochanter, femur, patella and tibia with granules. Leg IV: Coxa IV: robust apical transversal prolateral apophysis, with ventral process, with the approximate trochanter size; retrolateral apophysis visible in dorsal view. Trochanter IV: prolateral small blunt apophysis; retrolateral side with small tubercles. Femur IV: short and robust; all tubercles on prolateral row with approximately the same size; dorsal row of tubercles with a large tubercle before the DBA, DBA branched with the largest branch pointing upwards, small tubercles after DBA; retrolateral row of with a big median apophysis, four big tubercles before and three large tubercles posterior to the median apophysis; all tubercles on the ventral row small. Tarsal formula: 4(3)-8(3)-8-5. *Male genitalia* (Fig. 18G – I). Ventral plate: Ventral face with microsetae on basal 2/3; pronounced apical groove (reaching the line of MS B); lateral process basal when compared to other species (e.g. *Mischonyx intervalensis* **sp. nov.**); three apical helicoidal MS C on each side; two MS E, ventral and slightly basal relative to MS C; small MS D, basal relative to MS C and between MS E and MS C; four spatular MS A, forming a diagonal baso-apical line; one spatular MS B, with the same size of MS A. Glans: Small dorsal process; flabellum triangular with serrated margin; no information regarding stylus (broken in the analyzed specimen). *Color*. Brown; dorsal scutum with tones of yellow; pedipalps and trochanters I–III yellow. *Female*. (paratype; MZSP XXXXX): Measurements: Dorsal scutum: L: 3.9; W: 3.4. Prosoma: L: 1.5; W: 2.0; Femur IV: L: 3.8. Dorsal scutum outline α, with a constriction at the chelicerae, area III and evident *coda*; small median tubercles on each area; median tubercles on Area III rounded; lateral tubercles of the dorsal scutum small and the most posterior are not fused; absence of prolateral apophysis on coxa IV, but with a small retrolateral apophysis; trochanter and femur IV unarmed.

***Gonyleptes* Kirby, 1818**

Gonyleptes Kirby, 1818: 450 (type species *Gonyleptes horridus* Kirby, 1818, by subsequent designation, Roewer, 1913)

Anoploleptes Piza, 1940: 56; B. Soares, 1943: 53; Kury, 2003: 133 [= *Mischonyx* Bertkau, 1818] (type species *Anoploleptes dubium* Piza, 1940, by original designation).

REMARKS: We reestablished *Anoploleptes* as a subjective junior synonym of *Gonyleptes* as first established by B. Soares (1943).

***Gonyleptes antiquus* Mello-Leitão, 1934**

Gonyleptes antiquus Mello-Leitão, 1934: 415. fig.6; 1935: 106. B. Soares, 1943: 53 (Male holotype; Brazil, São Paulo; IBSP 11).
Paragonyleptes antiquus: B. Soares, 1945: 11, fig.1.
Mischonyx antiquus: Kury, 2003: 133.
Anoploleptes dubium Piza, 1940: 56, fig. 4. (Male holotype; Brazil, São Paulo, Juquiá; MZSP 401).

REMARKS: *Gonyleptes antiquus* returns to its former genus, so the original combination is reestablished (see discussion below).

Identification key for Mischonyx males

1. Median armature on area I larger and lighter (in ethanol) than those on a area III (lighter than the general body color) 2
   Median armature on area I smaller and with the same color (in ethanol) of those on area III (lighter than the general body color) 3
2. Small individuals (3 –3.5 mm of dorsal scutum lenght); median armature on area II with same color (in ethanol) those on area I (lighter than general body color) ..... *Mischonyx minimus* **sp. nov.**
   Large individuals (7 – 8 mm of dorsal scutum lenght); median armature on area II with same color (in ethanol) of those on area III (darker than the body color) ..... *Mischonyx arlei*
3. More posterior lateral mid-bulge tubercles fused, forming larger tubercles, clearer than the rest of the body color 4
   Lateral mid-bulge tubercles not fused 6
4. Ellipsed tubercles on mesotergal area III strongly laterally compressed; only one clearly more developed apophysis on leg IV retrolateral row of tubercles ..... *Mischonyx spinifrons*
   Ellipsed tubercles on area III not strongly compressed laterally; more than one developed apophysis on leg IV, with retrolateral row of tubercles 5
5. DBA digitiform and uniramous ..... *Mischonyx poeta*
   DBA birramous ..... *Mischonyx tinguaensis* **sp. nov.**
6. At least one mesotergal area with well-developed median armature 7
   Mesotergal areas with small tubercles with the same size 9
7. All mesotergal areas and posterior part of dorsal scutum with well-developed median armature ..... *Mischonyx squalidus*
   Mesotergal areas II –III only with well-developed median armature 8
8. DBA branched, retrolateral branch being the largest; prolateral row of tubercles on leg IV with medial tubercles more developed ..... *Mischonyx processigerus*
   DBA falciform, not branched and; prolateral row of tubercles on leg IV with tubercles of the same size ..... *Mischonyx insulanus*
9. Median tubercles on mesotergal area III small 10
   Median tubercles on mesotergal area III well-developed 11
10. Leg IV robust, with well-developed armature; DBA well-developed; dorsal row of tubercles from leg IV with four well-developed tubercles after DBA; recordedfrom Santa

Catarina state ..... *Mischonyx clavifemur*

Leg IV long and thin, with few well-developed armatures located terminally; DBA small and sharp; without dorsal row of tubercles after DBA ..... *Mischonyx intermedius*

11. DBA branched 12

DBA not branched 13

12. Retrolateral branch of DBA evidently larger than other branch; two apophysis on the leg IV dorsal row of tubercles, after DBA; prolateral apophysis of coxa IV with a prominent ventral process ..... *Mischonyx intervalensis* **sp. nov.**

Both branches of DBA of the same size; two well-developed apophysis on leg IV retrolateral row of tubercles ..... *Mischonyx reitzi*

13. DBA robust and sharp, with a tubercle emerging from its median part and almost as high as the whole body 14

DBA smaller than the body height 15

14. DBA pointing upwards; after DBA, only one well-developed tubercle on the dorsal row ..... *Mischonyx parvus*

DBA pointing anteriorly; no well-developed tubercles on the dorsal row, after the DBA; lateral mid-bulge tubercles clearer than the general body color (in ethanol) …..... *Mischonyx fidelis*

15. DBA with the same approximate size of the other tubercles on the dorsal row .... *Mischonyx kaisara*

DBA more developed than the tubercles on the dorsal row ..... *Mischonyx anomalus*

One extra row of tubercles between dorsal and prolateral rows; median tubercles on Leg IV prolateral row of tubercles more developed; one apophysis on the leg IV terminal third of the retrolateral row of tubercles ..... *Mischonyx scaber*

Discussion

Biogeographical remarks

In general, harvestmen present a high degree of endemism in the Atlantic Forest (Pinto-da-Rocha, Da Silva & Bragagnolo, 2005). Species distributions throughout the order are restricted to specific areas of few thousands of square kilometers, with few exceptions (Pinto-da-Rocha, Da Silva & Bragagnolo, 2005). Most species of *Mischonyx* agree with this pattern. One of these exceptions is *M. squalidus*. There are records of this species from Espirito Santo until Rio Grande do Sul states, occurring not only in Atlantic Rainforest but also in cerrado areas (Figs. 01 –03), which are considerably drier than the Atlantic Rain Forest (Resende, Pinto-da-Rocha & Bragagnolo, 2012). Mestre & Pinto-da-Rocha (2004) demonstrated that this species presents anthropic behavior, being found, for example, in residential areas and planting sites. Probably this anthropic behavior helps the species to disperse and colonize new areas more efficiently than most of harvestmen species.

Looking at the distribution area of each species, it is clear that most of *Mischonyx* species have their records restricted to only one or few points, close to each other. Apparently, most of its species present a high degree of endemism, as other harvestmen (Da Silva, Pinto-da-Rocha & Morrone, 2017). Serra do Órgãos, Mantiqueira, south coast of Rio de Janeiro and Serra do Mar areas of endemism hold 11 from the 16 species of the genus. According to Pinto-da-Rocha, Da Silva & Bragagnolo (2005) and Da Silva, Pinto-da-Rocha

& Morrone (2017), south coast of Rio de Janeiro and Serra dos Órgãos areas are the most species rich, which agrees with the data found in this research. This is important information for conservational matters, once the few remaining harvestmen habitats that still exist are suffering by anthropic pressure (Morellato & Haddad, 2000) and, to maintain the diversity of the whole group, these areas deserve better attention regarding the creation of new protected areas (Da Silva, Pinto-da-Rocha & Morrone, 2017, Nogueira *et al.* 2019a, b).

Divergence time of Mischonyx clade

Given that there are no significant differences on the relationships of the internal branches between B1 and the TE analyses (MP3 and ML3) and that Bayesian is the only optimality criteria capable of estimating divergence time, we are going to work with B1 hypothesis to discuss divergence time and biogeography.

There are two other published articles using different genus of Atlantic Forest harvestmen, both gonyleptids, and dating the divergence time of clades: Bragagnolo *et al.* (2015), which used *Promitobates* as study object, and Peres *et al.* (2019), analyzing *Sodreana*. The divergence time of *Mischonyx* (~50Mya) agrees with that of *Promitobates*. *Sodreana* has divergence time more recent than the other two (~35.5 Mya). *Sodreana* occurs in a more restricted area when compared to the other two genera. While it occurs from Paraná until the southern limit of Serra do Mar de São Paulo, *Promitobates* occurs from Santa Catarina until the northern edge of São Paulo state and *Mischonyx* occurs from Santa Catarina until northern Rio de Janeiro state (excluding *M. squalidus* range, which is wider). Hence, this wider distribution from the last two genera when compared to *Sodreana* could be related to their older diversification.

As stated by Da Silva, Pinto-da-Rocha & Morrone (2017), "The main geographical barriers associated with the general historical patterns are the Valleys of the Doce, Paraıba do Sul, and Ribeira do Iguape Rivers and the Todos os Santos Bay". Within *Mischonyx* genus, the split between the two major lineages occurred at ~45 Mya, agrees with the beginning of formation of Valley of Ribeira do Iguape river, 50 –56 Mya (Almeida & Carneiro, 1998; Pinto-da-Rocha, Da Silva & Bragagnolo, 2005; Da Silva, Pinto-da-Rocha & Morrone, 2017).

In one of those lineages, the split dividing species from SMSP from the species from SSP, PR and SC occurred at ~48 Mya, which could have occured by the rise of Serra do Mar (65 –50 Mya) (Almeida & Carneiro, 1998; Pinto-da-Rocha, Da Silva & Bragagnolo, 2005). Still inside this lineage, the split between *M. intervalensis* **sp. nov.**, species occurring at the north of Ribeira do Iguape River (SSP AoE), from the species from the south of this river (PR and SC AoE) occurs at ~28 Mya. This split agrees with Peres *et al.* (2019) findings regarding the split of *Sodreana* species from the north and south of this valley. After the formation of the valley, it passed through uplift and denudation events persisting from Upper Cretaceous to the Paleogene/ Neogene (Franco-Magalhães *et al.*, 2010; Franco-Magalhães, Hackspacher & Glasmacher, 2010), a period that agrees with the split cited above.

Inside the other lineage, the first split occurs at ~45 Mya, diverging *M. intermedius* from the remaining species. This species is the only one from Esp AoE and probably the distensive tectonic activity from the tertiary period, which separates Rio Doce, Paraíba do

Sul and São Francisco basins (Cherem *et al.*, 2012; Morais *et al.*, 2005) have isolated it from the sister species from Org, LSRJ and Mnt AoE. Many other studies with different taxa corroborate the relevance of Doce River disjunction in shaping biogeographical patterns (Müller, 1973; Prance, 1982; Amorim & Pires (1996); Pellegrino *et al.*, 2005; Sigrist & Carvalho 2009; Brunes *et al*., 2010; Thomé *et al*., 2010; Silva *et al*., 2012; Cabanne *et al*., 2014; Da Silva, Pinto-da-Rocha & Morrone, 2017). Afterwards, the split of *M. processigerus* (Mnt AoE) from species from LSRJ and Org occurred at ~29 Mya, agreeing with the formation of Paraíba do Sul valley and its change of course, during Oligocene-Miocene (Almeida & Carneiro, 1998; Pinto-da-Rocha, Da Silva & Bragagnolo, 2005; Cherem *et al.*, 2012)

In general, the divergence time of *Mischonyx* species are older than 5 Mya (excepting *M. clavifemur* **comb.nov.** diverging from *M. reitzi* **comb.nov.** and *M. parvus* **comb.nov.** diverging from *M. squalidus*), which agrees with *Promitobates* speciation events (Bragagnolo *et al.*, 2015). Authors who support the Pleistocene refugia hypothesis, propose that it happened at ~5 Mya (Ravelo *et al*., 2004, Carnaval & Moritz, 2008; Carnaval *et al.*, 2009; Holbourn *et al*., 2014). Therefore, the ancient cooling in Miocene/Pliocene probably have shaped most of the divergences between species inside the genus and the Pleistocene refugia contributed in the most recent speciation events to shape the extant diversity.

Finally, it is important to stress that *M. squalidus* appears in all analyses using molecular and TE as sister to *M. parvus* **comb.nov.**, inside the clade with species from LSRJ. So, it is reasonable to state that it probably diverged at this AoE in the past and, posteriorly, spread all over the Atlantic Forest and Cerrado areas, as discussed in the preview session. Therefore, from now on, in discussions regarding the AoE and the relationship among clades, we will consider *M. squalidus* as belonging to LSRJ AoE.

The hypothesis of TE under maximum likelihood as the optimality criteria (ML3)

We choose ML3 grounded in the following arguments.

In MP3, *M. tinguaensis* **sp. nov.** presents more than 30 autapomorphies. This represents almost a third of all morphological characters. Given the number of morphological changes in the other branches and even looking at morphological changes in other harvestmen research (Bragagnolo & Pinto-da-Rocha, 2012; Da Silva & Gnaspini, 2010; Da Silva & Pinto-da-Rocha, 2010; Pinto-da-Rocha & Bragagnolo, 2010), it seems unlikely that this single species has passed through genetic drift or selection that would have changed the lineage that much. Therefore, the hypothesis of ML3 seems less improbable.

Moreover, *M. tinguaensis* **sp. nov.**, in MP3 is inside a clade formed strictly by *M. spinifrons* **comb.nov.**, while in ML3 it is in a separated lineage, diverging after *M. processigerus*. By the *M. tinguaensis* **sp. nov.** position in MP3, *M. spinifrons* **comb.nov.** would not be monophyletic. This makes no morphological sense, once *M. tinguaensis* **sp. nov.** has too many apomorphies and separates *M. spinifrons* **comb.nov.** individuals that do not have any morphological divergence to each other. Inside the clade formed by *M. kaisara* and *M. insulanus* there is a similar issue. While in ML3 all individuals of *M. kaisara* are clustered together and *M. insulanus* as well, in MP3, the *M. insulanus* taxa are separating *M. kaisara* taxa, making this last species polyphyletic. Therefore, we think it

makes no sense to separate taxa which do not differ morphologically.

Finally, in MP3, the clade with species from Esp, Mnt, Org and LSRJ has no morphological characters supporting it. The *Mischonyx* clade itself is supported only by one morphological characteristic. Wipfler *et al.* (2015) support the idea that, in the field of phylogenetics, morphology is still important even with phylogenomic datasets, once "it provides independent data for checking the plausibility of molecular (...). It is the necessary basis for reconstructing character evolution on the phenotypic level and for developing complex evolutionary scenarios.". This is supported by Lee & Palci (2015) and Giribet (2015) as well. Hence, due to the lack of morphological character states supporting the nodes of interest in the MP3 analysis, the alternative hypothesis in ML3 is preferred, because its additional support in the form of morphology characters and by its topology, which does not separate morphologically identical taxa belonging to the same species. This convergence in data types, molecular and morphological, shows that the ML3 hypothesis should take priority.

Diagnosis of previews authors

Vasconcelos (2005a) describes some characteristics of *Mischonyx*, but does not propose a diagnosis for the genus. He only states that the genus would probably have two diagnostic characters: yellowish-reddish tubercles on lateral margin of mid-bulge and big median tubercles on area III. Pinto-da-Rocha *et al.* (2012) is the only recent work proposing a diagnosis for *Mischonyx*. In this diagnosis, the authors also stress as diagnostic characters the presence of well-developed median tubercles on mesotergal areas (and add their elliptic form) and the lateral tubercles of mid-bulge clearer than the rest of the body. Besides these characters, they consider the robust spines on the anterior border of dorsal scutum as a diagnostic character as well. However, the same work proposes that *Mischonyx* would be close to Hernandariinae subfamily, given their morphological features.

In this work, with the phylogenetics arguments, we agree with the diagnostic character proposed by both cited works: the elliptic median tubercles on area III. The tubercle shape changes in the clade holding *M. arlei* **comb.nov.**, *M. intermedius* and *M. minimus* **sp. nov.**, but, beside these species, all others inside *Mischonyx* have the elliptic tubercle. Along with that, our character "Lateral tubercles on anterior margin of dorsal scutum with the same size" (#7-0) is an approximation of the diagnostic character cited above. On the other hand, it is possible to see that *Mischonyx* is not close to Hernandariinae species added to the analysis (*Piassagera brieni* and *Pseudotrogulus telluris*). Not even in the analyses using morphological characters only (Figs. 04 and 05). This is in agreement with Pinto-da-Rocha *et al.* (2014), which places *Mischonyx squalidus* (*Mischonyx cuspidatus* in the article) far from Hernandariinae. To be certain about the phylogenetic proximity of *Mischonyx*, a more inclusive analysis must be performed, but, by our analyses along with Pinto-da-Rocha *et al.* (2014), we can consider that the genus is not closely related to Hernandariinae.

Other taxonomic~~al~~ and topological remarks

Recent publications on taxonomy and systematics of harvestmen considered *G. antiquus* member of *Mischonyx* (Kury, 2003; Vasconcelos, 2005a and Pinto-da-Rocha *et*

al., 2012). In fact, our morphological analysis places this species inside the genus as well, agreeing with those authors. However, molecular and TE analyses consistently place this species far from *Mischonyx* (Figs. 06 –14). In ML3, it is sister to *Ampheres leucopheus*, a Caelopyginae member. This indicates a convergence of morphological characteristics in two lineages which are distant from each other considering their molecular evolutionary history.

On the other hand, MP2, which does not include morphological characters, places a clade with *Multumbo* and *Deltaspidium* species inside *Mischonyx*, as sister to the clade with species from SMSP, SSP, PR and SC AoE. This group makes no morphological or biogeographical sense, once these species are from Org and LSRJ AoE. However, when we include morphological characters, MP3 does not recover the same clade and excludes *Multumbo* and *Deltaspidium* from *Mischonyx* genus.

The two cases in the two last paragraphs evidence the importance of the combination of morphological and molecular data in solving problematic points in topologies. Wiens (2004) and Baker & Gatesy (2002) support the hypothesis that morphological data in the framework is important especially in cases that there are some problematic or unresolved relationships in molecular data. The research of De Sá *et al.* (2014) support this hypothesis by showing that, in their target group, there were problematic relationships among species, which were better elucidated by the use of morphological and behavioural characters from both the larvae and adults of the studied frog species. Here, we conclude that morphological characters also helped to bring robustness to the hypotheses and solve some problematic relationships in MP2, agreeing with Wipfler *et al.* (2015), Lee & Palci (2015) and Giribet (2015) which consider morphological characters fundamental even in phylogenomics era, once the combination of morphological and molecular data provide independent sources of evidence building one phylogenetic hypothesis and because morphological characters brings phenotypic plausibility to molecular data.

Conclusions

Mischonyx is monophyletic by both Total Evidence analysis (Maximum Likelihood and Maximum Parsimony), if adding *Michonyx arlei* **comb. nov** and removing *Mischonyx antiquus*, which returns to its former genus, becoming *Gonyleptes antiquus*. *Geraecormobiella* Mello-Leitão, 1931, *Ariaeus* Sørensen, 1932 and *Urodiabunus* Mello-Leitão, 1935 are junior synonyms of *Mischonyx* Bertkau, 1880. *Geraecormobiella convexa* Mello-Leitão, 1931 and *Geraeocormobius cheloides Mello-Leitão, 1940* are junior synonym of *Weyhia spinifrons* Mello-Leitão, 1923*; Ilhaia cuspidata* Roewer, 1913, *Ilhaia fluminensis* Mello-Leitão, 1922, *Gonazula gibbosa* Roewer, 1930, *Eduardoius granulosus* Mello-Leitão, 1931, *Giltaya solitaria* Mello-Leitão, 1932 and *Eduardoius lutescens* Roewer, 1943 are junior synonym of *Mischonyx squalidus* Bertkau, 1880; *Ilhaia sulina* Soares & Soares, 1947 is a junior synonym of *Xundarava anomala* Mello-Leitão, 1936. We describe three new species for the genus: *Mischonyx minimus* **sp. nov.**, *Mischonyx intervalensis* **sp. nov.** and *Mischonyx tinguaensis* **sp. nov.**. *Geraeocormobius reitzi* Vasconcelos, 2005, *Weyhia clavifemur* Mello-Leitão, 1927 and *Weyhia spinifrons* Mello-Leitão, 1923 were transferred to *Mischonyx*. *Weyhia parva* Roewer, 1917 was removed from the synonym with *Mischonyx squalidus*, Bertkau 1880 (see Kury, 2003: 134),

considered as a valid species and transferred to *Mischonyx*.

The new composition of the genus after all synonimizations, combinations and new species description is: *Mischonyx. anomalus* (Mello-Leitão, 1936); *Mischonyx arlei* (Mello-Leitão, 1935b) **comb.nov.**, *Mischonyx clavifemur*, (Mello-Leitão, 1927a) **comb.nov.**; *Mischonyx fidelis* (Mello-Leitão, 1931b); *Mischonyx insulanus* (H. Soares, 1972); *Mischonyx intermedius* (Mello-Leitão, 1935b); *Mischonyx intervalensis* **sp. nov.**; *Mischonyx kaisara* Vasconcelos, 2004; *Mischonyx minimus* **sp. nov.**; *Mischonyx parvus* (Roewer, 1917) **comb. nov.**; *Mischonyx poeta* Vasconcelos, 2005a; *Mischonyx processigerus* (Soares & Soares, 1970); *Mischonyx reitzi* (Vasconcelos, 2005) **comb.nov.**; *Mischonyx scaber* (Kirby, 1819); *Mischonyx spinifrons* (Mello-Leitão, 1923) **comb.nov.;** *Mischonyx squalidus* Bertkau, 1880; *Mischonyx tinguaensis* **sp. nov.**

The most plausible phylogenetic hypothesis was recovered using Total Evidence under Maximum Likelihood optimality criteria, due to less apomorphies of *M. tinguaensis* **sp. nov.**, high bootstrap supports inside *Mischonyx* and absence of morphological characters supporting clades in the other Total Evidence hypothesis (under maximum parsimony optimality criteria). *Mischonyx* clade is supported by: lateral tubercles on anterior margin of dorsal scutum with the same size, elliptic tubercles on area III, absence of prolateral apophysis on females, femur prolaterally curved, three to six apophysis on the apical half of retrolateral row on femur IV and brown as the general body color. There are two major clades inside *Mischonyx*: one holding species from LSRJ, Mnt, Org and Esp AoE, and the other with species from SMSP, SSP, PR and SC AoE. The divergence time of these clades are in agreement with geological events.

Acknowledgements

We thank Marcio B. da Silva, Cristina A. Rheims for their advices and suggestions. We thank Jimmy Cabra-Garcia, Brittany Damron, Daniel Chirivi and Jairo Moreno-González, Marília Pessoa Silva, Daniel Castro and André Nogueira for their help in field trips, opinions and advices during the whole process of production of this manuscript. We thank Manuel Antunes Junior, Beatriz Vieira Freire, Phillip Lenktaitis, Ênio Mattos for their help in DNA sequencing and SEM operation.

References

Acosta LE, Kury AB, Juárez, ML. 2007. New records of *Geraeocormobius sylvarum* (Arachnida, Opiliones, Gonyleptidae), with a remarkable disjunction in northwestern Argentina. *Boletín Sociedad Entomológica Aragonesa* 41:303 –306.

Almeida FFM, Carneiro CDR. 1998. Origem e evolução da Serra do Mar. *Revista Brasileira de Geociências* 28:135–150. DOI: 10.25249/0375-7536.1998135150.

Amorim DS, Pires MRS. 1996. Neotropical biogeography and a method for a maximum biodiversity estimation. In: Bicudo CEM, Menezes NA, Ed. *Biodiversity in Brazil. A First Approach*. São Paulo: Conselho Nacional de Desenvolvimento Cientıfico e Tecnológico, 183–219.

Arango CP, Wheeler WC. 2007. Phylogeny of the sea spiders (Arthropoda, Pycnogonida)

based on direct optimization of six loci and morphology. *Cladistics* 23: 255–293. DOI: 10.1111/j.1096-0031.2007.00143.x.

Baker RH, Gatesy J. 2002. Is morphology still relevant? In: DeSalle R, Wheeler W, Giribet G, ed. *Molecular Systematics and Evolution: Theory and Practice*, Birkhäuser, Basel, 163-174.

Benedetti AR. 2017. Análise filogenética do clado K92, com ênfase em Gonyleptinae, baseada em caracteres morfológicos e moleculares (Opiliones, Gonyleptidae). D. Phil. Thesis, Universidade de São Paulo, São Paulo. doi:10.11606/T.41.2018.tde-03042018-100718.

Benedetti AR, Pinto-da-Rocha R. 2019. Description of two new species of *Progonyleptoidellus* (Opiliones: Gonyleptidae), with a cladistic analysis of the genus, an overview of relationships in the K92 group, and taxonomic notes on *Deltaspidium*. *Zootaxa* 4691(5):461–490. doi:10.11646/zootaxa.4691.5.3.

Bertkau P. 1880. Verzeichnis der von Prof. Ed. von Beneden auf seiner im Auftrage der Belgischen regierung untemommenen wissenschaftlichen Reise nach Brasilien und La Plata i. J. 1872–1875 *gesammelten Arachniden. Mém. cour. Acad. Belgique* 43:1–120.

Bouckaert R, Vaughan TG, Barido-Sottani J, Duchêne S, Fourment M, Gavryushkina A. 2019. BEAST 2.5: An advanced software platform for Bayesian evolutionary analysis. *PLoS computational biology* 15(4):e1006650. https://doi.org/10.1371/journal.pcbi.1006650.

Bragagnolo C, Pinto-da-Rocha R. 2009. Review of the Brazilian harvestman genus Roeweria Mello-Leitão, 1923 (Opiliones: Gonyleptidae). *Zootaxa* 2270:39–52.

Bragagnolo C, Pinto-da-Rocha R. 2012. Systematic review of *Promitobates* Roewer, 1913 and cladistic analysis of Mitobatinae Simon, 1879 (Arachnida: Opiliones:Gonyleptidae). *Zootaxa* 3308:1-48.

Bragagnolo C, Pinto-da-Rocha R, Antunes M, Clouse RM. 2015. Phylogenetics and phylogeography of a long-legged harvestman (Arachnida: Opiliones) in the Brazilian Atlantic Rain Forest reveals poor dispersal, low diversity and extensive mitochondrial introgression. *Invertebrate Systematics* 29:386–404. https://doi.org/10.1071/IS15009.

Brunes TO, Sequeira F, Haddad CFB, Alexandrino J. 2010. Gene and species trees of a Neotropical group of treefrogs: Genetic diversification in the Brazilian Atlantic Forest and the origin of a polyploid species. *Molecular Phylogenetics and Evolution* 57:1120–1133.

Cabanne, G. S., Trujillo-Arias, N., Calderon, L., D'Horta, F. M., & Miyaki, C. Y. (2014). Phenotypic evolution of an Atlantic Forest passerine (Xiphorhynchus fuscus): Biogeographic and systematic implications. Biological Journal of the Linnean Society, 113, 1047–1066.

Carnaval AC, Moritz C. 2008. Historical climate modelling predicts patterns of current biodiversity in the Brazilian Atlantic Forest. *Journal of Biogeography* 35:1187–1201 DOI: 10.1111/j.1365-2699.2007.01870.x.

Carnaval AC, Hickerson MJ, Haddad CFB, Rodrigues MT, Moritz C. 2009. Stability predicts genetic diversity in the Brazilian Atlantic Forest Hotspot. *Science* 323:785–789 DOI: 10.1126/science.1166955.

Cheng R-C, Kuntner M. 2014. Phylogeny suggests nondirectional and isometric evolution of sexual size dimorphism in argiopine spiders. *Evolution* 68: 2861–2872. DOI:10.1111/evo.12504.

Cherem LFS, Varajão CAC, Braucher R, Bourlés D, Salgado AAR, Varajão AC. 2012. Long-term evolution of denudational escarpments in southeastern Brazil. *Geomorphology* 173–174:118–127. DOI:10.1016/j.geomorph.2012.06.002.

Chernomor O, von Haeseler A, Minh BQ. 2016. Terrace aware data structure for phylogenomic inference from supermatrices. *Systematic Biology* 65:997–1008 DOI: 10.1093/sysbio/syw037.

Colgan DJ, McLauchlan A, Wilson GDF, Livingston SP, Edgecombe GD, Macaranas J, Cassis G, Gray MR. 1998. Histone H3 and U2 snRNA DNA sequences and arthropod molecular evolution. *Australian Journal of Zoology* 46: 419–437 DOI: 10.1071/ZO98048.

DaSilva MB, Gnaspini P. 2010. Systematic revision of Goniosomatinae (Arachnida: Opiliones: Gonyleptidae), with a cladistic analysis and biogeographical notes. *Invertebrate Systematics*. 23(6):530–624 DOI: 10.1071/IS09022.

DaSilva MB, Pinto-da-Rocha R. 2010. Systematic review and cladistic analysis of the Hernandariinae (Opiliones: Gonyleptidae). *Zoologia* 27(4):577-642 DOI: 10.1590/S1984-46702010000400010.

DaSilva MB, Pinto-da-Rocha R, Morrone, JJ. 2017. Historical relationships of areas of endemism of the Brazilian Atlantic rainforest: a cladistic biogeographic analysis of harvestman taxa (Arachnida: Opiliones). *Current Zoology* 63(5):525–535 DOI: 10.1093/cz/zow092.

De Ley P, Félix MA, Frisse LM, Nadler SA, Sternberg PW, Thomas WK. 1999. Molecular and morphological characterization of two reproductively isolated species with mirror image anatomy (Nematoda: Cephalobidae). *Nematology* 2:591–612.

De Sá RO, Grant T, Camargo AW, Heyer R, Ponssa ML, Stanley E. 2014. Systematics of the Neotropical Genus *Leptodactylus* Fitzinger, 1826 (Anura: Leptodactylidae): Phylogeny, the Relevance of Non-molecular Evidence, and Species Accounts. *South American Journal of Herpetology* 9(1):1–128. DOI: 10.2994/SAJH-D-13-00022.1

Dias BC, Souza ES, Hara MR, Willemart RH. 2014. Intense leg tapping behavior by the

harvestman *Mischonyx cuspidatus* (Gonyleptidae): an undescribed defensive behavior in Opiliones? *The Journal of Arachnology* 42(1):123–125. DOI: 10.1636/Hi12-06.1.

Dias BC, Willemart RH. 2013. The effectiveness of post-contact defenses in a prey with no pre-contact detection. *Zoology* 116(3):168–174 DOI: 10.1016/j.zool.2012.12.001.

Dias JM. 2017. O uso do olfato nos opiliões *Neosadocus maximus* e *Mischonyx cuspidatus* (Arachnida: Opiliones: Laniatores). Masters Dissertation. Universidade de São Paulo. São Paulo. DOI: 10.11606/D.41.2018.tde-03042018-083949.

Edgecombe GD, Giribet G. 2006. A century later – a total evidence re-evaluation of the phylogeny of scutigeromorpha centipedes (Myriapoda: Chilopoda). *Invertebrates Systematics* 20:503–525 DOI: 10.1071/IS05044.

Ewing B, Green P. 1998. Base-calling of automated sequencer traces using Phred. II, Error probabilities. *Genome Research* 8:186–194.

Ewing B, Hillier L, Wendl MC, Green P. 1998. Base-calling of automated sequencer traces using Phred. I. *Accuracy assessment Genome Research* 8:175–185 DOI: 10.1101/gr.8.3.175.

Franco-Magalhães AOB, Hackspacher PC, Glasmacher UA, Saad AR. 2010. Rift to post-rift evolution of a “passive” continental margin: The Ponta Grossa Arch, SE Brazil. *International Journal of Earth Sciences* 99:1599–1613. DOI: 10.1007/s00531-010-0556-8.

Franco-Magalhães AOB, Hackspacher PC, Saad AR. 2010. Exumação tectônica e reativação de paleolineamentos no Arco de Ponta Grossa: termocronologia por traços de fissão em apatitas. *Revista Brasileira de Geociências* 40:184–195 DOI: 10.25249/0375-7536.2010402184195.

Folmer O, Black M, Hoeh W, Lutz R, Vrijenhoek R. 1994. DNA primers for amplification of mitochondrial cytochrome c oxidase subunit I from diverse metazoan invertebrates. *Molecular Marine Biology and Biotechnology* 3:294–299.

Giribet G. 2015. Morphology should not be forgotten in the era of genomics – a phylogenetic perspective. *Zoologischer Anzeiger - A Journal of Comparative Zoology* 256:96-103 DOI: 10.1016/j.jcz.2015.01.003.

Goloboff PA. 1999. Analyzing large data sets in reasonable times: solutions for composite optima. *Cladistics* 15:415–428 DOI: 10.1006/clad.1999.0122.

Goloboff PA, Catalano SA. 2016. TNT version 1.5, including a full implementation of phylogenetic morphometrics. *Cladistics* 32: 221-238 DOI: 10.1111/cla.12160.

Goloboff P, Farris J, Nixon KC. 2008. TNT, a free program for phylogenetic analysis. *Cladistics* 24:774–786 DOI: 10.1111/j.1096-0031.2008.00217.x.

Gordon D, Abajian C, Green P. 1998. Consed: a graphical tool for sequence finishing. *Genome Research* 8:195–202 DOI: 10.1101/gr.8.3.195.

Gordon D, Desmarais C, Green P. 2001. Automated finishing with autofinish. *Genome Research* 11:614–625 DOI: 10.1101/gr.171401.

Grant T, Kluge A. 2009. Parsimony, explanatory power, and dynamic homology testing. *Systematics and Biodiversity* 7:357-363 DOI: 10.1017/S147720000999017X.

Holbourn A., Kuhnt W, Lyle M, Levay L, Romero O, Andersen N. 2014. Middle Miocene climate cooling linked to intensification of eastern equatorial Pacific upwelling. *Geology* 42:19–22. DOI: 10.1130/G34890.1.

ICZN 1999. International Code of Zoological Nomenclature. Fourth Edition. The International Trust for Zoological Nomenclature, London, UK.

Ji Y-J, Zhang D-X, He L-J. 2003. Evolutionary conservation and versatility of a new set of primers for amplifying the ribosomal internal transcribed spacer regions in insects and other invertebrates. *Molecular Ecology Notes* 3:581–585 DOI: 10. 1046/j.1471-8286.2003.00519.x.

Kalyaanamoorthy S, Minh BQ, Wong TKF, von Haeseler A. 2017. ModelFinder: Fast Model Selection for Accurate Phylogenetic Estimates. *Nature Methods* 14:587–589 DOI: 10.1038/nmeth.4285.

Katoh K, Misawa K, Kuma K, Miyata T. 2002. MAFFT: a novel method for rapid multiple sequence alignment based on fast Fourier transform. *Nucleic Acids Research* 33:511–518 DOI: 10.1093/nar/gkf436.

Kluge A, Grant T. 2006. From conviction to antisuperfluity: old and new justifications of parsimony in phylogenetic inference. *Cladistics* 22: 276–288 DOI: 10.1111/j.1096-0031.2006.00100.x.

Kury AB. 1990. Synonymic notes on Mitobates Sundevall, with redescription of the type species, *M. conspersus* (Perty) (Opiliones, Gonyleptidae, Mitobatinae). *Bulletin of the British Arachnological Society* 8(6):194–200.

Kury AB. 1992. A review of Metamitobates Roewer (Opiliones, Gonyleptidae, Mitobatinae). *Mitteilungen aus dem Zoologisches Museum in Berlin* 68(1):157–166.

Kury AB. 2003. Annotated catalogue of the Laniatores of the New World (Arachnida, Opiliones). *Revista Ibérica de Aracnología* 1:5–337.

Kury AB, Villareal MO. 2015. The prickly blade mapped: establishing homologies and chaetotaxy for macroseatae of penis ventral plate in Gonylepoidea (Arachinida, Opiliones, Laniatores). *Zoological Journal of Linnean Society* 174(1):1–46 DOI: 10.1111/zoj.12225.

Kury A, Medrano M. 2016. Review of terminology for the outline of dorsal scutum in Laniatores (Arachnida, Opiliones). *Zootaxa* 4097(1):130–134 DOI: 10.11646/zootaxa.4097.1.9.

Kury AB. 2020. Classification of Opiliones. Museu Nacional/UFRJ website. Online at: http://www.museunacional.ufrj.br/mndi/Aracnologia/opiliones.html (accessed: 10th August 2020).

Larsson, A. 2014. AliView: a fast and lightweight alignment viewer and editor for large datasets. Bioinformatics. 30(22):3276–3278 DOI: 10.1093/bioinformatics/btu531.

Lee MSY, Palci A. 2015. Morphological Phylogenetics in the Genomic Age. *Current Biology* 25(19):922–929 DOI: 10.1016/j.cub.2015.07.009.

Maddison WP, Maddison DR. 2017. Mesquite: a modular system for evolutionary analysis. Version 3.31 Available at: http://mesquiteproject.org.

Mello-Leitão CF. 1940. Sete gêneros e vinte e oito espécies de Gonyleptidae. *Archivos de Zoologia do Estado de São Paulo* 1(1):1–52.

Mendes AC. 2011. Phylogeny and taxonomic revision of Heteropachylinae (Opiliones: Laniatores: Gonyleptidae). *Zoological Journal of the Linnean Society* 163:437–483 DOI: 10.1111/j.1096-3642.2011.00706.x.

Mestre LAM, Pinto-da-Rocha R. 2004. Population dynamics of an isolated population of the harvestman *Ilhaia cuspidata* (Opiliones, Gonyleptidae), in araucaria forest (Curitiba, Paraná, Brazil). *Journal of Arachnology* 32(2):208–220 DOI: 10.1636/M02-61.

Meyer CP. 2003. Molecular systematics of cowries (Gastropoda: Cypraeidae) and diversification patterns in the tropics. *Biological Journal of Linnean Society* 79:401–459 DOI: 10.1046/j.1095-8312.2003.00197.x.

Minh BQ, Nguyen MAT, von Haesler A. 2013. Ultrafast approximation for phylogenetic bootstrap. *Molecular Biology and Evolution* 30:1118–1195 DOI: 10.1093/molbev/mst024.

Morais RMO, Mello CL, Costa FO, Ribeiro CS. 2005. Estudo faciológico de depósitos terciários (formações Barreiras e Rio Doce) aflorantes na porção emersa da Bacia do Espírito Santo e na região emersa adjacente à porção norte da Bacia de Campos. In: Congresso Abequa, 10, Guarapari. http://www.abequa.org.br/trabalhos/0291_rute_morais.pdf

Morellato LPC, Haddad CFB. 2000. Introduction: the Brazilian Atlantic Forest. *Biotropica* 32(4b):786 – 792 DOI: 10.1111/j.1744-7429.2000.tb00618.x.

Müller P. 1973. The dispersal centers of terrestrial vertebrates in the Neotropical realm: A study in the evolution of the Neotropical biota and its native landscape. *Biogeographica* 2:1–250.

Nguyen LT, Schmidt HA, von Haeseler A, Minh BQ. 2015. IQ-TREE: A fast and effective stochastic algorithm for estimating maximum likelihood phylogenies. *Molecular Biology and Evolution*. 32:268–274 DOI: 10.1093/molbev/msu300.

Nixon KC. 1999. The parsimony ratchet, a new method for rapid parsimony analysis. *Cladistic*s 15: 407–414 DOI: 10.1111/j.1096-0031.1999.tb00277.x.

Nixon KC. 2002. Winclada (BETA) ver. 1.00.08. New York, Published by author, Ithaca, 734–745.

Nogueira AA, Bragagnolo C, DaSilva MB, Martins T, Perbiche-Neves G, Pinto-da-Rocha R. 2019a. Historical signatures in the alpha and beta diversity patterns of Atlantic Forest harvestman communities (Opiliones-Arachnida). *Canadian Journal of Zoology* 97:631–643 DOI: 10.1139/cjz-2018-0032.

Nogueira AA, Bragagnolo C, DaSilva MB, Carvalho LS, Benedetti A, Pinto-da-Rocha R. 2019b. Spatial variation in phylogenetic diversity of communities of Atlantic Forest harvestmen (Opiliones, Arachnida). *Insect Conservation and Diversity* 12: 414–426 DOI: 10.1111/icad.12356.

Palumbi SR. 1996. Nucleic acids, II: the polymerase chain reaction. In: Hillis DM, Moritz C, Mable BK, eds. *Molecular Systematics. Sinauer Associates*. Sunderland 205–247.

Pellegrino KCM, Rodrigues MT, Waite AN, Morando M, Yonenaga-Yassuda Y, Sites JW. 2005. Phylogeography and species limits in the Gymnodactylus darwinii complex (Gekkonidae, Squamata): genetic structure coincides with river systems in the Brazilian Atlantic Forest. *Biological Journal of Linnean Society* 85:13–26 DOI: 10.1111/j. 1095-8312.2005.00472.x.

Peres EA, Benedetti AR, Hiruma ST, Sobral-Souza T, Pinto-da-Rocha R. 2019. Phylogeography of Sodreaninae harvestmen (Arachnida: Opiliones: Gonyleptidae): insights into the biogeography of the southern Brazilian Atlantic Forest. *Molecular Phylogenetics and Evolution* 138:1–16 DOI:10.1016/j.ympev.2019.05.028.

Peres EA, DaSilva MB, Antunes M, Pinto-Da-Rocha R. 2018. A short-range endemic species from south-eastern Atlantic Rain Forest shows deep signature of historical events: phylogeography of harvestmen Acutisoma longipes (Arachnida: Opiliones). *Systematics and Biodiversity* 16:171–187 DOI: 10.1080/14772000.2017.1361479.

Pinto-da-Rocha R. 1997. Systematic review of the Family Stygnidae Opiliones: Laniaores: Gonyleptoidea). *Arquivos de Zoologia* 33(4):163–342 DOI: 10.11606/issn.2176-7793.v33i4p163-342.

Pinto-da-Rocha R. 2002. Systematic review and cladistics analysis of the Caelopyginae (Opiliones, Gonyleptidae). *Arquivos Zoologia* 36:357–464 DOI: 10.1590/S1984-46702010000400010.

Pinto-da-Rocha R, DaSilva MB, Bragagnolo C. 2005. The Faunistic similarity and historic

biogeography of the harvestmen of southern and southeastern atlantic rain forest of Brazil. *The Journal of Arachnology* 33: 290–299 DOI: 10.1636/04-114.1.

Pinto-da-Rocha R, Bragagnolo C. 2010. Systematic revision and cladistic analysis of the Brazilian subfamily Sodreaninae (Opiliones: Gonyleptidae). *Invertebrate Systematics* 24:509–538 DOI: 10.1590/S1984-46702010000400010.

Pinto-da-Rocha R, Benedetti AR, Vasconcelos E, Hara MR. 2012. New systematic assignments in Gonyleptoidea (Arachnida, Opiliones, Laniatores). *Zookeys* 198: 25–68 DOI: 10.3897/zookeys.198.2337.

Pinto-da-Rocha R, Bragagnolo C, Marques FPL, Antunes Junior M. 2014. Phylogeny of harvestmen family Gonyleptidae inferred from a multilocus approach (Arachnida: Opiliones). *Cladistics* 30:519–539 DOI: 10.1111/cla.12065.

Prance GT. 1982. Forest refuges: Evidence from woody angiosperms. In Prance GT, ed. *Biological diversification in the tropics* New York: Columbia University Press, 137–158.

Prendini L, Weygoldt P, Wheeler WC. 2005. Systematics of the *Damon variegatus* group of African whip spiders (Chelicerata: Amblypygi): evidence from behaviour, morphology and DNA. *Organisms Diversity & Evolution* 5:203–236 DOI: 10.1016/j.ode.2004.12.004.

Rambaut A. 2010. FigTree v1.3.1. Institute of Evolutionary Biology, University of Edinburgh, Edinburgh. http://tree.bio.ed.ac.uk/software/figtree/

Rambaut A, Drummond AJ, Xie D, Baele G and Suchard MA. 2018. Posterior summarisation in Bayesian phylogenetics using Tracer 1.7. *Systematic Biology* 67(5):901–904 DOI: 10.1093/sysbio/syy032.

Ravelo AC, Andreasen DH, Lyle M, Olivarez-Lyle A, Wara MW. 2004. Regional climate shifts caused by gradual global cooling in the Pliocene epoch. *Nature* 429: 263–267 DOI: 10.1038/nature02567.

Resende LPA, Pinto-da-Rocha R, Bragagnolo C. 2012. The harvestmen fauna (Arachnida: Opiliones) of the Parque Estadual Carlos Botelho, and the Floresta Nacional de Ipanema, São Paulo, Brazil. *Biota Neotropica* 12(4):146–155. DOI: 10.1590/S1676-06032012000400016.

Reyda FB, Olson PD. 2003. Cestodes of Peruvian freshwater stingrays. *Journal of Parasitology* 89:1018–1024 DOI: 10.1645/GE-3143.

Rocha DFO, Wouters FC, Zampieri DS, Brocksom TJ, Machado G, Marsaioli AJ. 2013. Harvestmen phenols and benzoquinones: characterisation and biosynthetic pathway. *Molecules* 18: 11429–11451 DOI: 10.3390/molecules180911429.

Roewer CF. 1923 Die Weberknechte der Erde. Systematische Bearbeitung der bisher

bekannten Opiliones. Gustav Fischer, Jena, 1116 pp. Available at: http://www.museunacional.ufrj.br/mndi/Aracnologia/pdfliteratura/Roewer/WDE%201923.htm (Accessed 11 August 2020).

Sánchez-Pacheco SJ, Torres-Carvajal O, Aguirre-Peñafiel V, Sales Nunes PM, Verrastro L, Rivas GA, Rodrigues MT, Grant T, Murphy RW. 2017. Phylogeny of *Riama* (Squamata: Gymnophthalmidae), impact of phenotypic evidence on molecular datasets, and the origin of the Sierra Nevada de Santa Marta endemic fauna. *Cladistics* 34(3):260–291. DOI: 10.1111/cla.12203.

Sereno PC. 2007. Logical basis for morphological characters in phylogenetics. *Cladistics* 23(6):565–587 DOI: 10.1111/j.1096-0031.2007.00161.x.

Sharma P, Giribet G. 2011. The evolutionary and biogeographic history of the armoured harvestmen – Laniatores phylogeny based on the molecular markers, with the description of two new families of Opiliones (Arachnida). *Invertebrate Systematics* 25:106–142 DOI: 10.1071/IS11002.

Sigrist MS, Carvalho CJB. 2009. Historical relationships amongst areas of endemism in the tropical South America using Brooks Parsimony Analysis (BPA). *Biota Neotropica* 9:79–90 DOI: 10.1590/S1676-06032009000400009.

Silva SM, Moraes-Barros N, Ribas CC, Ferrand N, Morgante JS. 2012. Divide to conquer: A complex pattern of biodiversity depicted by vertebrate components in the Brazilian Atlantic Forest. *Biological Journal of the Linnean Society* 107:39–55 DOI: 10.1111/j.1095-8312.2012.01919.x.

Strong EE, Lipscomb D. 1999. Character coding and inapplicable data. *Cladistics* 15:363–371 DOI: 10.1006/clad.1999.0114.

Schwarz G. 1978. Estimating the dimension of a model. *The Annals of Statistics* 6(2):461–464.

Thomé MTC, Zamudio KR, Giovanelli JGR, Haddad CFB, Baldissera FA, Alexandrino J. 2010. Phylogeography of endemic toads and post-Pliocene persistence of the Brazilian Atlantic Forest. *Molecular phylogenetics and Evolution* 55:1018–1031 DOI: 10.1016/j.ympev.2010.02.003.

Varón A, Vinh LS, Wheeler WC. 2010. POY version 4: phylogenetic analysis using dynamic homologies. *Cladistics* 26:72–85 DOI: 10.1111/j.1096-0031.2009.00282.x.

Vasconcelos EG. 2003. Revisão Sistemática de *Mischonyx* Bertkau, 1880 (Opiliones: Laniatores: Gonyleptidae). Masters Dissertation, Universidade Federal do Rio de Janeiro.

Vasconcelos EG. 2004. Nova espécie de *Mischonyx* Bertkau, 1880 do litoral norte do Estado de São Paulo, Brasil (Opiliones, Laniatores, Gonyleptidae). *Revista Ibérica de Aracnologia* 10:129–132 DOI: 10.1590/S0073-47212005000300001.

Vasconcelos EG. 2005a. Nova espécie de *Mischonyx* do estado do Rio de Janeiro, Brasil (Arachnida, Opiliones, Gonyleptidae). *Iheringia. Série Zoologia* 95(3):229–232 DOI: 10.1590/S0073-47212005000300001.

Vasconcelos EG. 2005b. Notes on *Geraecormobius clavifemur* (Mello-Leitão, 1927) and description of *Geraecormobius reitzi* n.sp. (Arachnida: Opiliones: Gonyleptidae). *Zootaxa* 1088:1–10 DOI: 10.11646/zootaxa.1088.1.1.

Vaidya G, Lohman DJ, Meier R. 2011. SequenceMatrix: concatenation software for the fast assembly of multi-gene datasets with character set and codon information. *Cladistics* 27:171–180 DOI:10.1111/j.1096-0031.2010.00329.x.

Wheeler WC. 1996. Optimization Alignment: the end of multiple sequence alignment in phylogenetics? *Cladistics* 12:1–9 DOI: 10.1006/clad.1996.0001.

Wheeler WC. 2001a. Homology and the optimization of DNA sequence data. *Cladistics* 17:3 – 11 DOI: 10.1006/clad.2000.0154.

Wheeler WC. 2001b. Homology and DNA sequence data. In: Wagner GP, ed. *The Character Concept in Evolutionary Biology*. New York: Academic Press, 303–318.

Wheeler WC. 2003. Iterative pass optimization of sequence data. *Cladistics* 19:254–260 DOI: 10.1016/S0748-3007(03)00047-1.

Wiens JJ. 2004. The Role of Morphological Data in Phylogeny Reconstruction, *Systematic Biology* 53(4):653–661 DOI: 10.1080/10635150490472959.

Willemart RH, Pellegatti-Franco F. 2006. The spider *Enoploctenus cyclothorax* (Araneae, Ctenidae) avoids preying on the harvestmen *Mischonyx cuspidatus* (Opiliones: Gonyleptidae). *The Journal of Arachnology* 34(3):649–652 DOI: 10.1636/S05-70.1.

Wipfler B, Pohl H, Yavorskaya MI, Beutel RG. 2016. A review of methods for analysing insect structures – the role of morphology in the age of phylogenomics. *Current Opinion in Insect Science* 18:60–68. DOI: 10.1016/j.cois.2016.09.004.

Table 1(on next page)

Sequenced genes per taxon with their respective identification vouchers and GenBank access number (Outgroup only).

Each code represents the GenBank access number for each gene sequence. Blank cells represent individuals that we could not acquire sequences.

Sequence ID	ITS	28S	COI	16S	12S	CAD	H3
Ampheres_leucopheus_0377	MT957104	MT990789	MT992270	MW000844	MW000802	MW017372	MW017447
Deltaspidium_asperum_2201	MT957119	MT990804	MT992285	MW000859	MW000818	MW017385	MW017418
Deltaspidium_orguense_0520	MT957106	MT990791	MT992272	MW000858	MW000804	MW017374	MW017454
Deltaspidium_tenue		MT990783	MT992264	MW000857	MW000796	MW017370	MW017436
Gonyleptes_antiquus_3707	MT957132	MT990822	MT992301	MW000847	MW000834	MW017397	MW017416
Gonyleptes_antiquus_3708	MT957133	MT990823	MT992302	MW000848	MW000835	MW017398	MW017417
Gonyleptes_horridus_0103	MT957100	MT990784	MT992265	MW000841	MW000797		MW017448
Heliella_singularis_1837	MT957113	MT990798	MT992279	MW000839	MW000812		MW017412
Multumbo_dimorphicus_0069	MT957096	MT990778	MT992259	MW000865	MW000791		MW017455
Multumbo_terrenus_2136	MT957117	MT990802	MT992283	MW000864	MW000816	MW017383	MW017425
Piassagera_brieni_0141		MT990787	MT992268	MW000842	MW000800		MW017409
Promitobates_ornatus_0054		MT990776	MT992257	MW000837	MW000789		MW017406
Pseudotroglus_telluris_2118	MT957115	MT990800	MT992281	MW000843	MW000814	MW017381	MW017411
Roeweria_virescens_0081		MT990780	MT992261	MW000838	MW000793		MW017407
Sodreana_sodreana_0056	MT957095	MT990777	MT992258	MW000852	MW000790	MW017366	MW017410

Table 2 (on next page)

Sequenced genes per taxon with their respective identification vouchers and GenBank access number (Ingroup only).

Each code represents the GenBank access number for each gene sequence. Blank cells represent individuals that we could not acquire sequences.

Sequence ID	ITS	28S	COI	16S	12S	CAD	H3
Mischonyx_anomalus_0122	MT957102	MT990786	MT992267	MW000854	MW000799		MW017452
Mischonyx_anomalus_0693	MT957108	MT990793	MT992274	MW000853	MW000807	MW017376	MW017423
Mischonyx_anomalus_1638	MT957112	MT990797	MT992278	MW000840	MW000811	MW017379	MW017421
Mischonyx_anomalus_2953	MT957122	MT990808	MT992289	MW000856	MW000821	MW017388	MW017424
Mischonyx_clavifemur_0079	MT957097	MT990779	MT992260	MW000862	MW000792	MW017367	MW017449
Mischonyx_clavifemur_0845	MT957109	MT990794	MT992275	MW000863	MW000808		MW017422
Mischonyx_fidelis_4115A	MT957135	MT990825	MT992304	MW000872		MW017400	MW017441
Mischonyx_fidelis_4115B	MT957136	MT990826	MT992305	MW000867		MW017401	MW017442
Mischonyx_insulanus_1455	MT957111	MT990796	MT992277	MW000869	MW000810	MW017378	
Mischonyx_insulanus_3066	MT957123	MT990811	MT992290	MW000855		MW017389	MW017408
Mischonyx_intermedius_4116A	MT957137	MT990827	MT992306	MW000850	MW000831	MW017402	MW017426
Mischonyx_intermedius_4116B	MT957138	MT990809	MT992307	MW000849	MW000832	MW017403	MW017427
Mischonyx_intermedius_4117A	MT957139	MT990810	MT992308	MW000851	MW000833	MW017404	MW017428
Mischonyx_intervalensis_0099	MT957099	MT990782	MT992263	MW000845	MW000795	MW017369	MW017451
Mischonyx_intervalensis_3709	MT957134	MT990824	MT992303	MW000846	MW000836	MW017399	MW017420
Mischonyx_kaisara_0143	MT957103	MT990788	MT992269		MW000801		MW017414
Mischonyx_kaisara_1374	MT957110	MT990795	MT992276	MW000868	MW000809	MW017377	MW017405
Mischonyx_kaisara_2345	MT957120	MT990805	MT992286	MW000866	MW000819	MW017386	MW017415
Mischonyx_kaisara_3575	MT957124	MT990814	MT992293	MW000860	MW000824		MW017413
Mischonyx_minimus_3649	MT957128	MT990818	MT992297	MW000879	MW000828	MW017393	MW017443
Mischonyx_parvus_3621A	MT957125	MT990815	MT992294	MW000875	MW000825	MW017390	MW017437
Mischonyx_parvus_3621B	MT957126	MT990816	MT992295	MW000877	MW000826	MW017391	MW017438
Mischonyx_parvus_3651A	MT957131	MT990821	MT992300	MW000876	MW000806	MW017396	MW017439
Mischonyx_poeta_3650A	MT957129	MT990819	MT992298	MW000880	MW000829	MW017394	MW017445
Mischonyx_poeta_3650B	MT957130	MT990820	MT992299	MW000881	MW000830	MW017395	MW017446
Mischonyx_processigerus_0463	MT957105	MT990790	MT992271	MW000870	MW000803	MW017373	MW017450
Mischonyx_processigerus_3648	MT957127	MT990817	MT992296	MW000871	MW000827	MW017392	MW017444
Mischonyx_reitzi_0672	MT957107	MT990792	MT992273	MW000861	MW000805	MW017375	MW017419
Mischonyx_spinifrons_0111	MT957101	MT990785	MT992266	MW000884	MW000798	MW017371	MW017431
Mischonyx_spinifrons_2120	MT957116	MT990801	MT992282	MW000885	MW000815	MW017382	MW017432
Mischonyx_spinifrons_2151	MT957118	MT990803	MT992284	MW000886	MW000817	MW017384	MW017430
Mischonyx_spinifrons_2809	MT957121	MT990807	MT992288	MW000882		MW017387	MW017433

Mischonyx_spinifrons_3363		MT990812	MT992291	MW000887	MW000822		MW017434
Mischonyx_spinifrons_3375		MT990813	MT992292	MW000883	MW000823		MW017435
Mischonyx_squalidus_0085	MT957098	MT990781	MT992262	MW000873	MW000794	MW017368	MW017453
Mischonyx_squalidus_2026	MT957114	MT990799	MT992280	MW000874	MW000813	MW017380	MW017440
Mischonyx_tinguaensis_2361		MT990806	MT992287	MW000878	MW000820		MW017429

Figure 1

General geographical distribution of *Mischonyx* species.

Legends are in the right of the image. The red line represents the Tropic of Capricorn and the black grid represents the full meridians and parallels.

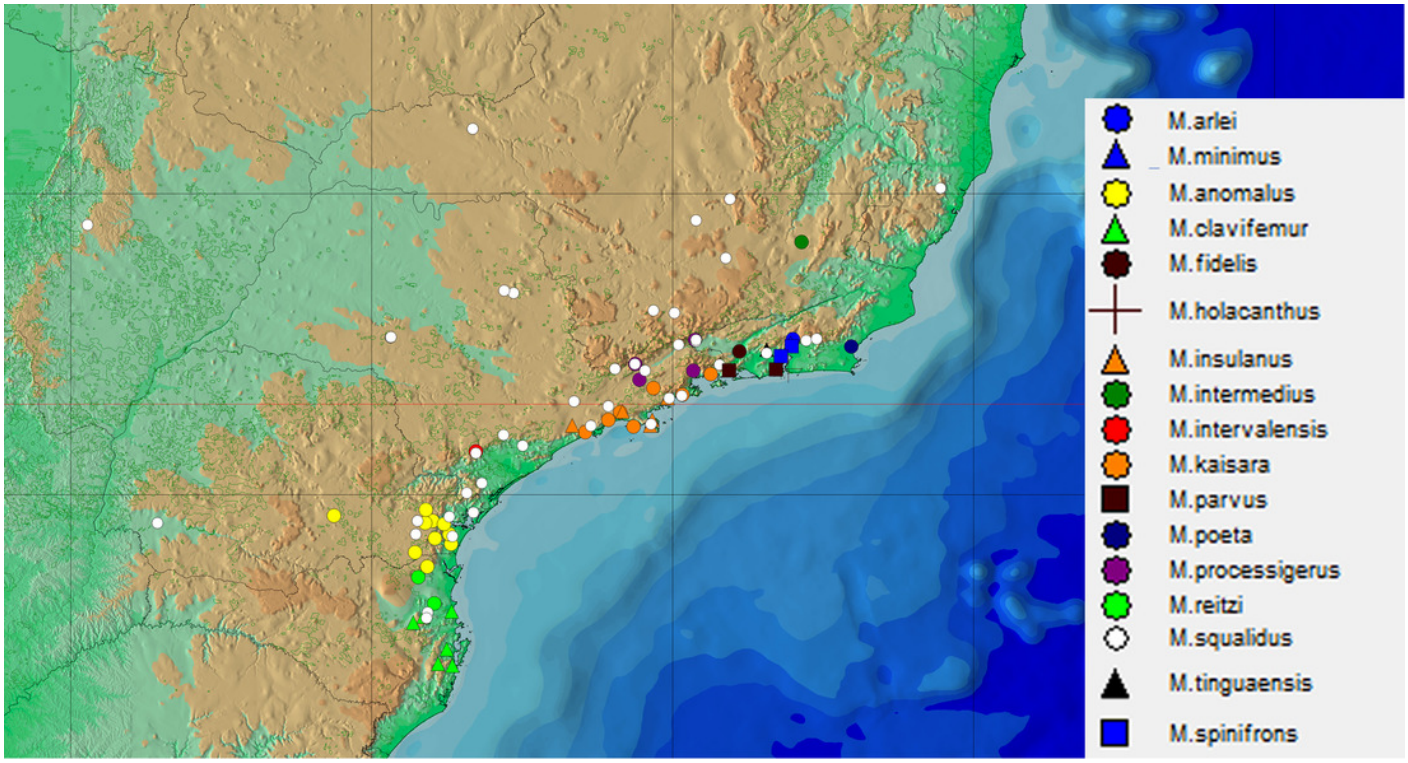

Figure 2

Geographical distribution of *Mischonyx* species from Paraná and Santa Catarina states.

Legends are in the right of the figure. The black grid represents the full meridians and parallels.

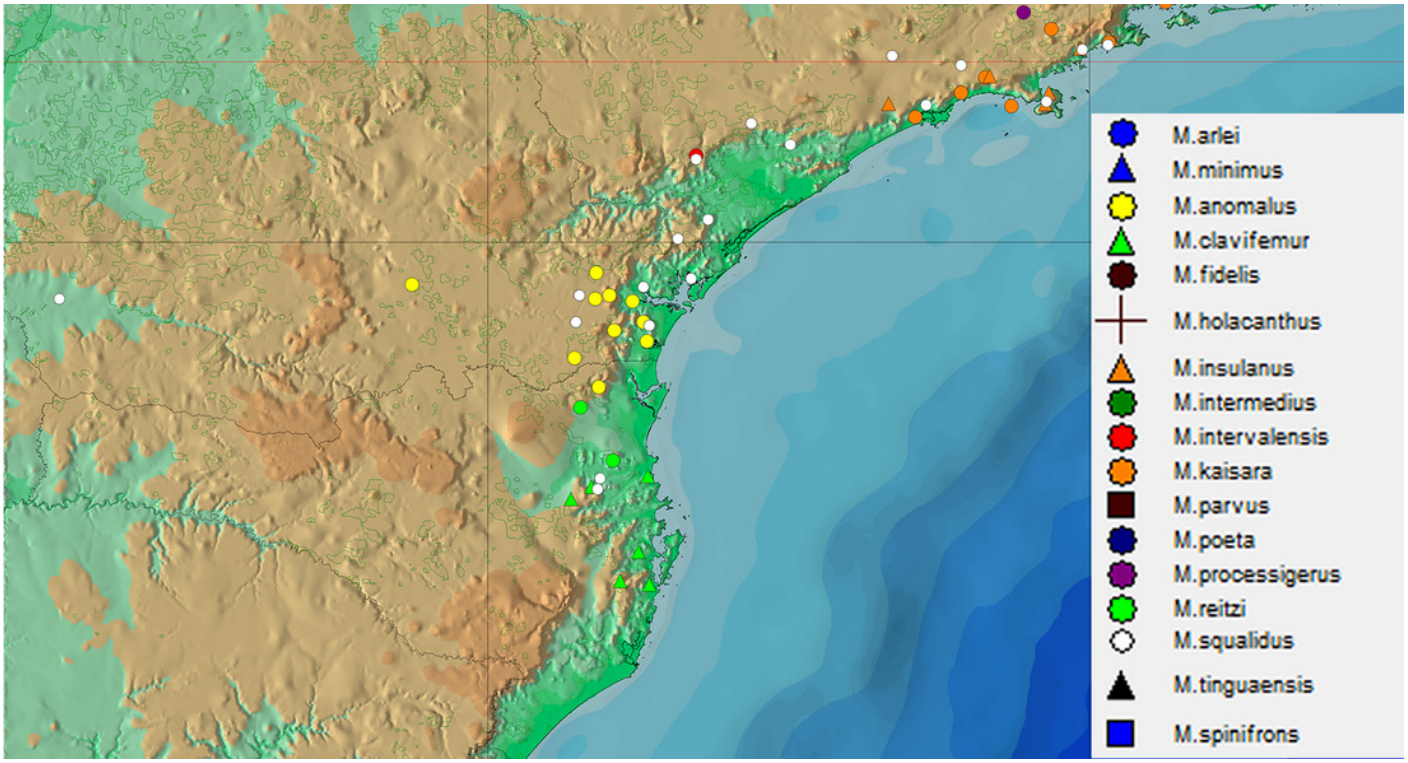

Figure 3

Geographical distribution of *Mischonyx* species from São Paulo, Rio de Janeiro e Minas Gerais states.

Legends are in the right of the figure. The red line represents the Tropic of Capricorn and the black grid represents the full meridians and parallels.

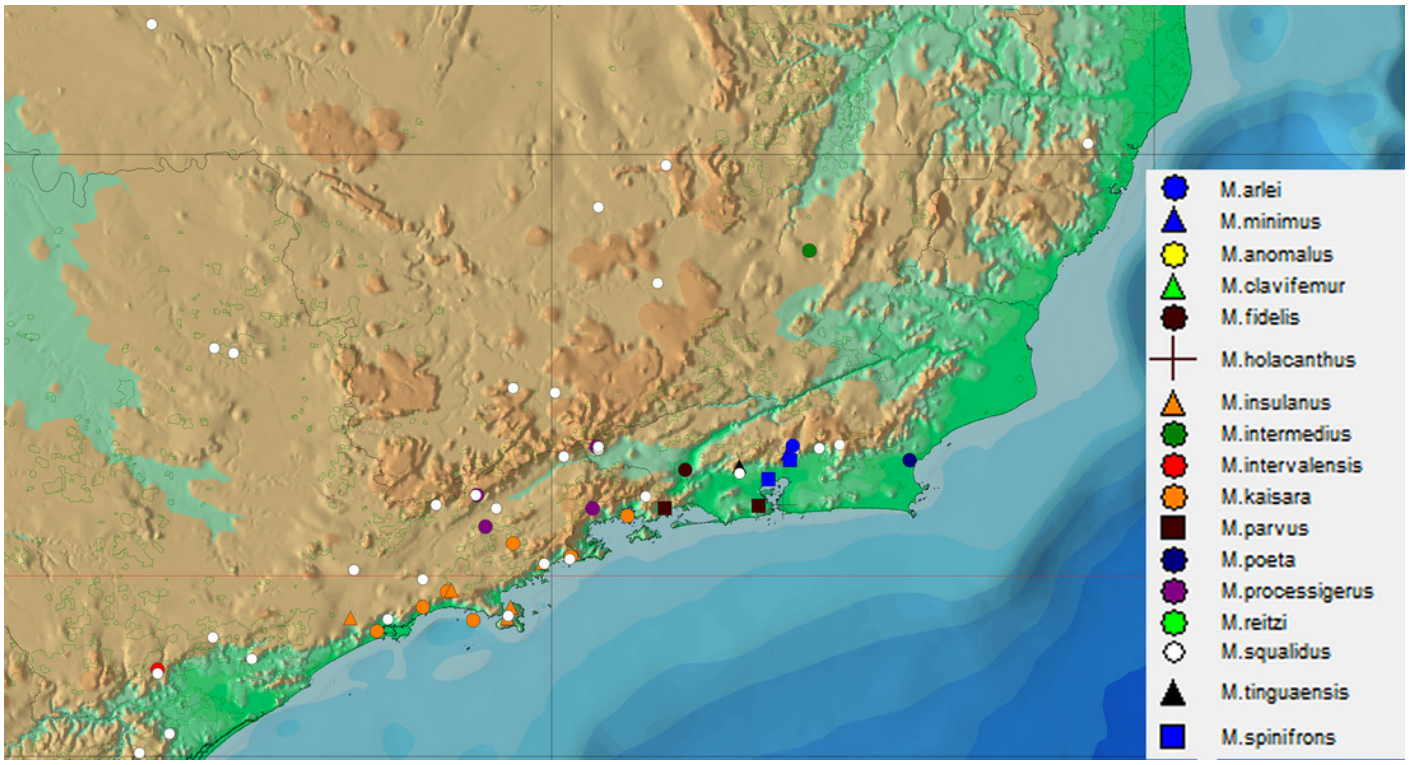

Figure 4

Maximum Likelyhood hypothesis with morphological data only (ML1).

The values near the nodes are the Bootstrap values of each one. Numbers after the species name are the LAL Vouchers of each individual.

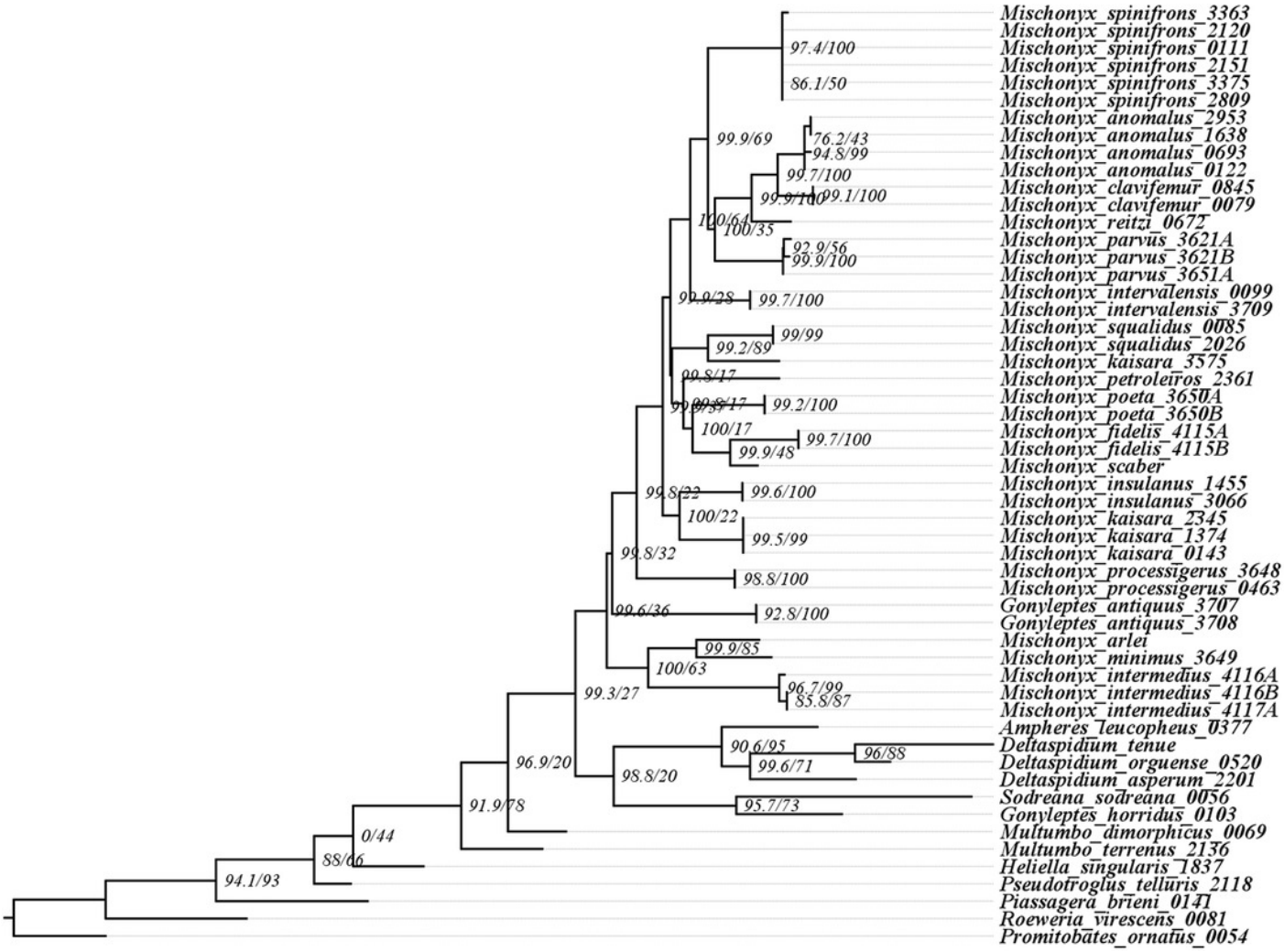

Figure 5

Most parsimonious trees with morphological data only, with 655 steps (MP1), showing *Mischonyx* clade only.

The values near the nodes are the Bootstrap/ Bremer values of each one. The circles in each node represent the unambiguous changes only. Black circles represent non homoplastic and empty circles represent homoplastic synapomorphies. Numbers after the species name are the LAL Vouchers of each individual.

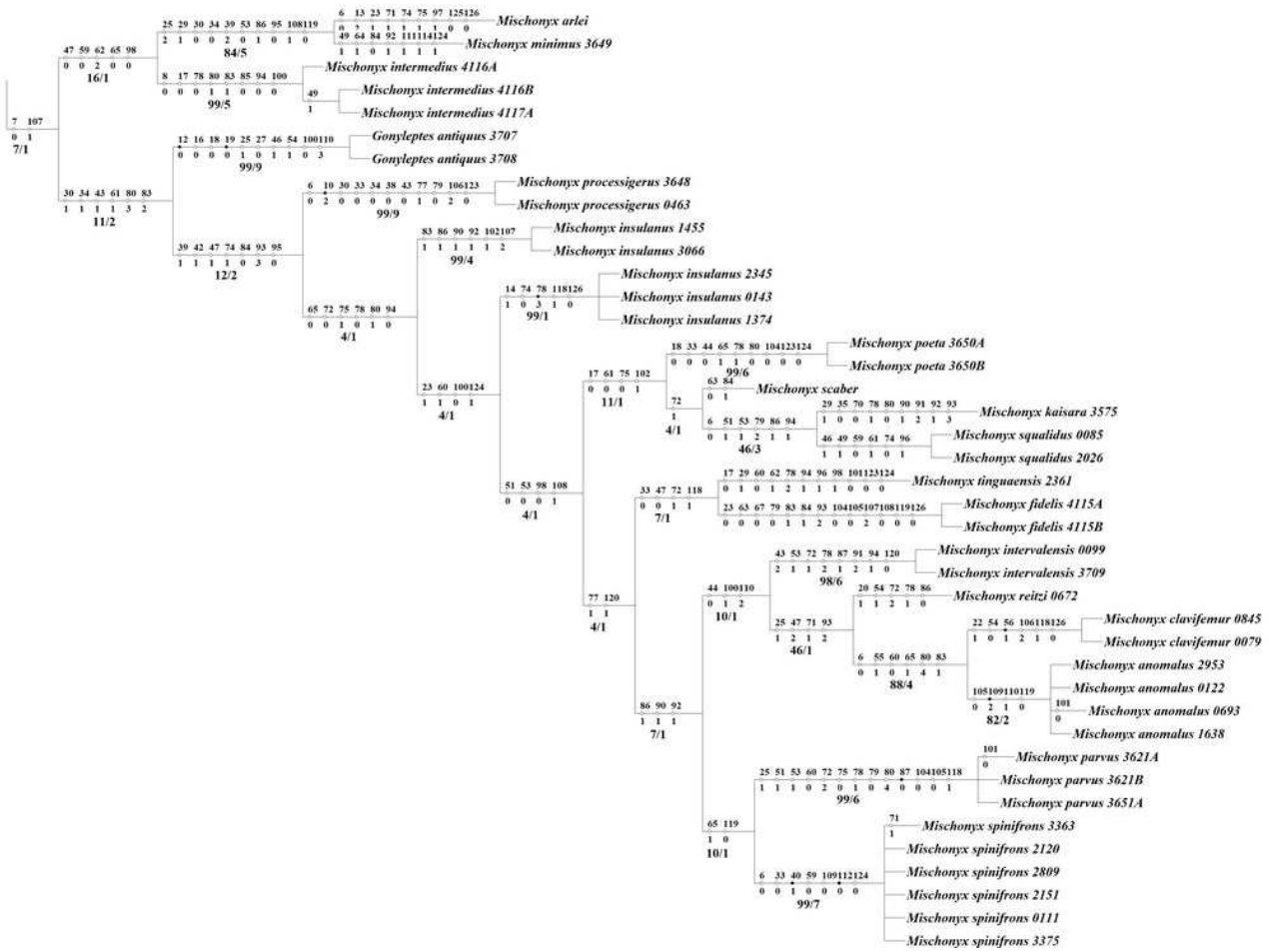

Figure 6

Maximum Likelyhood hypothesis with molecular data only (ML2).

The values near the nodes are the bootstrap values of each one. Numbers after the species name are the LAL Vouchers of each individual. The colored clades are according to their location, respective to each Area of Endemism. Light green: SC; yellow: PR; Red: SSP; orange: SMSP; blue: Org; dark green: Esp; purple: Boc; brown: LSRJ and *M. squalidus*.

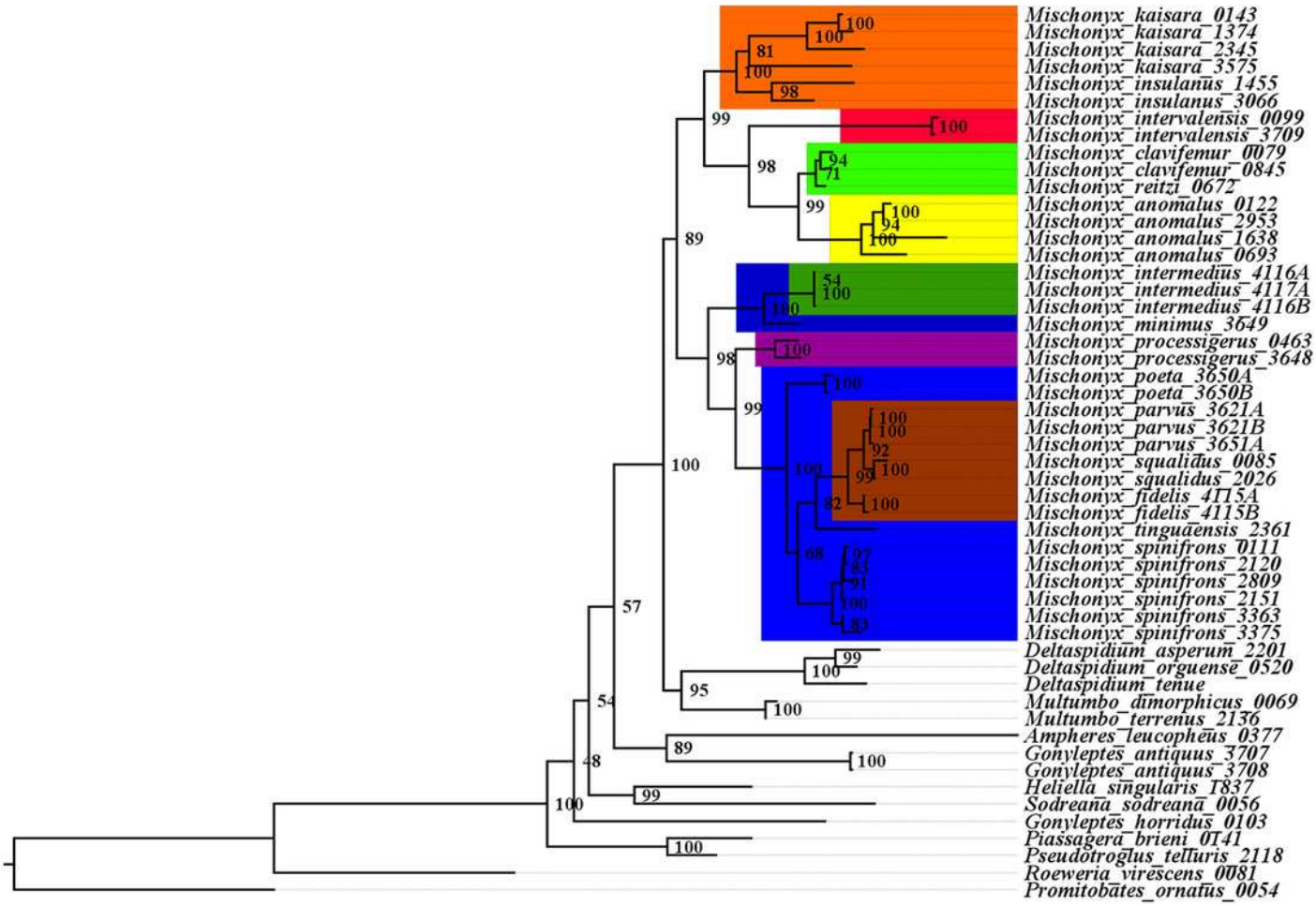

Figure 7

Parsimony hypothesis with molecular data only (MP2).

The values near the nodes are the bootstrap values of each one. Numbers after the species name are the LAL Vouchers of each individual. The colored clades are according to their location, respective to each Area of Endemism. Light green: SC; yellow: PR; Red: SSP; orange: SMSP; blue: Org; dark green: Esp; purple: Boc; brown: LSRJ and *M. squalidus*.

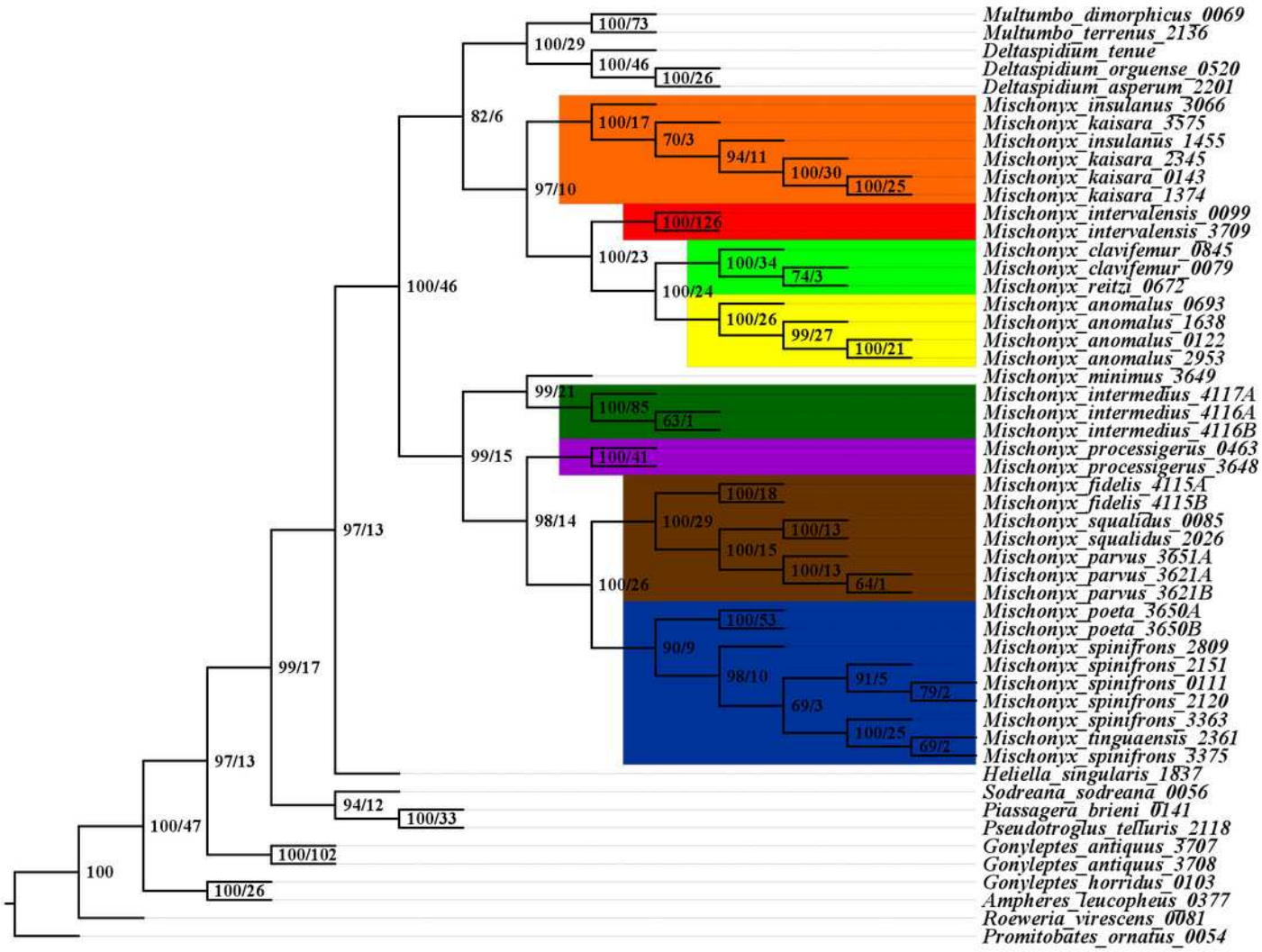

Figure 8

Bayesian hypothesis with molecular data only (B1).

The values near the nodes are the node ages and the bars on each node are the 95% HPD values of each one. Numbers after the species name are the LAL Vouchers of each individual. The colored clades are according to their location, respective to each Area of Endemism. Light green: SC; yellow: PR; Red: SSP; orange: SMSP; blue: Org; dark green: Esp; purple: Boc; brown: LSRJ and *M. squalidus*.

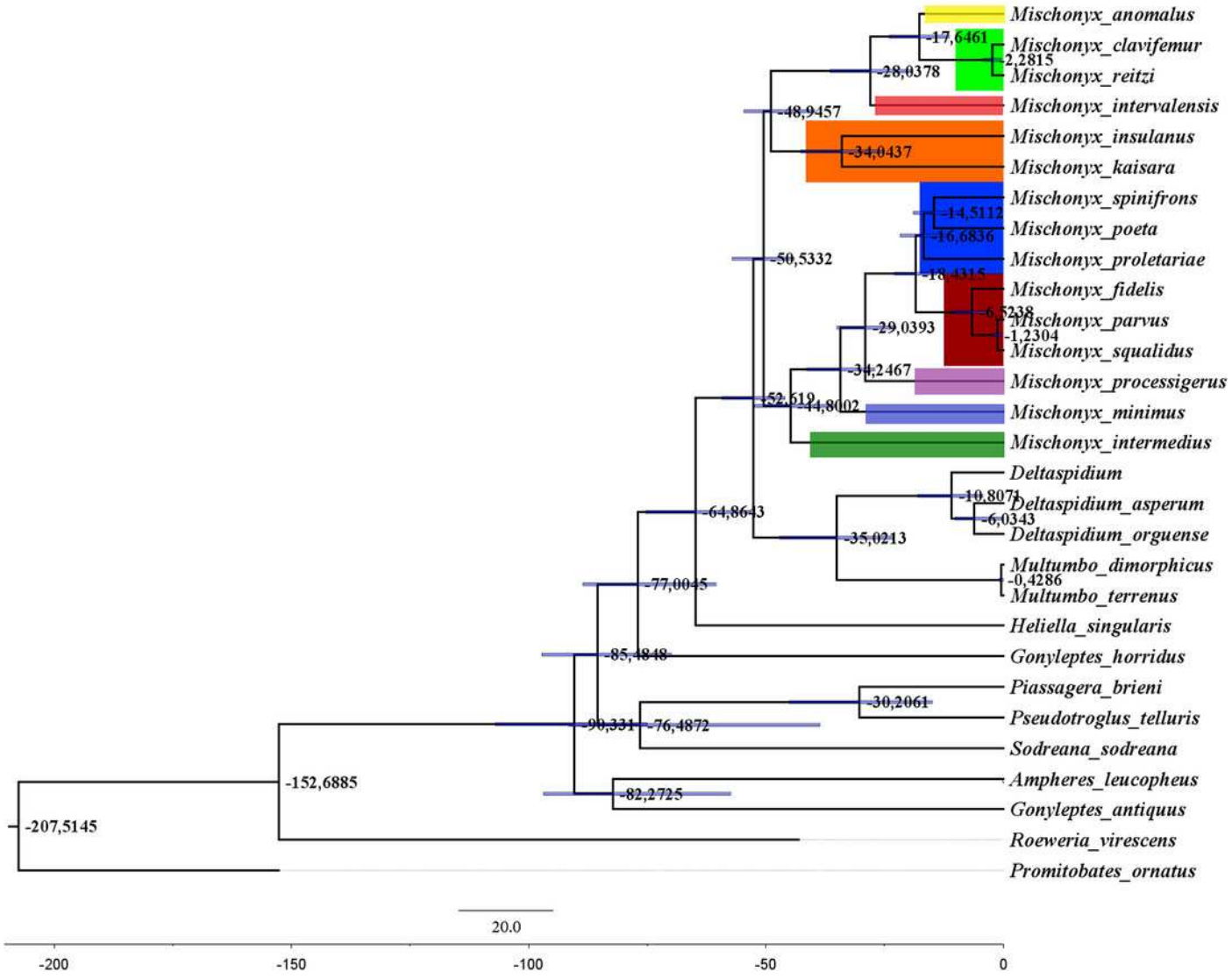

Figure 9

Total Evidence Maximum Likelyhood hypothesis topology (ML3).

The values near the nodes are the bootstrap values of each one. Numbers after the species name are the LAL Vouchers of each individual. The colored clades are according to their location, respective to each Area of Endemism. Light green: SC; yellow: PR; Red: SSP; orange: SMSP; blue: Org; dark green: Esp; purple: Boc; brown: LSRJ and *M. squalidus*.

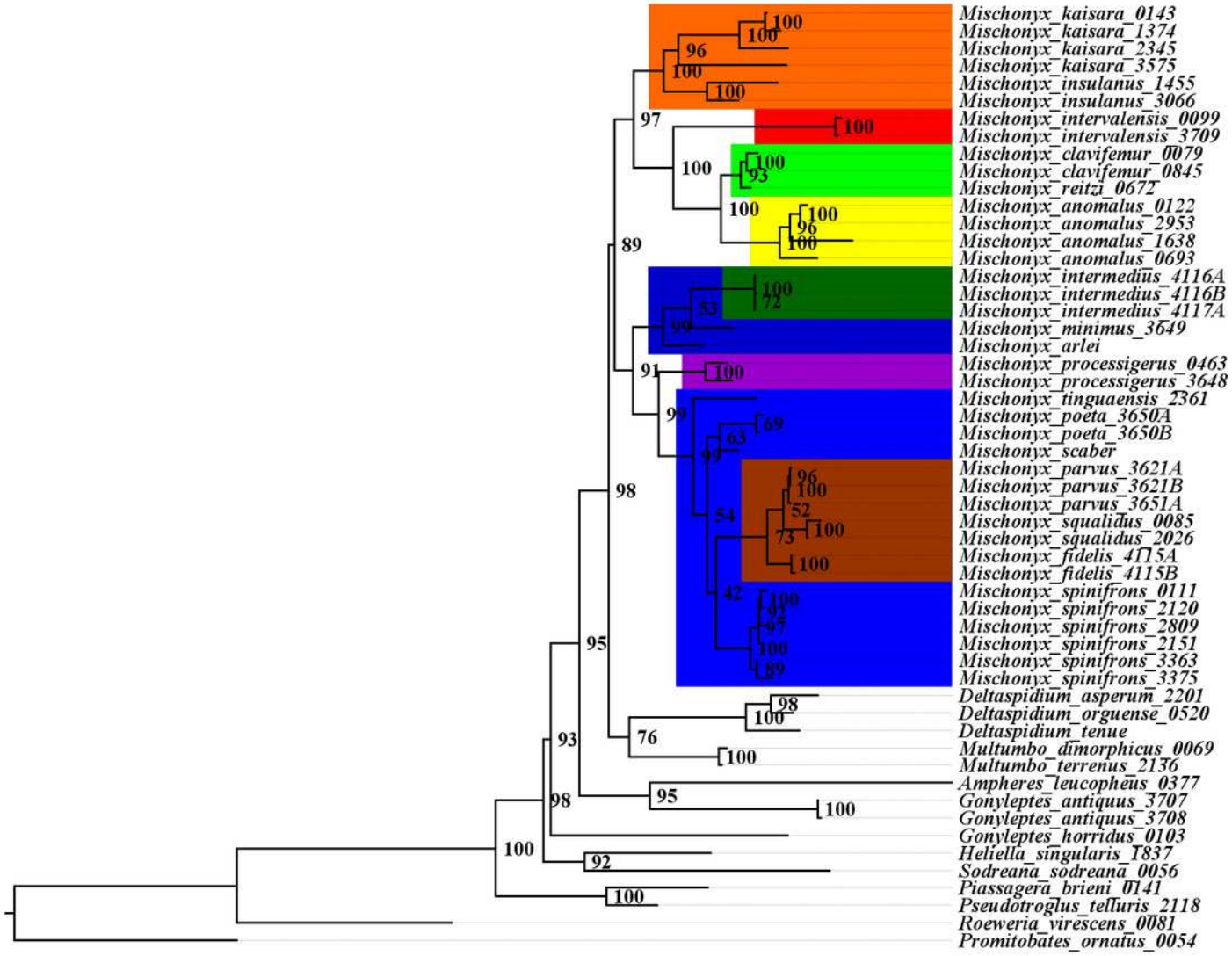

Figure 10

Total Evidence Maximum Likelihood hypothesis (ML3) with characters change plotted in each node, representing only the external group.

The circles in each node represent the unambiguous changes only. Black circles represent non homoplastic and empty circles represent homoplastic synapomorphies. Numbers after the species name are the LAL Vouchers of each individual.

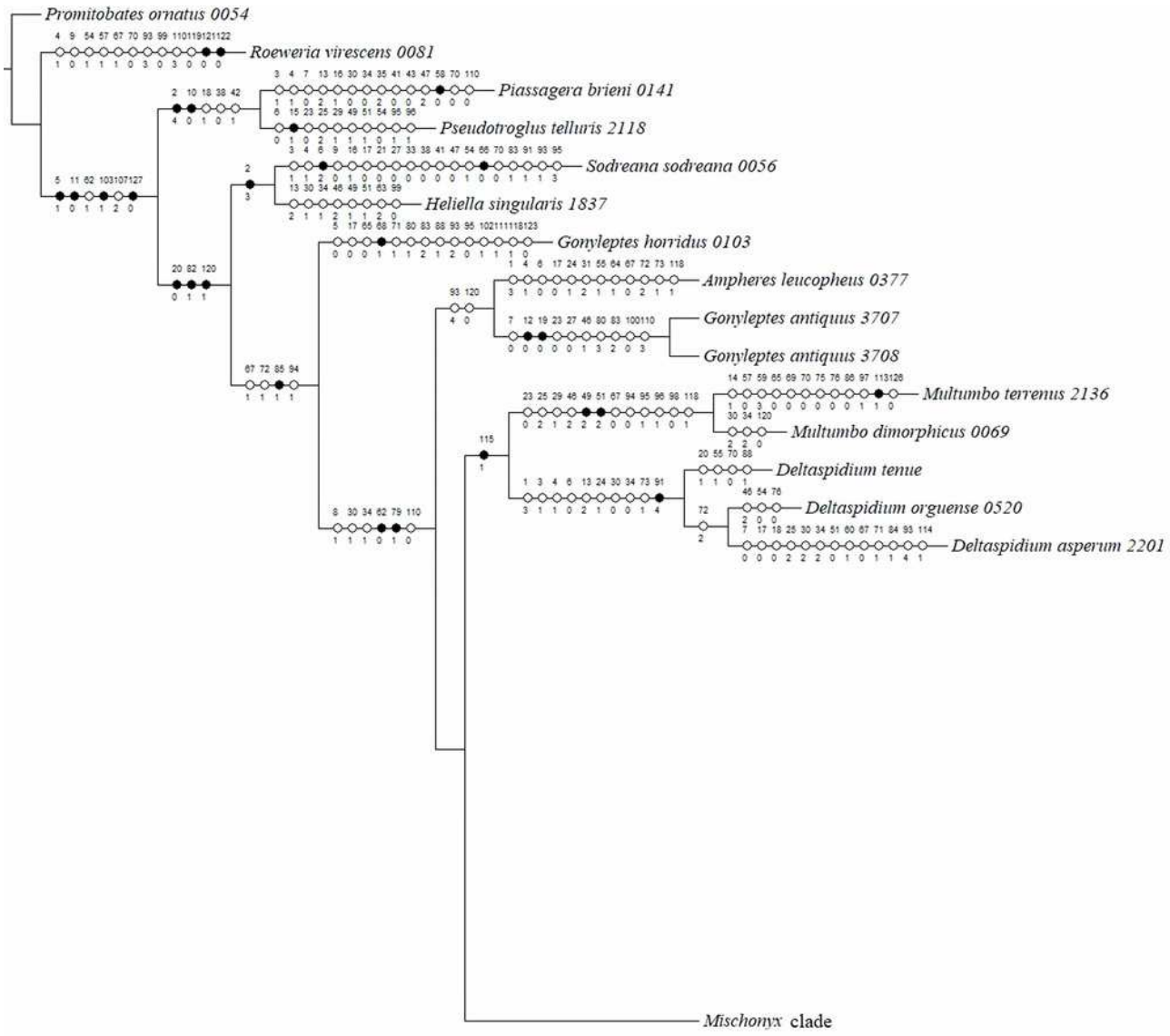

Figure 11

Total Evidence Maximum Likelihood hypothesis (ML3) with characters change plotted in each node, representing *Mischonyx* internal relationships.

The circles in each node represent the unambiguous changes only. Black circles represent non homoplastic and empty circles represent homoplastic synapomorphies. Numbers after the species name are the LAL Vouchers of each individual.

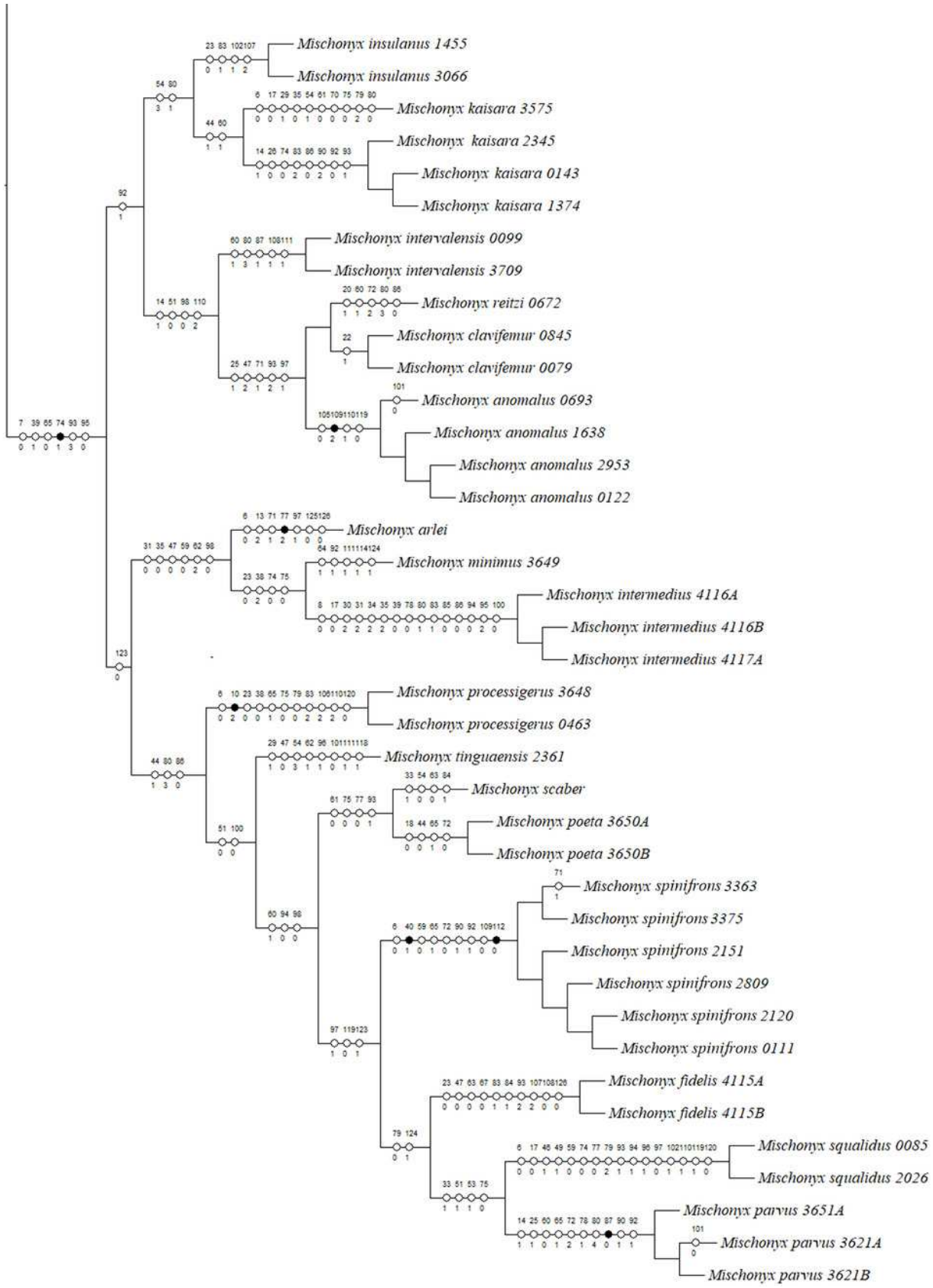
Mischonyx insulanus 1455
Mischonyx insulanus 3066
Mischonyx kaisara 3575
Mischonyx kaisara 2345
Mischonyx kaisara 0143
Mischonyx kaisara 1374
Mischonyx intervalensis 0099
Mischonyx intervalensis 3709
Mischonyx reitzi 0672
Mischonyx clavifemur 0845
Mischonyx clavifemur 0079
Mischonyx anomalus 0693
Mischonyx anomalus 1638
Mischonyx anomalus 2953
Mischonyx anomalus 0122
Mischonyx arlei
Mischonyx minimus 3649
Mischonyx intermedius 4116A
Mischonyx intermedius 4116B
Mischonyx intermedius 4117A
Mischonyx processigerus 3648
Mischonyx processigerus 0463
Mischonyx tinguaensis 2361
Mischonyx scaber
Mischonyx poeta 3650A
Mischonyx poeta 3650B
Mischonyx spinifrons 3363
Mischonyx spinifrons 3375
Mischonyx spinifrons 2151
Mischonyx spinifrons 2809
Mischonyx spinifrons 2120
Mischonyx spinifrons 0111
Mischonyx fidelis 4115A
Mischonyx fidelis 4115B
Mischonyx squalidus 0085
Mischonyx squalidus 2026
Mischonyx parvus 3651A
Mischonyx parvus 3621A
Mischonyx parvus 3621B

Figure 12

Total Evidence Parsimony hypothesis topology (MP3).

The values near the nodes are the bootstrap values of each one. Numbers after the species name are the LAL Vouchers of each individual. The colored clades are according to their location, respective to each Area of Endemism. Light green: SC; yellow: PR; Red: SSP; orange: SMSP; blue: Org; dark green: Esp; purple: Boc; brown: LSRJ and *M. squalidus*.

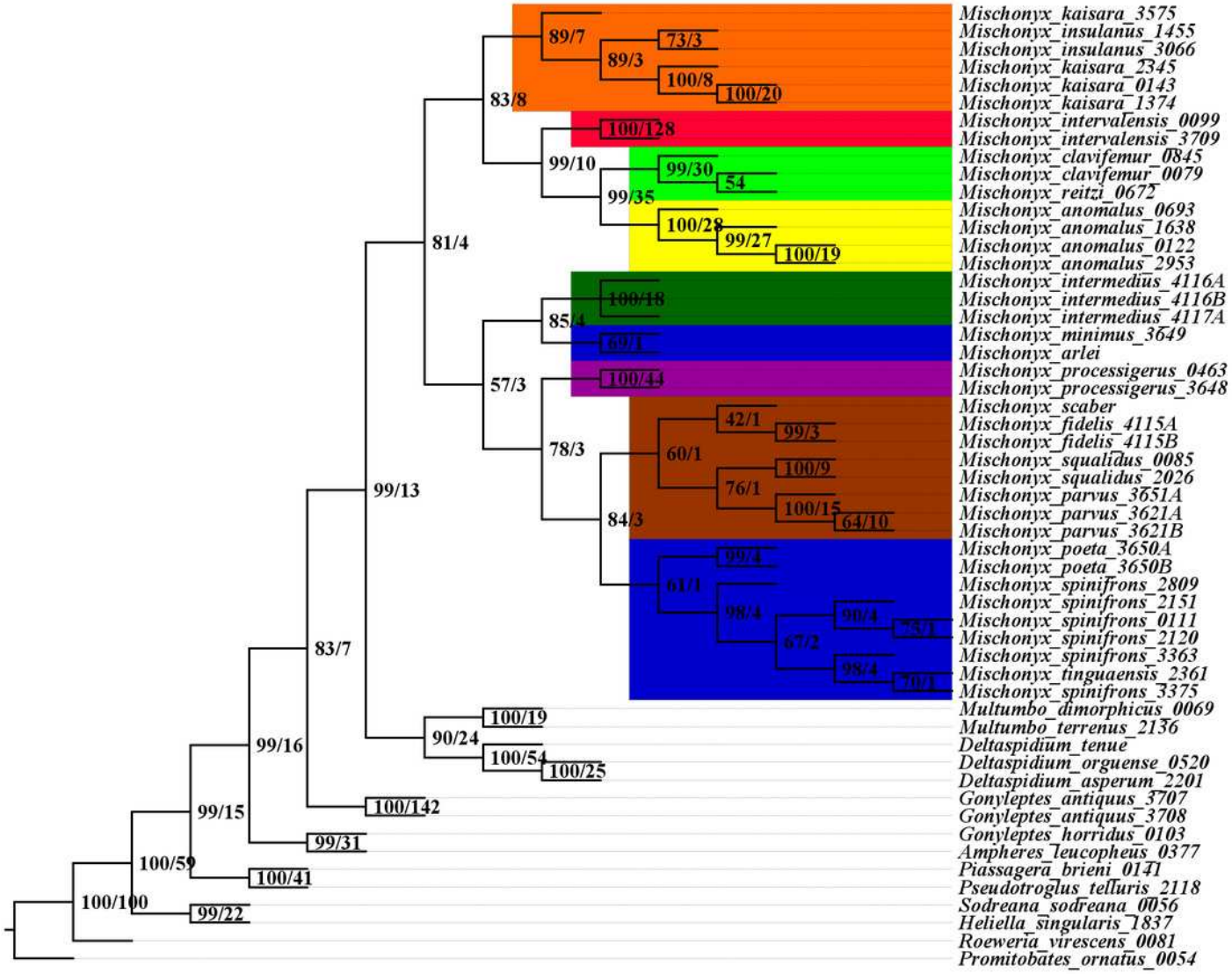

Figure 13

Total Evidence Maximum Parsimony hypothesis (MP3) with characters change plotted in each node, representing only the external group.

The circles in each node represent the unambiguous changes only. Black circles represent non homoplastic and empty circles represent homoplastic synapomorphies. Numbers after the species name are the LAL Vouchers of each individual.


Promitobates ornatus 0054
Roeweria virescens 0081
Sodreana sodreana 0056
Heliella singularis 1837
Piassagera brieni 0141
Pseudotroglus telluris 2118
Ampheres leucopheus 0377
Gonyleptes horridus 0103
Gonyleptes antiquus 3707
Gonyleptes antiquus 3708
Multumbo terrenus 2136
Multumbo dimorphicus 0069
Deltaspidium tenue
Deltaspidium orguense 0520
Deltaspidium asperum 2201
Mischonyx clade

Figure 14

Total Evidence Maximum Parsimony hypothesis (MP3) with characters change plotted in each node, representing *Mischonyx* internal relationships.

The circles in each node represent the unambiguous changes only. Black circles represent non homoplastic and empty circles represent homoplastic synapomorphies. Numbers after the species name are the LAL Vouchers of each individual.

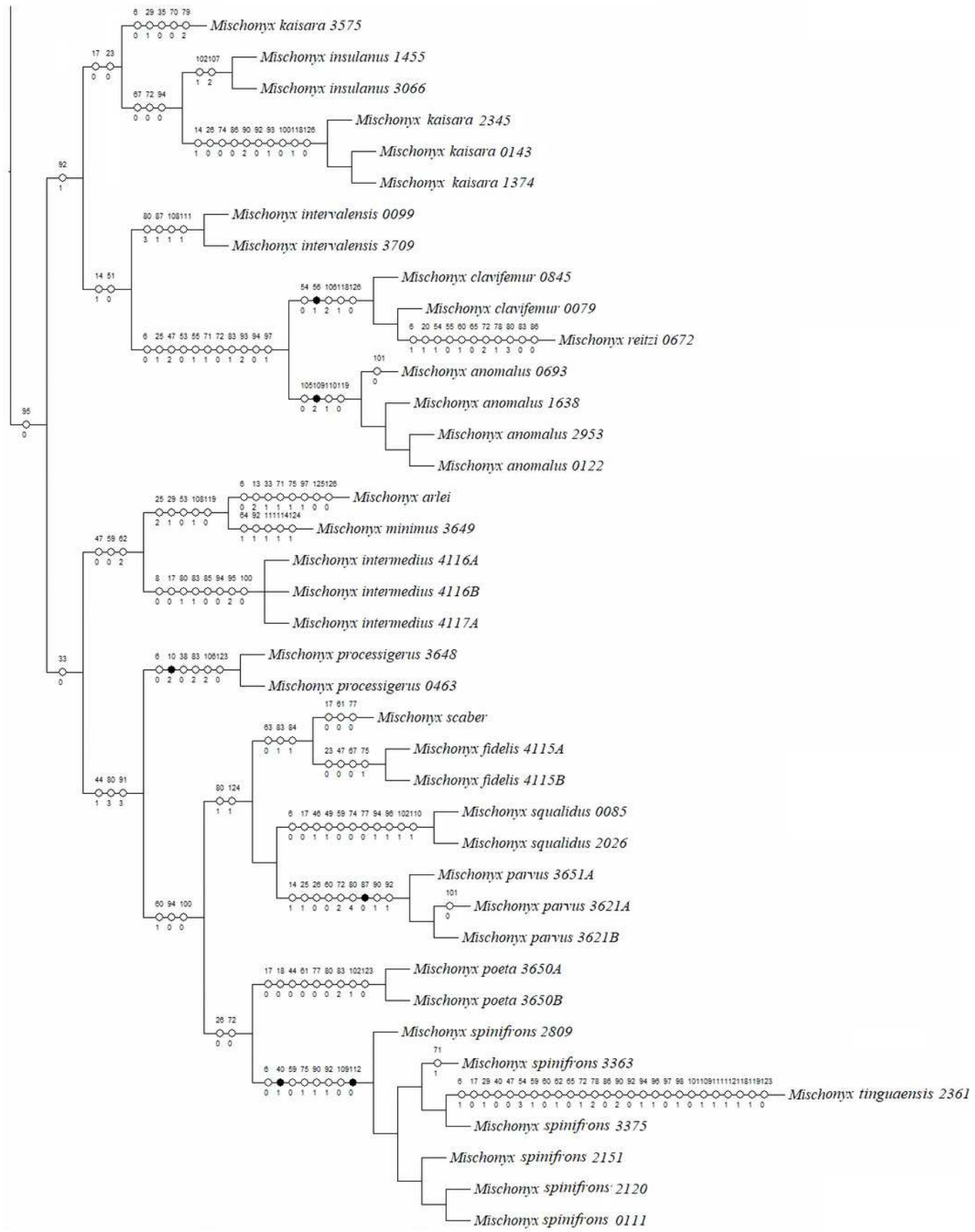
Mischonyx kaisara 3575
Mischonyx insulanus 1455
Mischonyx insulanus 3066
Mischonyx kaisara 2345
Mischonyx kaisara 0143
Mischonyx kaisara 1374
Mischonyx intervalensis 0099
Mischonyx intervalensis 3709
Mischonyx clavifemur 0845
Mischonyx clavifemur 0079
Mischonyx reitzi 0672
Mischonyx anomalus 0693
Mischonyx anomalus 1638
Mischonyx anomalus 2953
Mischonyx anomalus 0122
Mischonyx arlei
Mischonyx minimus 3649
Mischonyx intermedius 4116A
Mischonyx intermedius 4116B
Mischonyx intermedius 4117A
Mischonyx processigerus 3648
Mischonyx processigerus 0463
Mischonyx scaber
Mischonyx fidelis 4115A
Mischonyx fidelis 4115B
Mischonyx squalidus 0085
Mischonyx squalidus 2026
Mischonyx parvus 3651A
Mischonyx parvus 3621A
Mischonyx parvus 3621B
Mischonyx poeta 3650A
Mischonyx poeta 3650B
Mischonyx spinifrons 2809
Mischonyx spinifrons 3363
Mischonyx tinguaensis 2361
Mischonyx spinifrons 3375
Mischonyx spinifrons 2151
Mischonyx spinifrons 2120
Mischonyx spinifrons 0111

Figure 15

Mischonyx minimus sp. nov. male holotype drawings.

A, dorsal view; B, lateral view; C, dorsal view of the right leg; D, retrolateral view of the right leg. The tubercles painted in gray are whitish in ethanol. Scale bars = 1 mm.

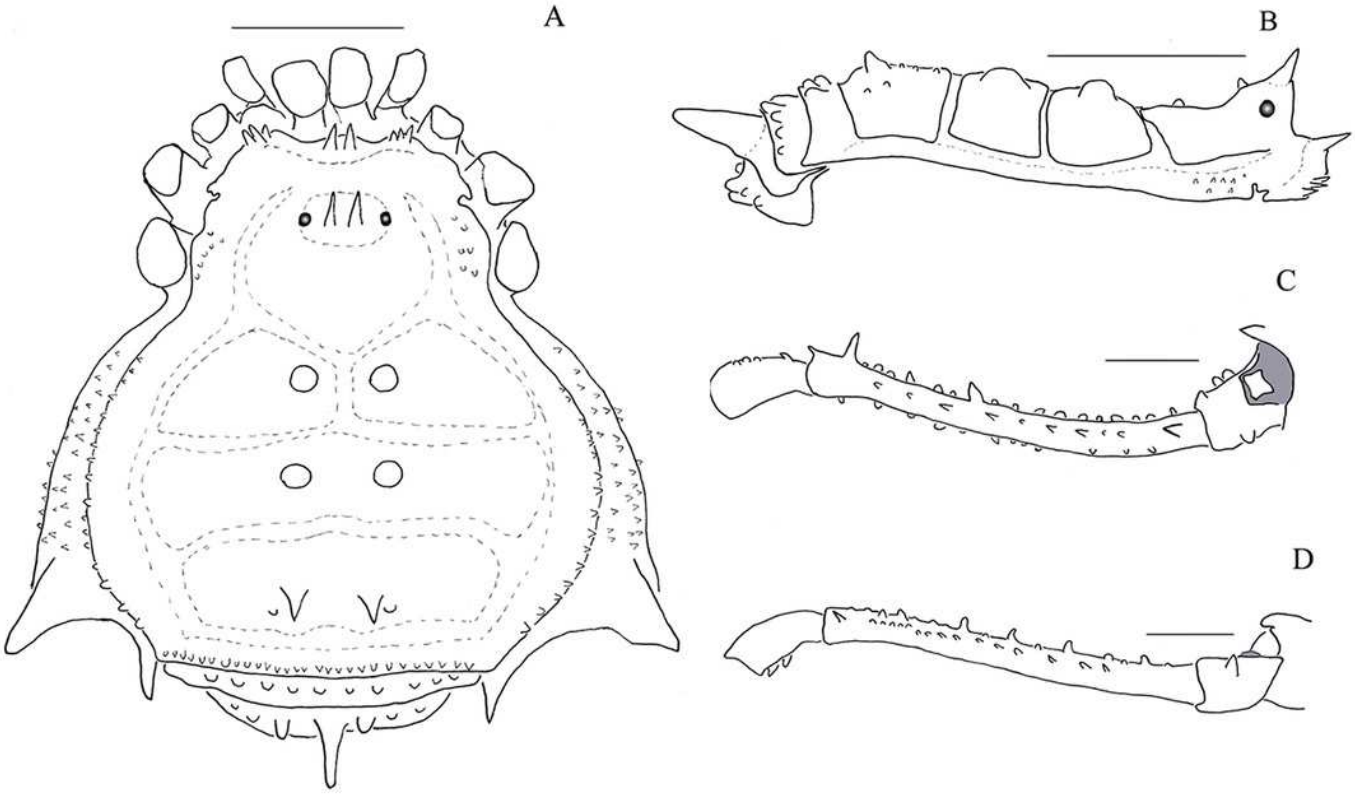

Figure 16

Mischonyx intervalensis sp. nov. male holotype and female paratype drawings.

A, C, Male holotype, dorsal and lateral view, respectively; B, Female paratype, dorsal view; D, E Right leg of the male holotype right, dorsal and retrolateral view, respectively. Scale bars = 1 mm.

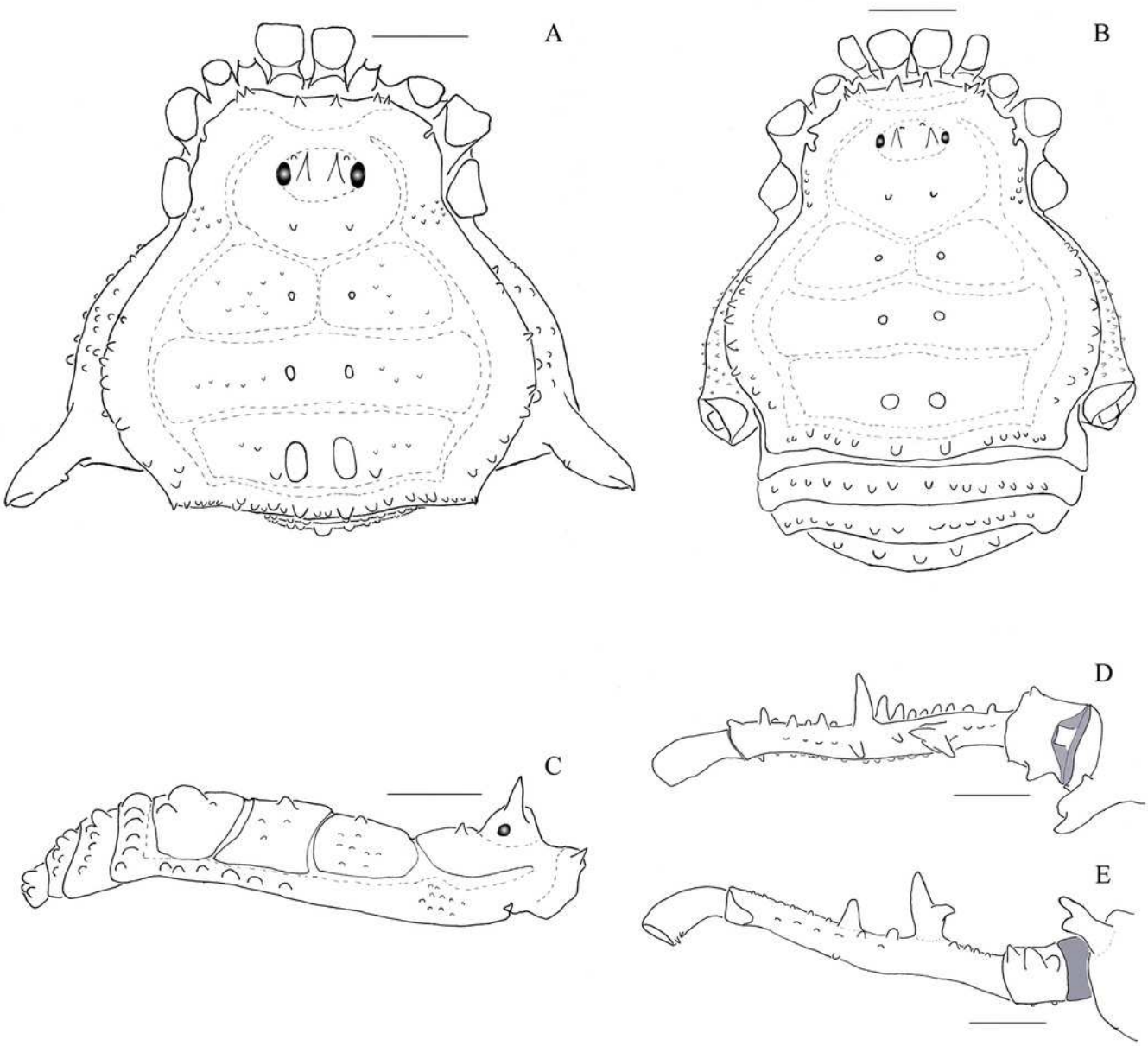
A
B
C
D
E

Figure 17

Mischonyx tinguaensis sp. nov. male holotype and female paratype drawings.

A, C, Male holotype, dorsal and lateral view, respectively; B, Female paratype, dorsal view; D, E Right leg of the male holotype right, dorsal and retrolateral view, respectively. Scale bars = 1 mm.

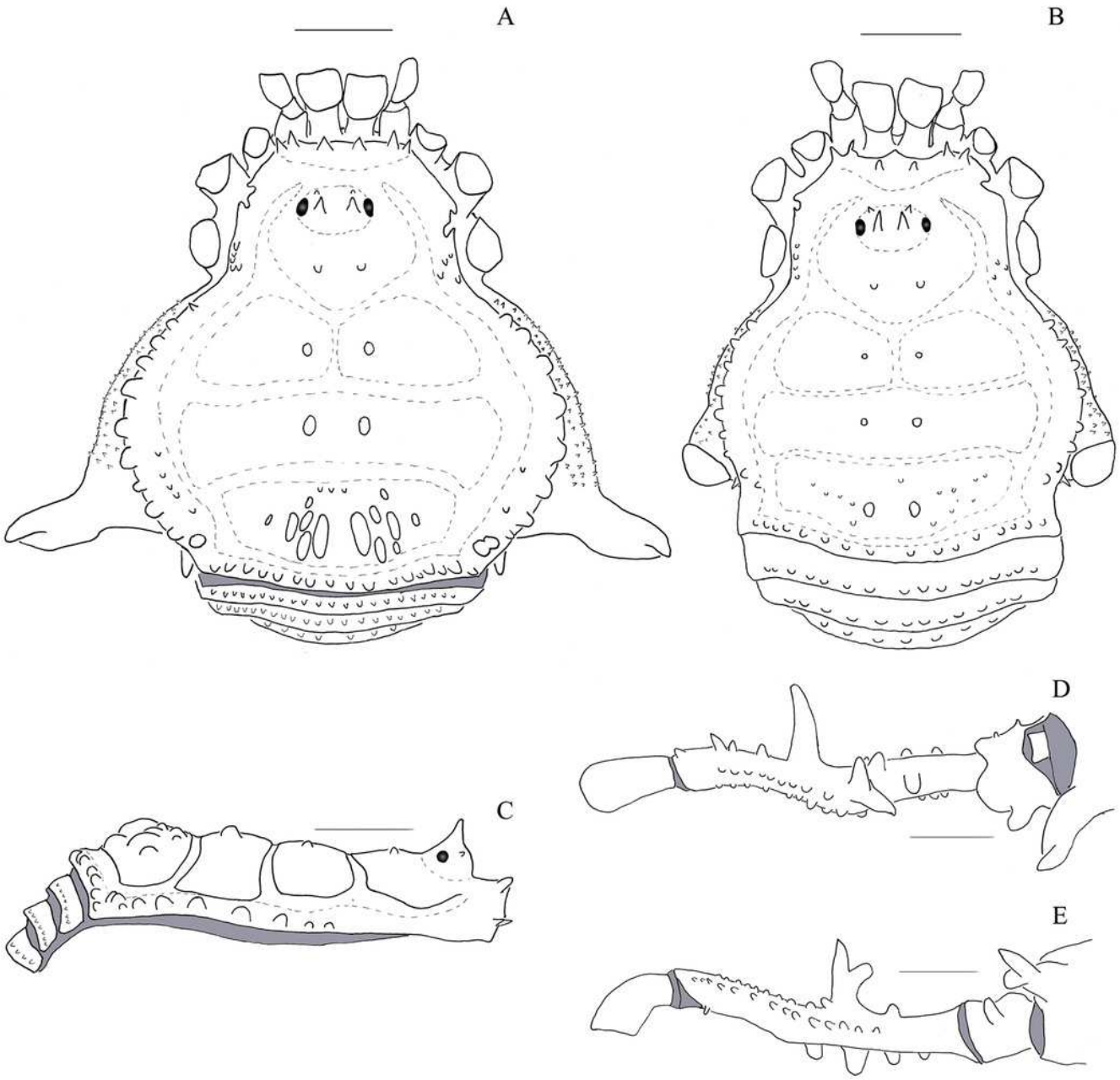
A
B
C
D
E

Figure 18

Penis of the new species.

A – C. Dorsal, right lateral and ventral views, respectively, of the penis of *Mischonyx minimus* **sp. nov.** paratype (3649). D – F. Dorsal, right lateral and ventral views, respectively, of the penis of *Mischonyx tinguaensis* **sp. nov.** paratype (2361). G – I. Dorsal, right lateral and ventral views, respectively, of the penis of *Mischonyx intervalensis* **sp. nov.** paratype (0099).

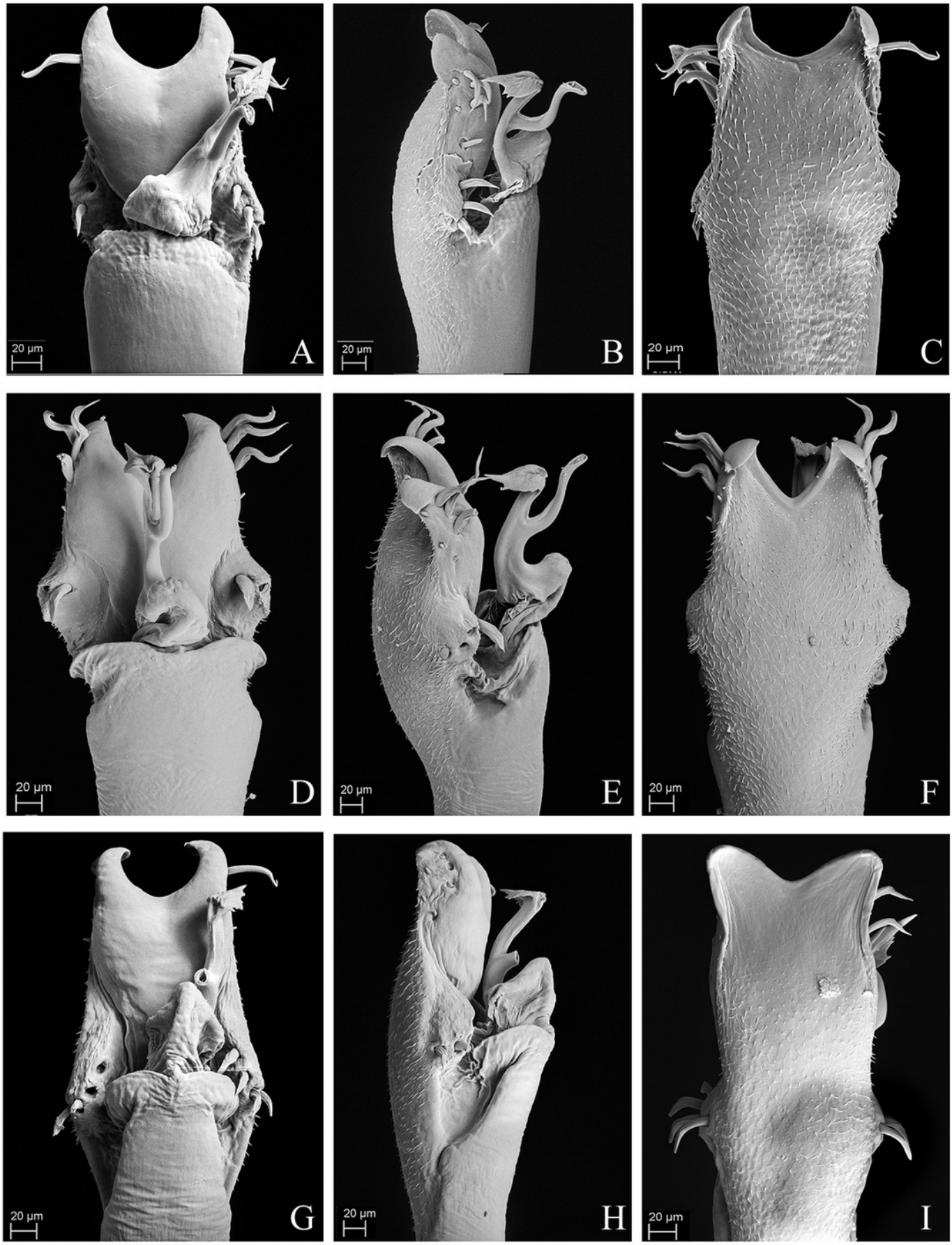
20 µm
A
20 µm
B
20 µm
C
20 µm
D
20 µm
E
20 µm
F
20 µm
G
20 µm
H
20 µm
I

Figure 19

Mischonyx anomalus and *Mischonyx arlei* holotypes.

A and C. *Mischonyx anomalus*, dorsal and lateral views, respectively. B and D. *Mischonyx arlei*, dorsal and lateral views, respectively. Scale bars: 1 mm.

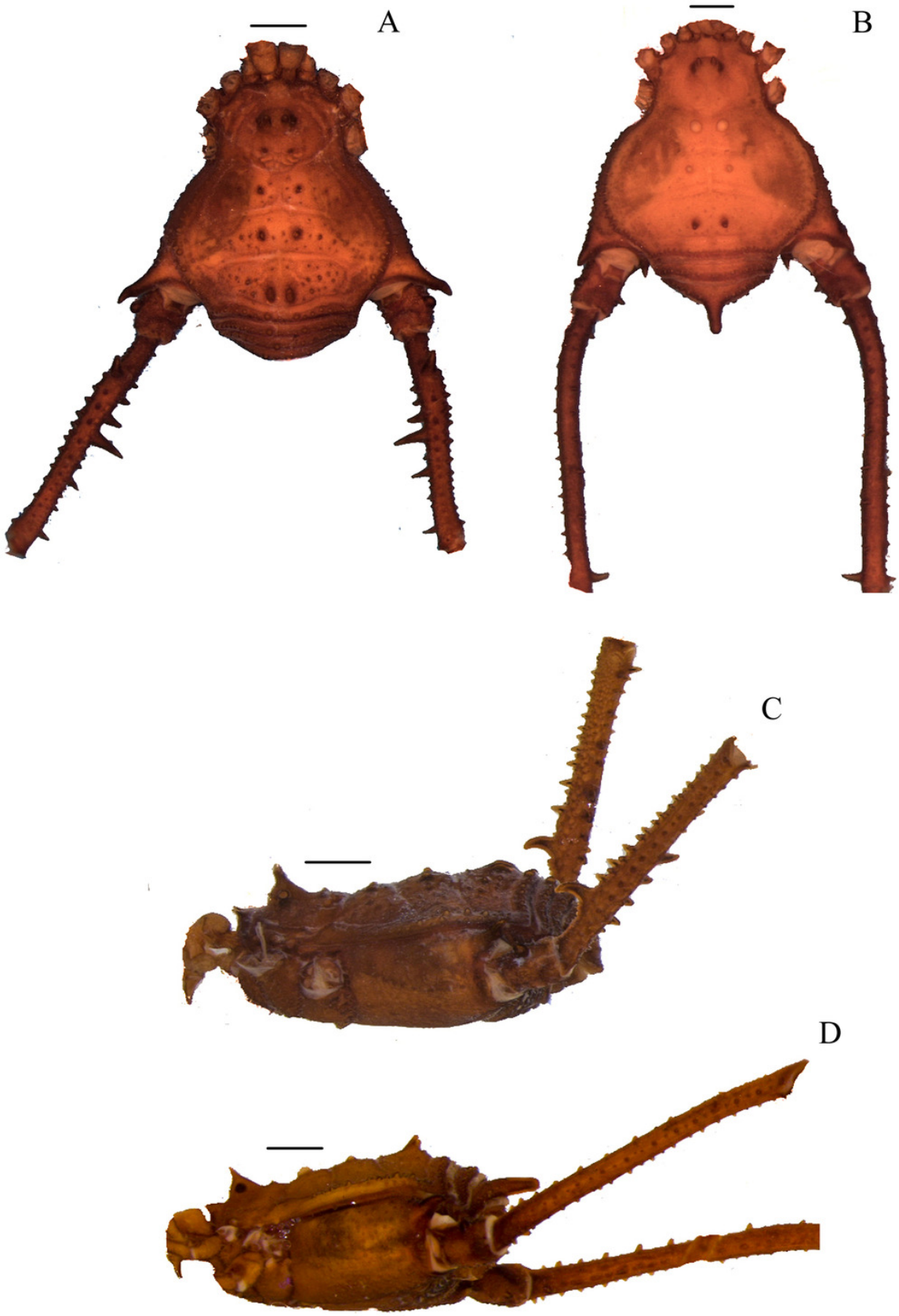
A
B
C
D

Figure 20

Mischonyx clavifemur holotype and *Mischonyx fidelis* (4115A).

A and C. *Mischonyx clavifemur*, dorsal and lateral views, respectively. B and D. *Mischonyx fidelis*, dorsal and lateral views, respectively. Scale bars: 1 mm.

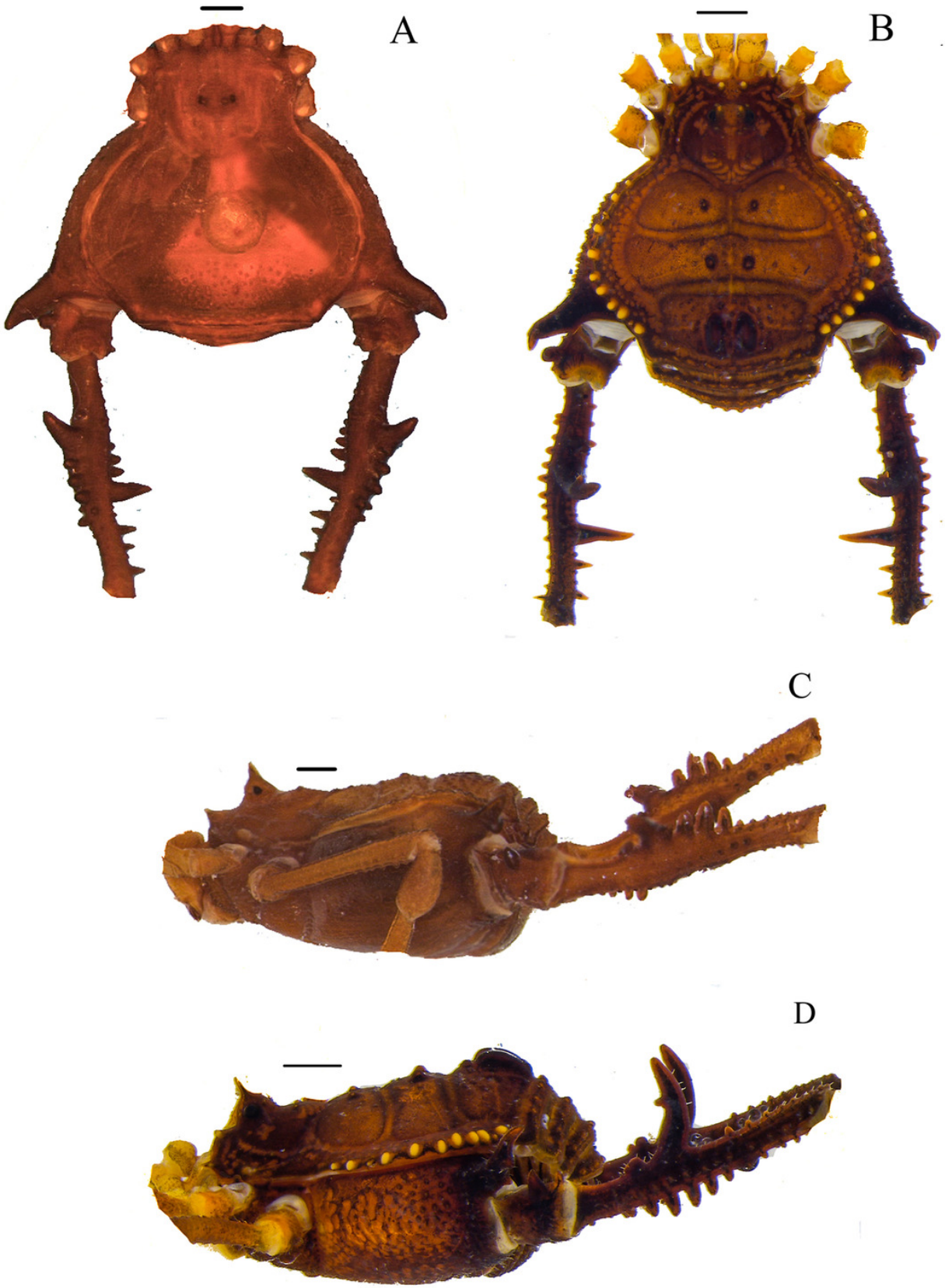
A
B
C
D

Figure 21

Mischonyx insulanus and *Mischonyx intermedius* holotypes.

A and C. *Mischonyx insulanus*, dorsal and lateral views, respectively. B and D. *Mischonyx intermedius*, dorsal and lateral views, respectively. Scale bars: 1 mm.

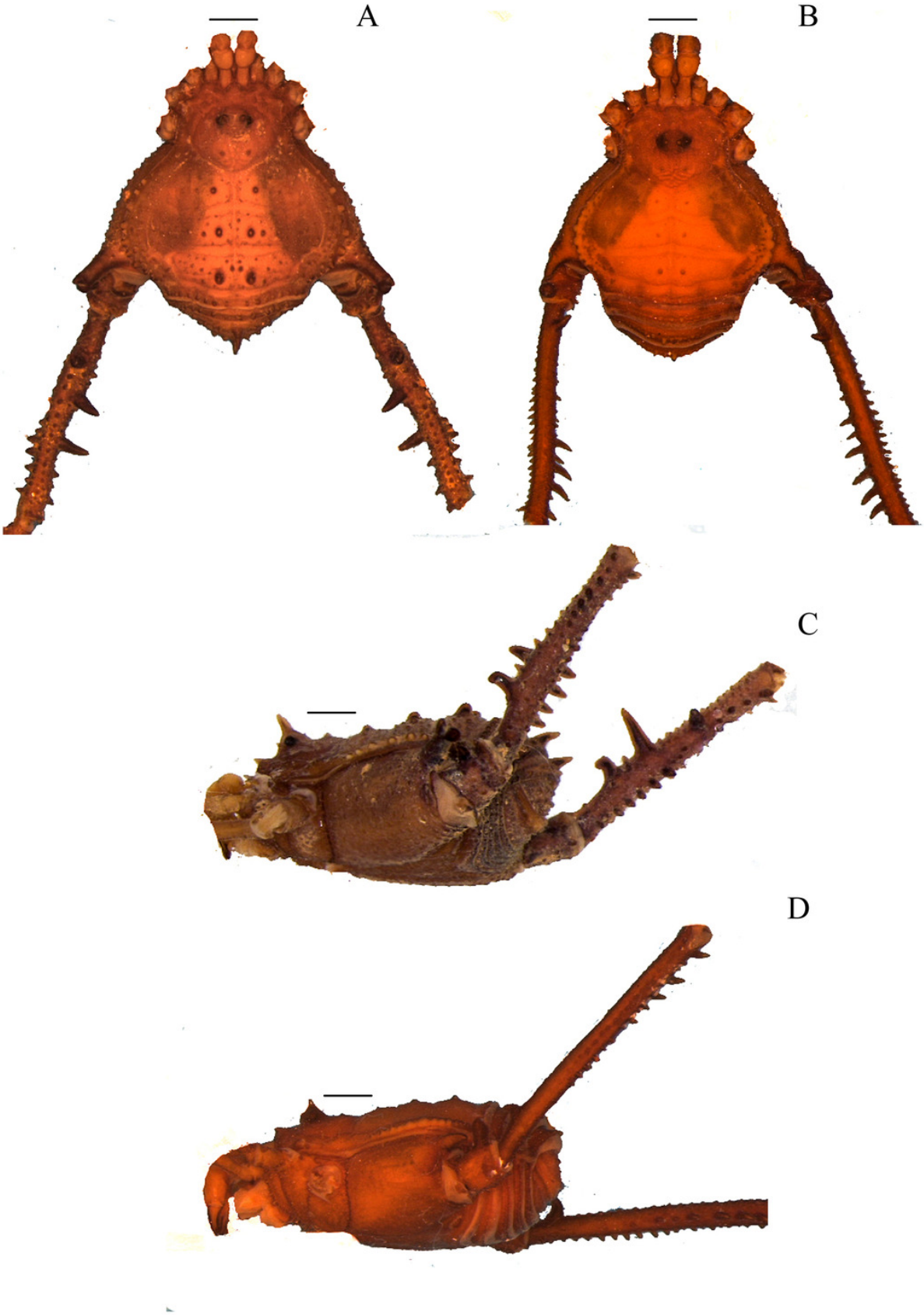
A
B
C
D

Figure 22

Mischonyx intervalensis sp. nov. holotype and *Mischonyx kaisara*.

A and C. *Mischonyx intervalensis* **sp. nov.**, dorsal and lateral views, respectively. B and D. *Mischonyx kaisara*, dorsal and lateral views, respectively. Scale bars: 1 mm.

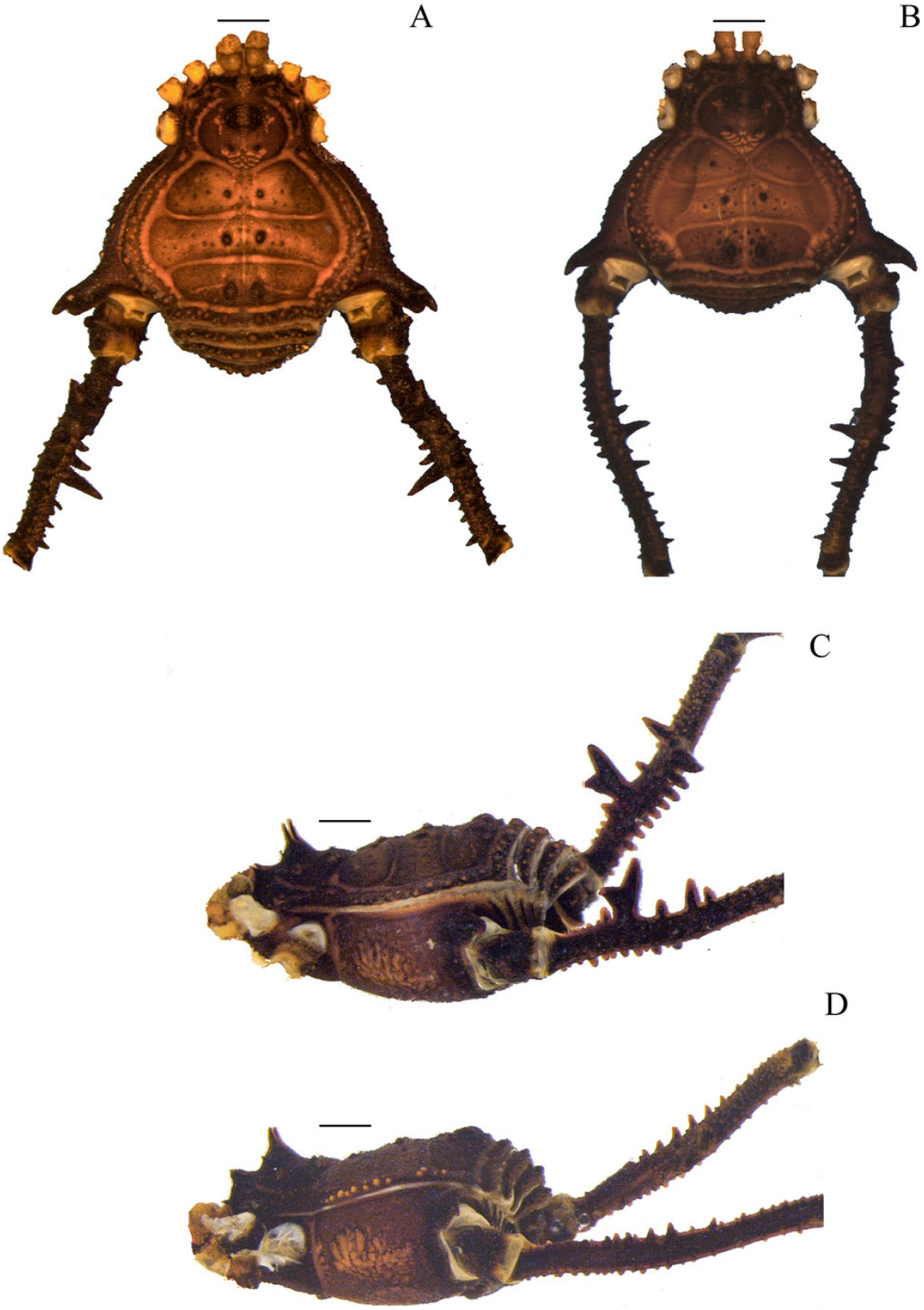
A
B
C
D

Figure 23

Mischonyx minimus sp. nov. and *Mischonyx parvus* holotypes.

A and C. *Mischonyx minimus* **sp. nov.**, dorsal and lateral views, respectively. B and D. *Mischonyx parvus*, dorsal and lateral views, respectively. Scale bars: 1 mm.

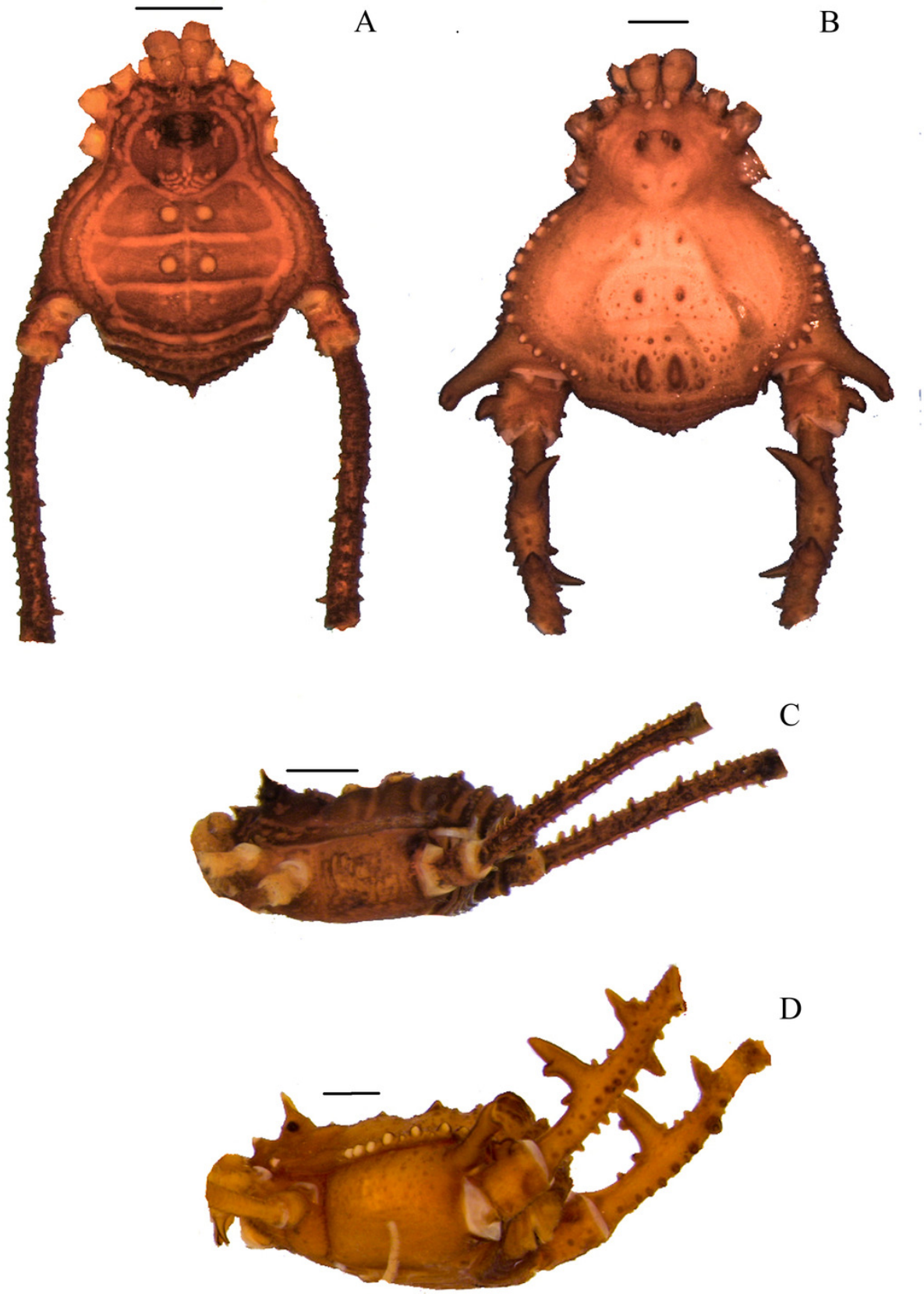
A
B
C
D

Figure 24

Mischonyx poeta and *Mischonyx processigerus* paratypes.

A and C. *Mischonyx poeta*, dorsal and lateral views, respectively. B and D. *Mischonyx processigerus*, dorsal and lateral views, respectively. Scale bars: 1 mm.

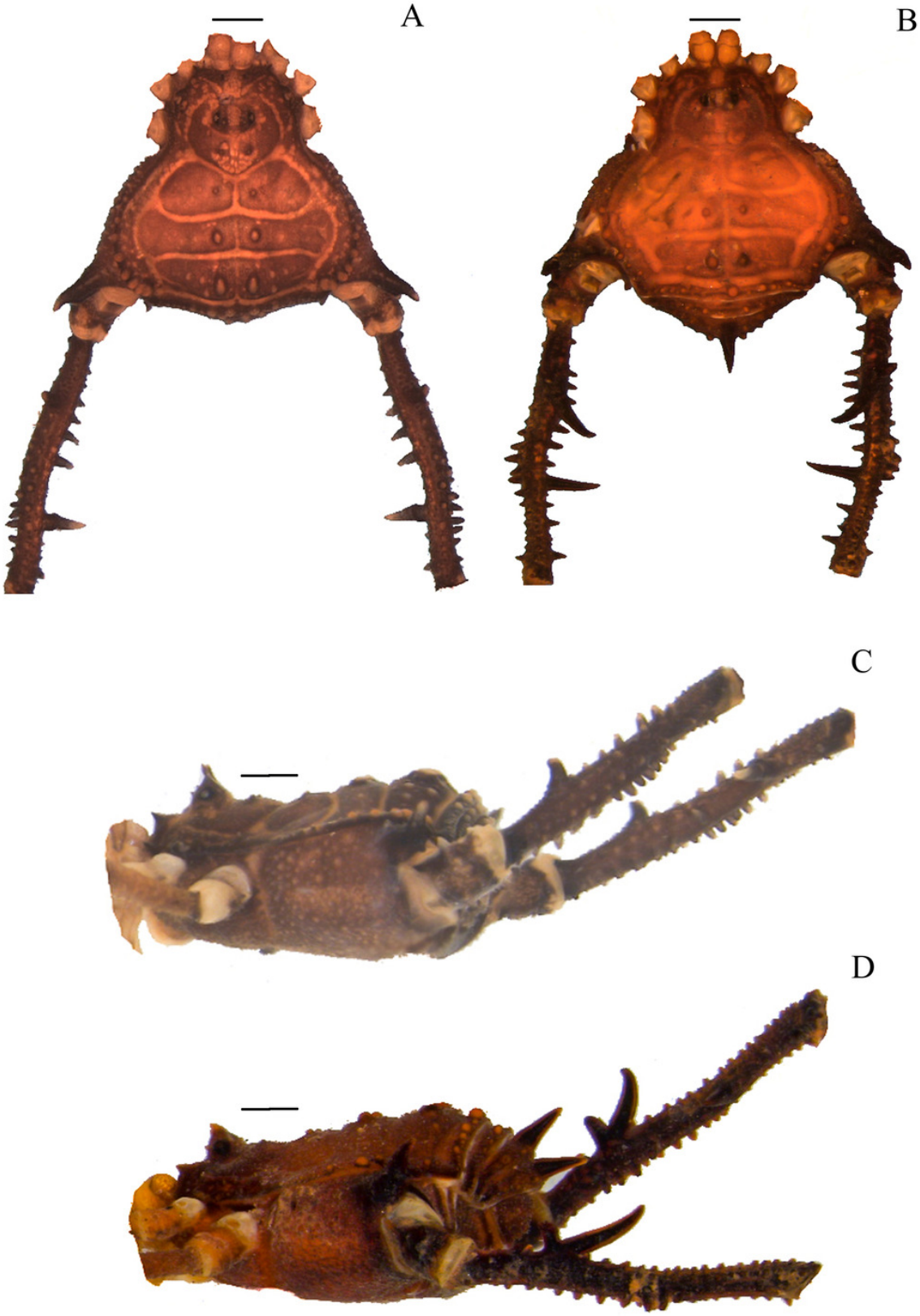
A
B
C
D

Figure 25

Mischonyx reitzi (0672) and *Mischonyx scaber*.

A and C. *Mischonyx reitzi*, dorsal and lateral views, respectively. B and D. *Mischonyx scaber*, dorsal and lateral views, respectively. Scale bars: 1 mm.

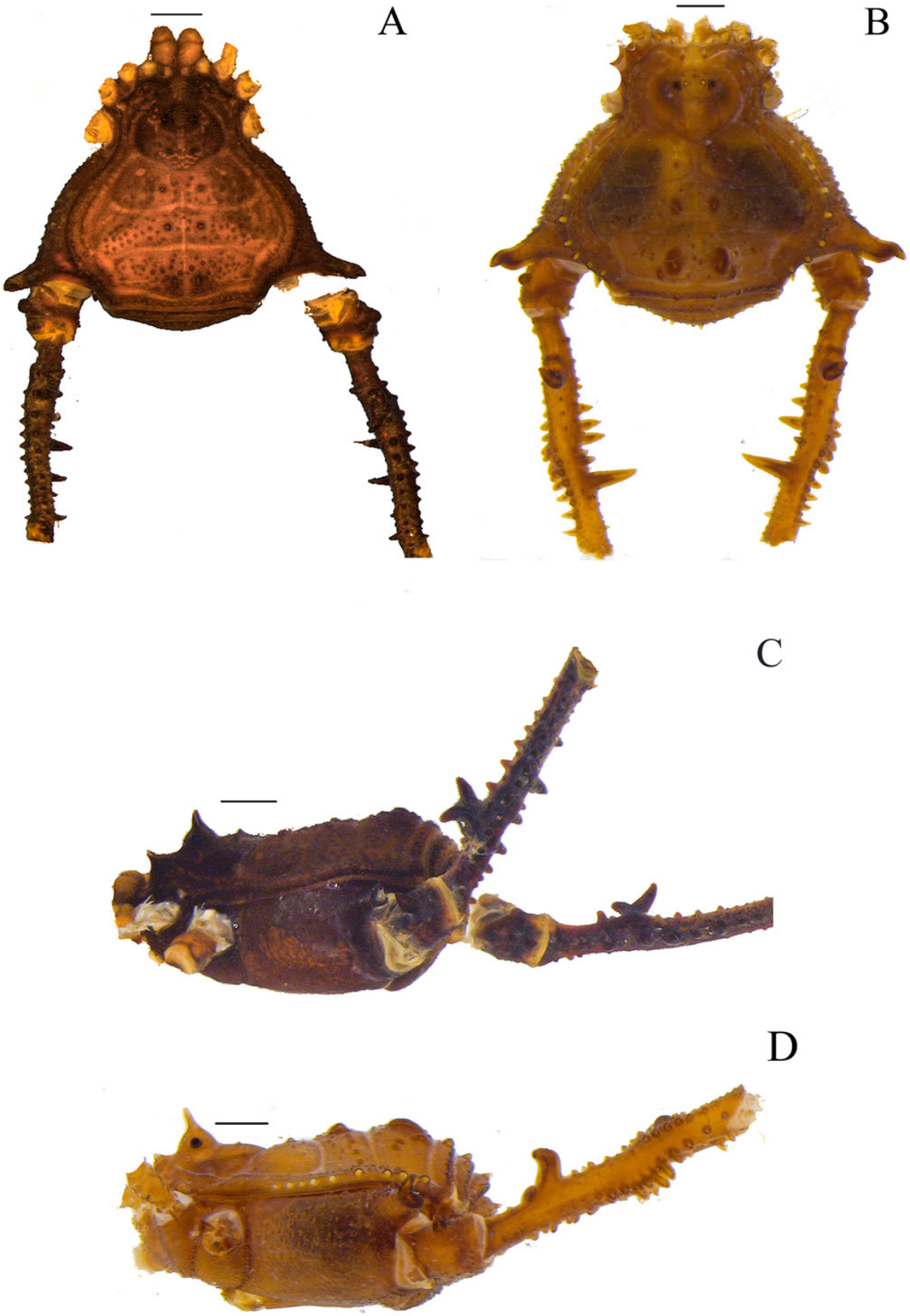
A
B
C
D

Figure 26

Mischonyx spinifrons (*M. bresslaui* paratype) and *Mischonyx squalidus* (*M. cuspidatus* holotype).

A and C. *Mischonyx spinifrons*, dorsal and lateral views, respectively. B and D. *Mischonyx squalidus*, dorsal and lateral views, respectively. Scale bars: 1 mm.

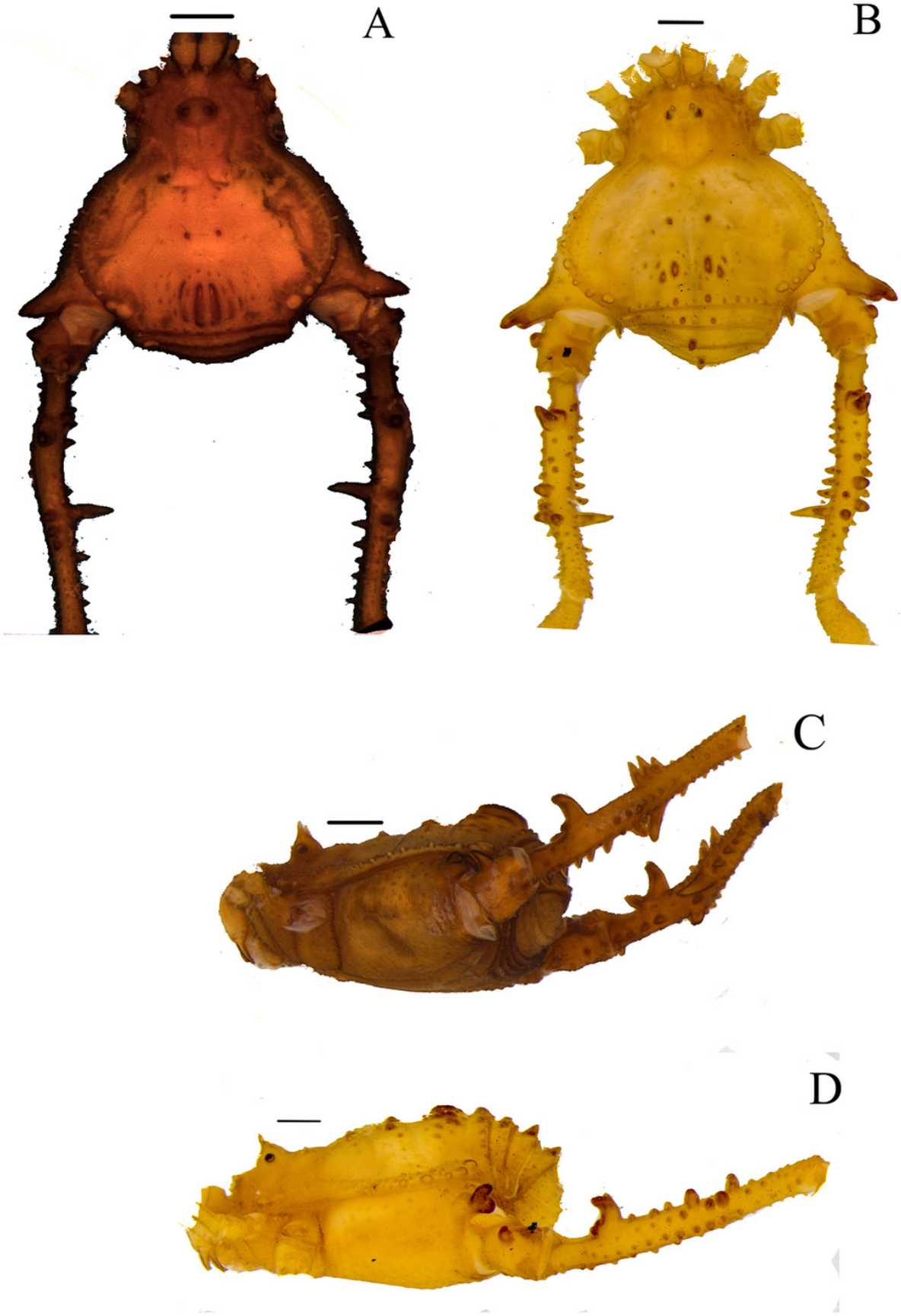
A
B
C
D

Figure 27

Mischonyx tinguaensis sp. nov. holotype.

A. dorsal view. B. lateral. Scale bars: 1 mm.


A


B

Figure 28

Penis of *Mischonyx anomalus, M. arlei* and *M. clavifemur*.

A – C. Dorsal, right lateral and ventral views, respectively, of *Mischonyx anomalus*. D – F. Dorsal, right lateral and ventral views, respectively, of the penis of *Mischonyx arlei*. G – I. Dorsal, right lateral and ventral views, respectively, of the penis of *Mischonyx clavifemur.*

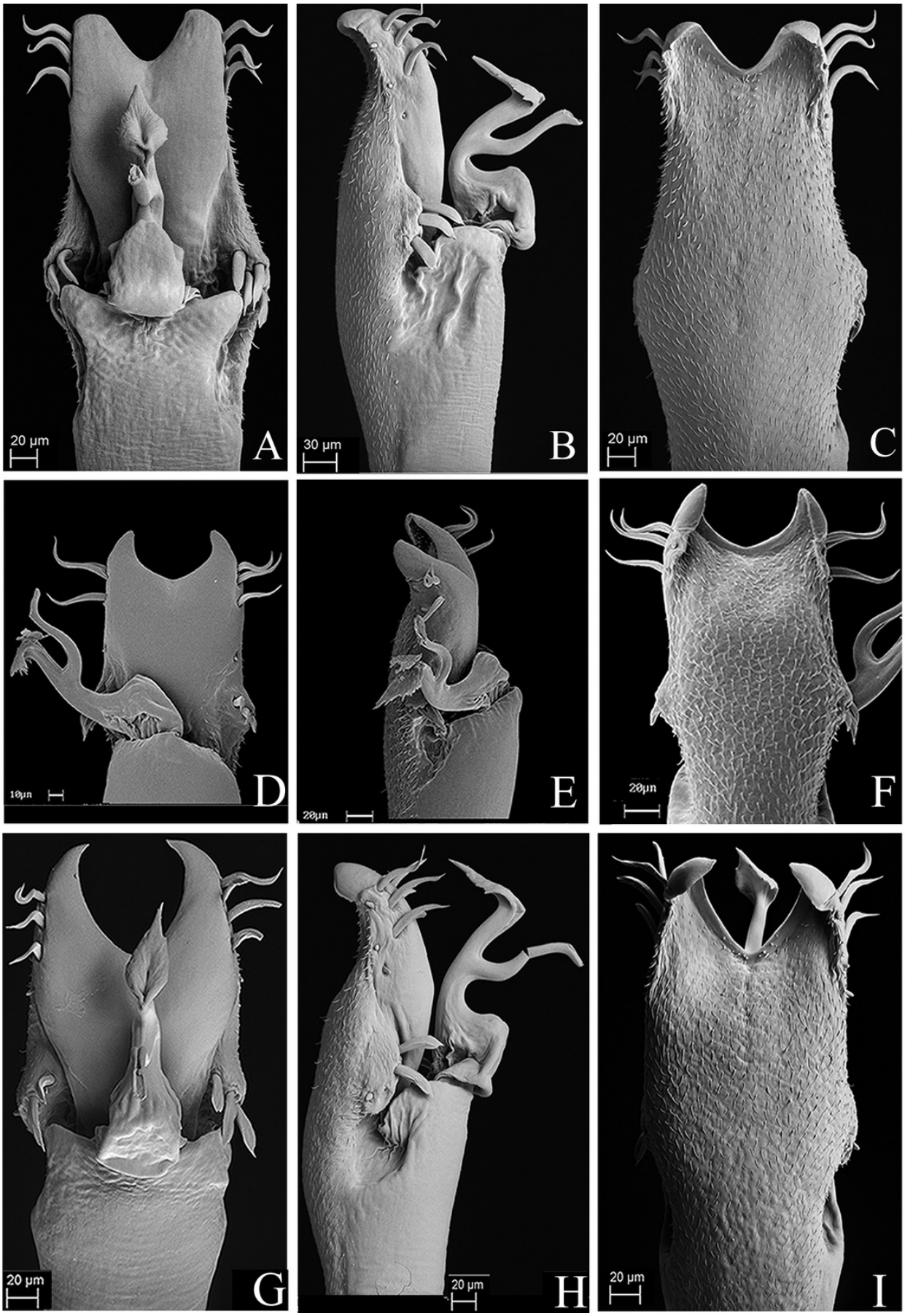
20 µm
A
30 µm
B
20 µm
C
10µm
D
20µm
E
20µm
F
20 µm
G
20 µm
H
20 µm
I

Figure 29

Penis of *Mischonyx fidelis*, *M. insulanus* and *M. intermedius*.

A – C. Dorsal, right lateral and ventral views, respectively, of the penis of *Mischonyx fidelis.* D – F. Dorsal, right lateral and ventral views, respectively, of *Mischonyx insulanus*. G – I. Dorsal, right lateral and ventral views, respectively, of the penis of *Mischonyx intermedius*.

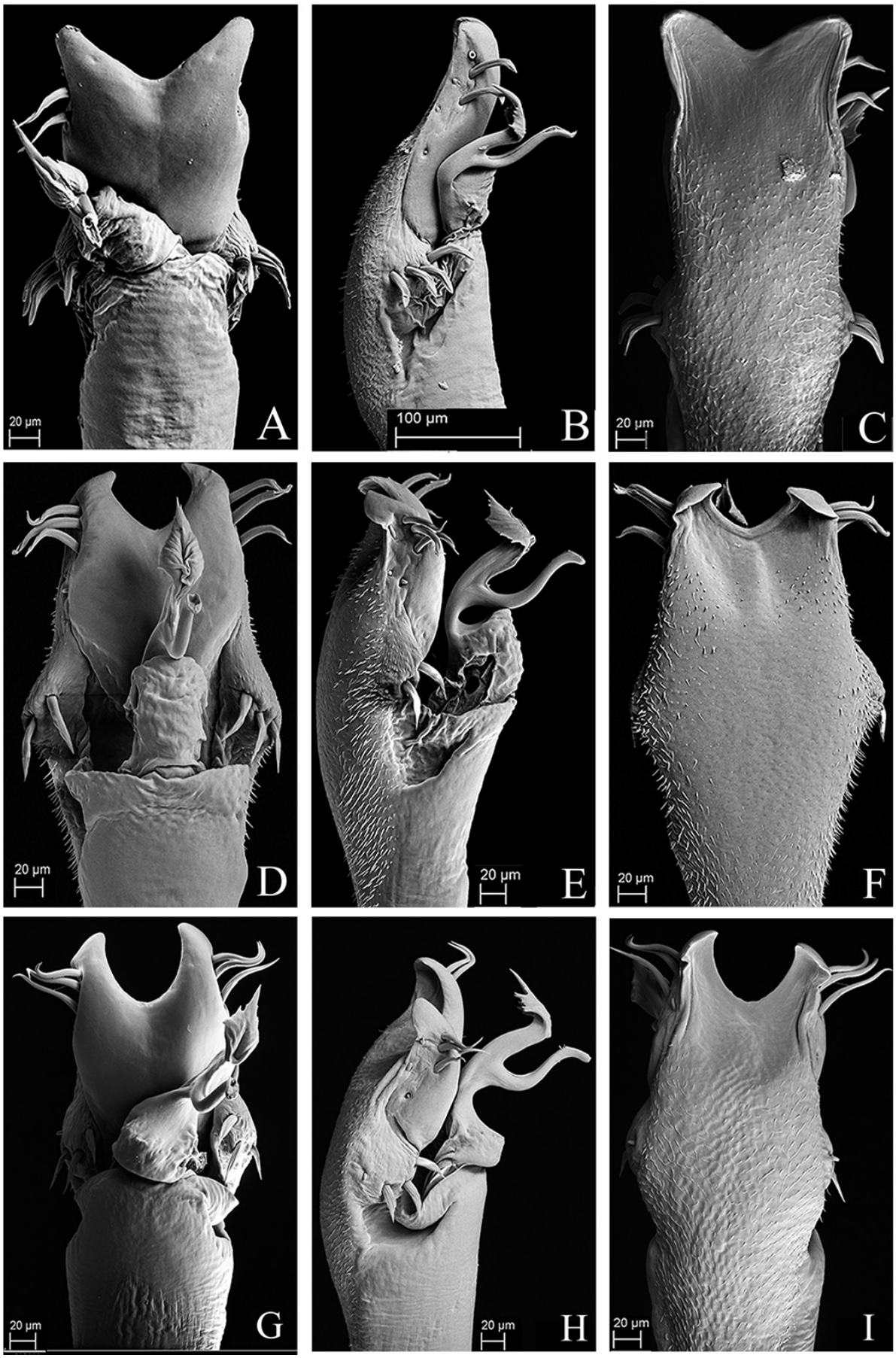
20 µm
A
100 µm
B
20 µm
C
20 µm
D
20 µm
E
20 µm
F
20 µm
G
20 µm
H
20 µm
I

Figure 30

Penis of *Mischonyx kaisara*, *M. parvus* and *M. poeta*.

A – C. Dorsal, right lateral and ventral views, respectively, of the penis of *Mischonyx kaisara.*

D – F. Dorsal, right lateral and ventral views, respectively, of the penis of *Mischonyx parvus.*

G – I. Dorsal, right lateral and ventral views, respectively, of *Mischonyx poeta.*

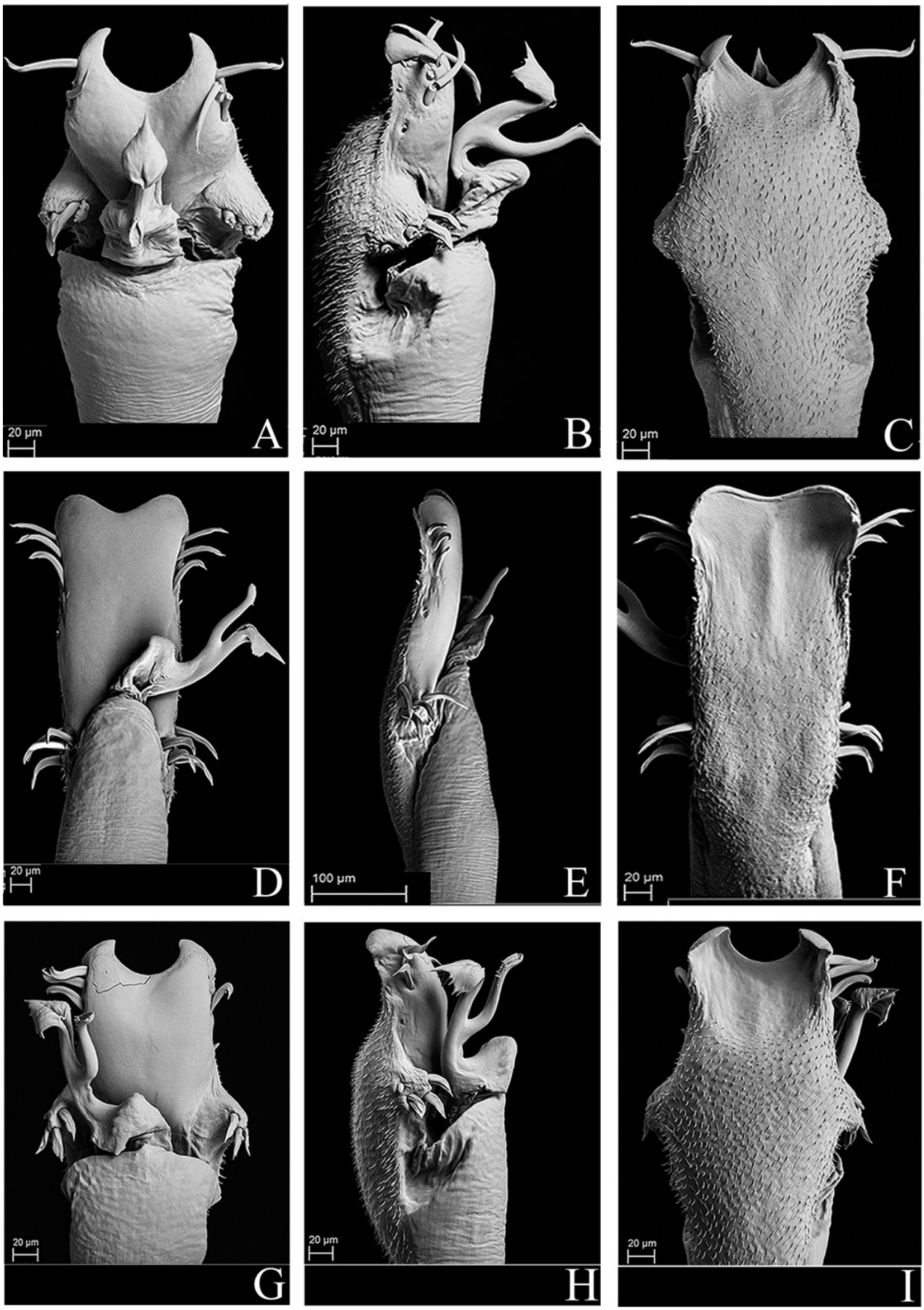
20 µm
A
20 µm
B
20 µm
C
20 µm
D
100 µm
E
20 µm
F
20 µm
G
20 µm
H
20 µm
I

Figure 31

Penis of *Mischonyx processigerus*, *M. spinifrons* and *M. squalidus*.

A – C. Dorsal, right lateral and ventral views, respectively, of the penis of *Mischonyx processigerus*. D – F. Dorsal, right lateral and ventral views, respectively, of the penis of *Mischonyx spinifrons*. G - I. Dorsal, right lateral and ventral views, respectively, of the penis of *Mischonyx squalidus.*

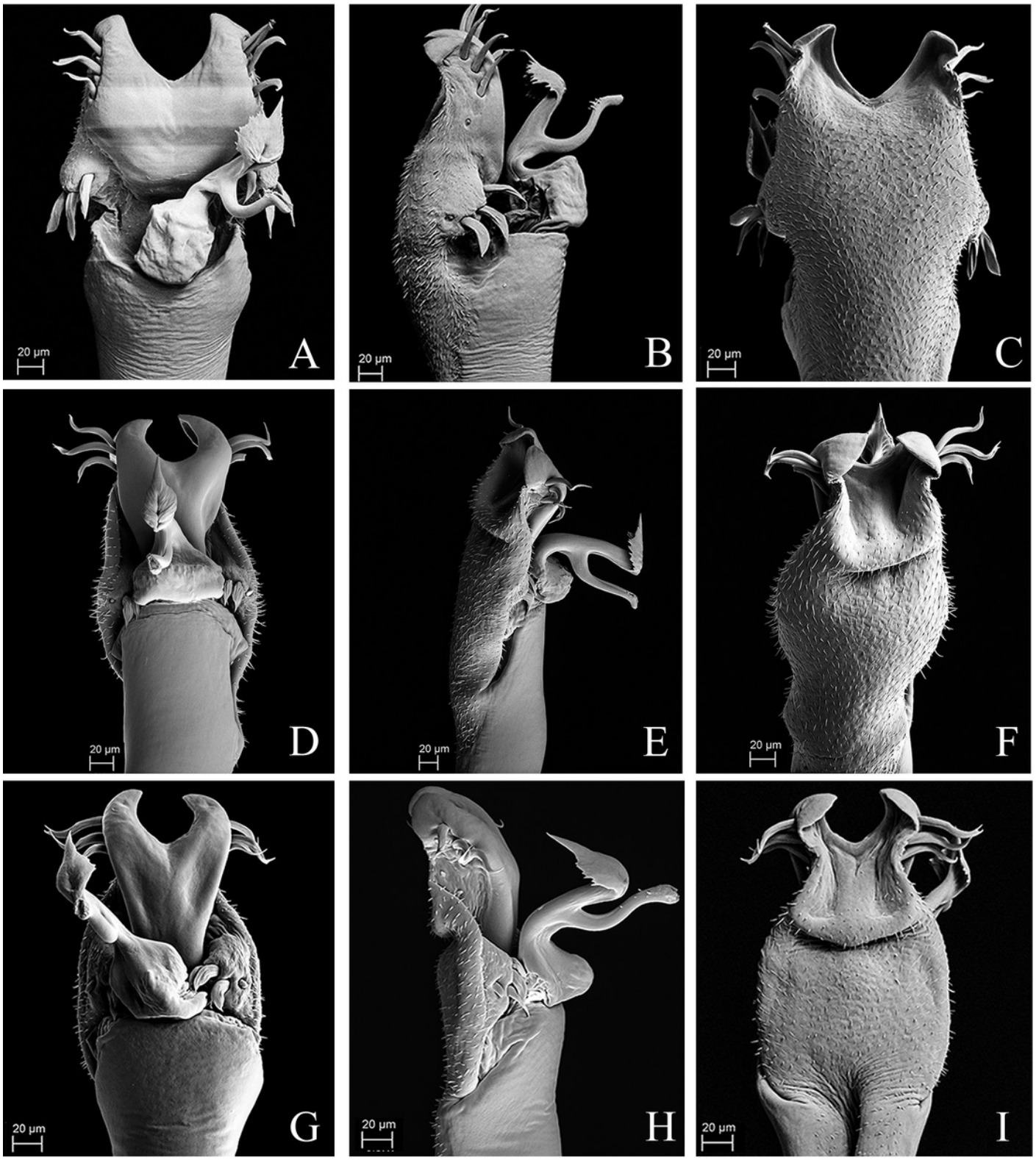
20 µm
A
20 µm
B
20 µm
C
20 µm
D
20 µm
E
20 µm
F
20 µm
G
20 µm
H
20 µm
I

Figure 32

Penis of *Mischonyx reitzi*.

A - C. Dorsal, right lateral and ventral views, respectively, of the penis of Mischonyx reitzi

Scale bars = 1 m.